Morphogenesis and migration: investigating the roles of Rap1 in epithelial cell behaviors during *Drosophila* oogenesis

by

Christopher Luke Bernard Messer

B.S., University of Alabama in Huntsville, 2017

AN ABSTRACT OF A DISSERTATION

submitted in partial fulfillment of the requirements for the degree

DOCTOR OF PHILOSOPHY

Division of Biology
College of Arts and Sciences

KANSAS STATE UNIVERSITY
Manhattan, Kansas

2023

Abstract

Epithelia line many of the body's surfaces and organs where they perform essential functions like nutrient absorption and wound healing. Epithelia are consistently challenged during development and as a part of normal tissue homeostasis. Moreover, most cancers originate in epithelia. Normal developmental apoptosis, cell division, and cell rearrangements test epithelial integrity and cell-cell adhesions. How epithelial cells maintain cell-to-cell adhesions and tissue integrity despite challenges imposed by the tissue environment is poorly understood. The small GTPase Rap1 has roles in cell polarity, cell-cell adhesion, and cell migration. In this dissertation I use the *Drosophila* ovary to investigate how Rap1 contributes to epithelial integrity and cell migration. *Drosophila* oogenesis provides a robust, genetically accessible model to study Rap1 function in epithelia. First, I utilize the *Drosophila* ovariole, a string of progressively developing egg chambers within the ovary, to understand how Rap1 contributes to epithelial integrity in a growing tissue. As oogenesis progresses, egg chambers elongate, which presents a challenge to the overlying follicular epithelium. I found that Rap1 was required to maintain tissue and cell shapes and promote cell viability during tissue elongation. Egg chambers deficient for Rap1 had distorted tissue shapes, stretched individual cells, and failed enrichment of the homophilic cell-cell adhesion protein E-Cadherin. Moreover, Rap1 deficient egg chambers lost follicle cells via apoptosis as indicated by an increase in caspase activity. These results support dual functions for Rap1 in promoting normal epithelial integrity and cell viability during tissue growth of the ovary. While Rap1 has numerous roles in development and disease, signaling partners that facilitate Rap1 function remain unclear. Therefore, I next used the *Drosophila* border cell model of collective cell migration to screen for potential Rap1 effectors required for migration. Border cell migration is a powerful *in vivo* model of collective cell migration. A group of four to six

migratory border cells, along with the central pair of organizing polar cells, migrate across the egg chamber to reach the oocyte. Border cells maintain adhesions to one another and overall cluster polarity. Properly regulated Rap1 activity is essential for efficient migration. I used the strong border cell migration defects reported for constitutively active Rap1, $Rap1^{V12}$, to screen for X-chromosome deficiency regions that partially restored migration to the oocyte. I identified seven X-chromosome deficiencies that restored migration to $Rap1^{V12}$ expressing border cells. Furthermore, I mapped three of these regions to single genes, and report *fz4*, *Usp16-45*, and *sno* as candidate Rap1 interacting genes in border cell migration. Taken together these results demonstrate a requirement for Rap1 in epithelial integrity and cell viability during oogenesis and identify three candidate effectors that facilitate border cell migration. Results from this study are broadly relevant, as epithelial morphogenesis and collective cell migration are highly conserved features of metazoan development.

Morphogenesis and migration: investigating the roles of Rap1 in epithelial cell behaviors during *Drosophila* oogenesis

by

Christopher Luke Bernard Messer

B.S., University of Alabama in Huntsville, 2017

A DISSERTATION

submitted in partial fulfillment of the requirements for the degree

DOCTOR OF PHILOSOPHY

Division of Biology
College of Arts and Sciences

KANSAS STATE UNIVERSITY
Manhattan, Kansas

2023

Approved by:

Major Professor
Dr. Jocelyn A. McDonald

Copyright

Abstract

Epithelia line many of the body's surfaces and organs where they perform essential functions like nutrient absorption and wound healing. Epithelia are consistently challenged during development and as a part of normal tissue homeostasis. Moreover, most cancers originate in epithelia. Normal developmental apoptosis, cell division, and cell rearrangements test epithelial integrity and cell-cell adhesions. How epithelial cells maintain cell-to-cell adhesions and tissue integrity despite challenges imposed by the tissue environment is poorly understood. The small GTPase Rap1 has roles in cell polarity, cell-cell adhesion, and cell migration. In this dissertation I use the *Drosophila* ovary to investigate how Rap1 contributes to epithelial integrity and cell migration. *Drosophila* oogenesis provides a robust, genetically accessible model to study Rap1 function in epithelia. First, I utilize the *Drosophila* ovariole, a string of progressively developing egg chambers within the ovary, to understand how Rap1 contributes to epithelial integrity in a growing tissue. As oogenesis progresses, egg chambers elongate, which presents a challenge to the overlying follicular epithelium. I found that Rap1 was required to maintain tissue and cell shapes and promote cell viability during tissue elongation. Egg chambers deficient for Rap1 had distorted tissue shapes, stretched individual cells, and failed enrichment of the homophilic cell-cell adhesion protein E-Cadherin. Moreover, Rap1 deficient egg chambers lost follicle cells via apoptosis as indicated by an increase in caspase activity. These results support dual functions for Rap1 in promoting normal epithelial integrity and cell viability during tissue growth of the ovary. While Rap1 has numerous roles in development and disease, signaling partners that facilitate Rap1 function remain unclear. Therefore, I next used the *Drosophila* border cell model of collective cell migration to screen for potential Rap1 effectors required for migration. Border cell migration is a powerful *in vivo* model of collective cell migration. A group of four to six

migratory border cells, along with the central pair of organizing polar cells, migrate across the egg chamber to reach the oocyte. Border cells maintain adhesions to one and overall cluster polarity. Properly regulated Rap1 activity is essential for efficient migration. I used the strong border cell migration defects reported for constitutively active Rap1, $Rap1^{V12}$, to screen for X-chromosome deficiency regions that partially restored migration to the oocyte. I identified seven X-chromosome deficiencies that restored migration to $Rap1^{V12}$ expressing border cells. Furthermore, I mapped three of these regions to single genes, and report *fz4*, *Usp16-45*, and *sno* as candidate Rap1 interacting genes in border cell migration. Taken together these results demonstrate a requirement for Rap1 in epithelial integrity and cell viability during oogenesis and identify three candidate effectors that facilitate border cell migration. Results from this study are broadly relevant, as epithelial morphogenesis and collective cell migration are highly conserved features of metazoan development.

Table of Contents

List of Figures

List of Tables

Acknowledgements

First, I would like to thank my advisor, **Dr. Jocelyn McDonald** for her patience and indefatigable support. It is through her guidance that I have been able to attain the knowledge necessary to produce this document and continue my training as a developmental biologist. The availability she provides her trainees is unparalleled and it is her tireless attention to detail that has taught me to be a more rigorous scientist. This work was also guided by the generous support and commentary provided by my committee, **Drs. Erika Geisbrecht, Michael Veeman, and Anna Zinovyeva.**

I would like to thank all members of the McDonald lab that I had the benefit of knowing during my time at K-State. I was supported heavily by my fellow graduate students, Emily Burghardt and Nirupama Kotian, undergraduate trainees Manuel Garcia and Gibson Shaver, postdoctoral fellow Yujun Chen, and lab manager Kevin Preuss. I was supported intellectually by each of these people in a variety of ways. From intense scientific discussions in front of a whiteboard to simple chitchat or the classic "hey, will you fatten these bugs for me? I gotta run home." All these individuals were extremely helpful, and their contributions were essential to my sanity and producing this work.

Finally, I would like to thank the lifelong friends that I have acquired within the bounds of Chalmers Hall. Emily Burghardt, Berenice Jiménez Marín, Rue Lerma-Reyes, and Gabi Shipman. All of you are dynamite and I love each of you. To Emily Burghardt and Berenice Jiménez Marín I give special thanks for not letting me run away to work for the railroad as I threatened to do many times.

Dedication

I dedicate this work to my mothers, Betty Messer, and Angie Wilson. It is their love, hard work, and encouragement that made higher education possible for me. Thanks Mom and Angie for working so hard during my youth so I could focus on doing well in school. I know it wasn't easy raising me and I give you both so much credit for teaching me how to work hard and be a good person. I know that I'll always have the skills you've shown me to fall back on. I love y'all so much.

Chapter 1 - Introduction

Epithelial cells are the most common cell type found in animals. The three types of epithelial cells, squamous, cuboidal, and columnar, serve as the building blocks for sheets and tubes that shape the developing embryo, serve as protective barriers, and aid in wound healing (Blanpain and Fuchs, 2009; Honda, 2017; Tai et al., 2019). Epithelial cells have a couple distinctive properties. First, they are polarized, having three generalized domains: apical; lateral; and basal (Buckley and St Johnston, 2022). Discrete distribution of polarity proteins is essential for proper organization of cellular contents and management of cargoes (Buckley and St Johnston, 2022). Second, they form robust contacts with neighboring cells including a variety of specialized cell-cell junctions. Adherens junctions, septate or tight junctions, gap junctions, and desmosomes all have individualized roles in regulating cell-cell contacts (Broussard et al., 2020; Buckley and St Johnston, 2022; Goodenough and Paul, 2009; Vasquez et al., 2021).

Adherens junctions specifically allow the supracellular coordination of forces required for organized behaviors like apical constriction, invagination, intercalation, and collective migration (Perez-Vale and Peifer, 2020; Pinheiro and Bellaïche, 2018). Tissue and organ morphogenesis often requires dramatic epithelial rearrangements that must be accommodated across a group of cells. Intercellular coordination is a common theme throughout epithelial morphogenesis with each adherens junction serving as a critical mechanosensory link in the developmental chain (Fernandez-Gonzalez and Peifer, 2022; Hunter and Fernandez-Gonzalez, 2017; Perez-Vale and Peifer, 2020; Pinheiro and Bellaïche, 2018). How cells coordinate individual behaviors to achieve tissue level morphogenesis is an exciting area of study. This thesis will introduce and expand upon two primary areas of inquiry: 1. How do epithelia maintain integrity during tissue growth? 2. How do epithelia coordinate cell migrations?

This introductory chapter will explore conserved behaviors of epithelial cells required for development focusing on how cells maintain proper connections with one another in a changing tissue landscape. This foundation will provide a framework to discuss the roles of Rap1 GTPase in epithelial morphogenesis and migration. In the first section, apical constriction and intercalation are used to explore how small groups of cells facilitate tissue folding or extension. The second section focuses on interactions between neighboring tissue types using *Drosophila* dorsal closure and *Drosophila* follicle cell migration as examples. The third section provides a review of *Drosophila* border cell migration; an in-vivo model of collective cell migration. Section four introduces Rap1 GTPase and section five introduces *Drosophila* oogenesis as a model system and previews the work presented in Chapters 2 and 3.

1. Local progress: single cells and small groups shape tissue development

Embryogenesis, the journey from zygote to organism, involves a complex series of cell divisions, rearrangements, and migrations. Common epithelial cell behaviors underlie major tissue level changes shaping metazoan development (Salazar-Ciudad, 2010). This section will detail how two conserved cellular behaviors, apical constriction and intercalation affect tissue level change. This section of the introductory chapter will review the signaling events, cell shape changes, and intercellular linkages that epithelial cells use to achieve final form and function while maintaining proper tissue integrity.

1.1 Apical constriction: a conserved driver of cell and tissue shape modulation

Apical constriction is a highly conserved cellular behavior with the power to remodel entire epithelial sheets (Martin and Goldstein, 2014; Sawyer et al., 2010). From sea urchin gastrulation to neural tube formation in vertebrates, apical constriction is a common mechanism of epithelial sheet bending in development (Martin and Goldstein, 2014; Sawyer et al., 2010). Apical constriction is also required in diverse aspects of tissue maintenance. Apical constriction facilitates the epithelial-mesenchymal transition required in murine epiblast (Williams et al., 2012), contributes to the timely elimination of apoptotic corpses from epithelial layers (Slattum et al., 2009), and is an active component of wound closure (Davidson et al., 2002). This section will use a well-defined model of apical constriction, *Drosophila* ventral furrow formation, to discuss how apical constriction is initiated, the intracellular machinery required, and how apical constriction is linked to tissue morphogenesis.

1.1.1 Coordinated apical constrictions pattern the ventral furrow of Drosophila embryos

One of the most stereotypic examples of apical constriction occurs during *Drosophila* mesoderm invagination. Just as cellularization is completed within the ventral domain, cells within the blastoderm epithelium invaginate to form an internalized tube that eventually becomes the mesoderm germ layer (Gheisari et al., 2020; Sweeton et al., 1991). A stripe of cells initially 12-15 cells wide but quickly extending to 18 cells wide becomes visibly flattened in a pattern than overlaps with *twist* transcription factor expression, providing the first evidence of apical constriction (Fig. 1.1; Leptin and Grunewald, 1990; Sweeton et al., 1991). As cells in this stripe constrict apically, their nuclei move basally, and they lengthen their lateral domains along the apical-basal axis (Leptin, 1999; Leptin and Grunewald, 1990; Sweeton et al., 1991). Intriguingly,

cells just a few diameters away from the ventral midline do not undergo apical constriction, but rather lengthen their lateral domains towards the ventral furrow (Fox and Peifer, 2007; Fuse et al., 2013; Rauzi et al., 2015). These cells have lower levels of myosin contractility yet higher cortical tension and the local contractility gradient of the tissue likely facilitates tissue folding (Heer et al., 2017; Rauzi et al., 2015).

1.1.2 Genetic regulation controls actomyosin driven cell shape change

Apical constriction is governed by genetic regulation. Two early zygotic transcription factors, *twist* (*twi*) and *snail* (*sna*), are required for ventral furrow formation (Leptin and Grunewald, 1990). Both *twi* and *sna* are activated by Dorsal, but *twi* is required to maintain *sna* levels (Gheisari et al., 2020; Wong et al., 2014). *Twi* expression initiates a signaling cascade that drives apical constriction (Fig. 1.1 A). Downstream of *twi*, dorsoventral (DV) gradients of *transcript 48* (*t48*) and *folded gastrulation* (*fog*) are established through transcriptional timing starting first at the ventral midline and extending outward (Lim et al., 2017). Fog acts as a ligand for G-protein-coupled-receptors (GPCRs) Mist and Smog, which act through Concertina (Cta) to promote Rho1 activation via RhoGEF2 (Garcia De Las Bayonas et al., 2019; Kerridge et al., 2016; Manning et al., 2013; Parks and Wieschaus, 1991). T48 facilitates RhoGEF2 recruitment to the apical membrane (Kölsch et al., 2007; Lim et al., 2017). The Rho1 effector Rho Kinase (Rok) then phosphorylates and activates non-muscle myosin II (hereafter myosin) which provides the motor forces required for cell shape change (Fig. 1.1 A; Barrett et al., 1997; Dawes-Hoang et al., 2005).

A common theme in ventral furrow formation is the interplay between genetically encoded cellular behaviors and mechanical properties of the tissue. In *sna* mutants, for example, myosin typically fails to accumulate normally, and ventral furrow formation is impeded (Martin

et al., 2009). These defects can be rescued, however, by applying mechanical force on ventral cells, suggesting a dynamic relationship between genetic regulation and the biophysical properties of the tissue (Pouille et al., 2009). Indeed, closer examination of myosin activity reveals a more sophisticated mechanism than the textbook "purse string" model of apical constriction in tissue folding (Martin et al., 2010). In fact, two distinct pools of myosin activity are involved in apical constriction of cells in the ventral furrow. In addition to the myosin localized to adherens junctions (AJ), there is a medioapical pool of myosin that undergoes pulsatile contractions to constrict the apical cell surface (Fig. 1.1 B; Martin et al., 2009; Martin et al., 2010). These pulsatile contractions in conjunction with the AJ associated F-actin network drive apical constriction similarly to tightening a belt (Martin et al., 2009; Martin et al., 2010). Myosin contractility is followed by F-actin stabilization of cell diameter in a "ratcheting" type mechanism (Martin 2010). These mechanical properties of cellular behavior are governed ultimately by genetic encoding; *sna* is required to initiate the contraction, while *twi* stabilizes cell diameter (Martin et al., 2009).

1.1.3 AJs and actomyosin cables link single cell changes across the tissue

Actomyosin contractility can pull the apical cell membrane inward. As the apical domain of each cell decreases, the excess membrane generated must be removed to ensure efficient apical constriction and ventral furrow formation. This process is facilitated by the small GTPase Rab35, which in concert with Rab5, moves excess apical membrane to the Rab11 recycling endosome (Jewett et al., 2017; Miao et al., 2019). Thus, actomyosin contractility and cell ratcheting work together with members of the endocytic pathway to ensure mechanical force equals cell remodeling and shape change (Jewett et al., 2017; Miao et al., 2019).

Apical constriction of a single cell or group of cells would be unable to shape the local tissue environment without robust connections at AJs. AJs act as a relay mechanism linking the contractile forces generated in one cell to its neighbors providing regional tissue tension. Myosin organization also contributes to tissue tension. Myosin is retained at the cell cortex during the stabilization phase of apical constriction in a *twi*-dependent mechanism (Martin et al., 2010). Myosin maintained at the cell cortex is then assembled into supracellularly coupled myosin fibrils that allow transmission of forces generated at the cellular level across the tissue through dynamic coupling and uncoupling interactions between supracellular myosin and AJs that requires rapid turnover of F-actin (Jodoin et al., 2015; Martin et al., 2010). Efficient coupling of apically constricting cells to their neighbors at AJs drives the tissue folding observed in ventral furrow formation (Fig. 1.1 C; Martin et al., 2010).

1.2 Tissue elongation: intercalation drives epithelial lengthening

Apical constriction in a population of cells facilitates tissue folding. Similarly, intercalation of small groups of cells can drive tissue extension. Indeed, tissue elongation by intercalation is a common theme throughout developmental biology often helping develop the basic body plan of an animal or driving elongation of tube-like structures during organogenesis (Walck-Shannon and Hardin, 2014). Convergent extension in *Xenopus*, for example, facilitates elongation of the body axis while simultaneously closing the blastopore (Keller and Sutherland, 2020). Similarly, intercalation works to shape organ structure contributing to both elongation of trachea in *Drosophila* and development of vertebrate kidney and cochlea (Walck-Shannon and Hardin, 2014). Perhaps the best studied example of intercalation occurs during *Drosophila* gastrulation where a group of lateral cells within the blastoderm epithelium move posteriorly to increase the length of the embryo in a process called germband extension (Gheisari et al., 2020).

1.2.1 Pair-rule genes provide patterning required for polarized intercalation

During germband extension embryo length is increased along the anterior-posterior axis ~2.5 fold as width along the dorsal-ventral axis is halved (Campos-Ortega and Hartenstein, 1997; Irvine and Wieschaus, 1994). Polarized intercalation requires proper embryo patterning along the anterior-posterior axis. Mutations that disrupt anterior-posterior patterning have defective germband extension, while those causing patterning issues along the dorsoventral axis allow normal progression of germband extension (Irvine and Wieschaus, 1994). The pair-rule genes *even skipped* (*eve*) and *runt* (*run*) contribute directly to planar cell polarity helping enrich non-muscle myosin II (myosin) at anterior-posterior cell borders and Bazooka/PAR-3 at dorsoventral borders (Fig. 1.2 A; Irvine and Wieschaus, 1994; Zallen and Wieschaus, 2004).

A complete link between pair-rule gene expression and enrichment of cell surface proteins is poorly defined. The toll family receptor genes *toll-2*, *toll-6*, and *toll-8* are one set of targets linking pair-rule gene expression to myosin enrichment at the cell cortex. First, Toll-2, Toll-6, and Toll-8 are expressed in a pattern of transverse stripes across the anterior-posterior axis of the embryo that resembles pair-rule gene expression (Fig. 1.2 A; Paré et al., 2014; Paré et al., 2019) Single Toll mutants elongate normally, but targeting multiple Toll members simultaneously results in significant elongation defects. Thus, Toll-2, Toll-6, and Toll-8 have a combinatorial effect on germband extension (Paré et al., 2014). Triple Toll family receptor mutants have reduced intercalation and an inability to stabilize properly oriented cell to cell contacts upon cellular rearrangement (Paré et al., 2014). Furthermore, planar polarized myosin and Bazooka/Par3 were disrupted in these embryos positioning Toll receptor activity as one relay mechanism between pair-rule gene expression and the cellular machinery directly contributing to polarized intercalation (Fig. 1.2 A; Paré et al., 2014). Myosin polarity is partially retained at

compartment boundaries in Toll deficient embryos, however, suggesting an additional layer of polarity regulation. The transmembrane protein Tartan and its ligand, the teneurin Ten-m, work in parallel to Toll to coordinate planar polarity at epithelial compartment boundaries (Fig. 1.2 A; Paré et al., 2019). Further studies will be required to fully define the sophisticated regulatory system governing cellular polarity across the *Drosophila* embryo that allows successful intercalation in germband extension.

1.2.2 Actomyosin contractility drives the two types of intercalations observed in Drosophila germband extension

Pair-rule genes and downstream signaling components provide the genetic regulation required to properly polarize the *Drosophila* embryo in preparation for oriented intercalations. The mechanics required within a group of intercalating cells are still poorly understood. The two well-described types of intercalations observed during germband extension, T1 neighbor swapping and multicellular rosette resolution, both require modulation of adherens junctions driven by contractile myosin activity (Fig. 1.2 B-C; Gheisari et al., 2020). In T1 type transitions, tetrads of cells reorganize their adherens junctions, shrinking the initial contact between anterior-posterior cells to achieve a transition state, T2. In T2 equal contacts are shared amongst the four cells. The T2 transition state is resolved by forming a new junction orthogonal to the starting contact. This state is called T3 (Fig. 1.2 B; Bertet et al., 2004; Gheisari et al., 2020). Myosin is enriched along shrinking T1 junctions but appears only at low levels along newly formed T3 junctions suggesting an active role of myosin in junctional remodeling. Furthermore, inhibition of the myosin activator, Rho kinase (Rok), reveals defects in myosin recruitment and germband extension (Bertet et al., 2004). Successful progression from T1 to T3 states results in an

increased length along the anterior-posterior domain of 50% per resolved tetrad (Bertet et al., 2004).

The second type of intercalation, multicellular rosette resolution, occurs predominantly at stage 8 during the rapid phase of intercalation (Blankenship et al., 2006; Fernandez-Gonzalez et al., 2009). In this process, AJs from 2 to 8 linked anterior-posterior interfaces accumulate myosin in supracellular cables and collapse, forming rosettes ranging in size from 5 to 11 cells (Fig. 1.2 C; Blankenship et al., 2006; Fernandez-Gonzalez et al., 2009; Gheisari et al., 2020). Rosettes then resolve, creating new contacts between cells that had been 2-5 cell diameters apart along the dorsoventral axis. Cells that had once been anterior-posterior neighbors are separated and elongation occurs along the anterior-posterior direction of the embryo (Fig. 1.2 C; Blankenship et al., 2006; Gheisari et al., 2020). Actomyosin contractility is required to not only collapse linked AJs to form rosettes, but for the formation of new AJs as part of rosette resolution (Collinet et al., 2015; Yu and Fernandez-Gonzalez, 2016).

Dynamic myosin contractility is a key component of AJ remodeling during intercalation. Myosin flow towards vertical junctions causes them to shrink (Rauzi et al., 2010). AJ shrinkage, however, must be irreversible for efficient intercalation. Like apical constriction, this process requires removal of excess membrane components. The formin Diaphanous (Dia) and myosin are both required to initiate E-Cadherin endocytosis (Levayer et al., 2011). In addition, the small GTPase Rab35 localizes to spherical and tubular endomembrane compartments at shrinking vertical interfaces during germband extension (Jewett et al., 2017). Rab35 knockdown results in limited neighbor exchange (Jewett et al., 2017). Vertical contractions are followed by re-extension (Jewett et al., 2017). Thus, Rab35 may act as a molecular ratchet at vertical junctions

moving excess plasma membrane and associated proteins along to early endosomes (Jewett et al., 2017).

2. Community engagements: tissue interactions drive development

Tissue interactions involving multiple cell types are critical during development, immune responses, and tumor progression (Labernadie and Trepat, 2018). Large scale tissue-tissue interactions are conserved across animal development. Zebrafish epiboly, for example, involves the spreading of a squamous epithelial covering called the enveloping layer across the underlying yolk cell (Bruce, 2016). This process is driven by a contractile actomyosin ring within the yolk syncytial layer that provides the pulling force required to draw the enveloping layer over the developing embryo (Behrndt et al., 2012). Similarly, *C. elegans* epidermal cells migrate ventrally over neuroblasts during ventral enclosure (Chisholm and Hardin, 2005; Williams-Masson et al., 1997). Perhaps the best studied tissue-tissue interaction occurs between the lateral epidermis and central amnioserosa during *Drosophila* dorsal closure (Kiehart et al., 2017). The following section will explore epithelial behaviors at a tissue interface using *Drosophila* dorsal closure and egg chamber elongation as models. Extra emphasis will be placed upon cell-cell contacts both within the epithelial sheet and between epithelial sheets and neighboring tissues that allow for proper force coordination and successful morphogenesis.

2.1 Dorsal closure: neighboring cell types cooperatively seal the *Drosophila* embryo

During mid-embryogenesis the *Drosophila* germband consists of ventral, lateral, and dorsal epithelium with germband retraction leaving an eye-shaped epidermal gap in the dorsal domain. This dorsal hole is filled by a sheet of thin amnioserosa cells (Fig. 1.3 A; Hayes and Solon, 2017; Kiehart et al., 2017). These two cell types function together to ensure the successful sealing of the embryo. The squamous amnioserosa cells undergo pulsatile contractions while

each lateral epidermal cell sheet assembles actomyosin rich cables commonly referred to as "purse strings". Cumulatively the forces generated by each cell type result in stretching of the lateral epidermis dorsally until the two flanking edges meet and are sealed into a continuous epithelium by a purse string zipping mechanism (Kiehart et al., 2017).

2.1.1 Squamous amnioserosa undergo pulsed contractions and force generating apoptotic extrusion pulling epidermal sheets forward

Drosophila dorsal closure requires a unique balance of forces generated by two discrete tissues, the amnioserosa and the lateral epidermis. Prior to dorsal closure, germband retraction reveals the squamous amnioserosa that makes contact basally with the yolk cell (Fig. 1.3 A; Hayes and Solon, 2017; Narasimha and Brown, 2004). Integrin-mediated adhesion between the amnioserosa and the yolk cell contributes to efficient dorsal closure with the yolk likely providing stability to the thin amnioserosa (Kiehart et al., 2017; Narasimha and Brown, 2004). The squamous amnioserosa cells undergo pulsed oscillatory contractions driven by non-muscle myosin II (myosin) that function to draw flanking epidermal cells dorsally (Fig. 1.3 B; Hayes and Solon, 2017). Pulsed actomyosin contractions result in apical cell shape fluctuations that increase in frequency and decrease in magnitude as dorsal closure progresses (Blanchard et al., 2010). Both apical-medial and junctional fractions of myosin increased as dorsal closure progressed suggesting multiple pools of myosin activity are critical for amnioserosal contractions required for closure (Blanchard et al., 2010). Indeed, laser ablation experiments reveal similar recoil measurements when cells are wounded either at cell-cell junctions, or centrally, indicating a somewhat homogenous distribution of tension exists across the epithelial sheet (Ma et al., 2009). Importantly, integrin mediated cell-ECM anchoring is critical for dorsal closure. Integrin mutants have slower closure rates and it is thought that cell-substrate anchoring is required to

restrict cell motion and modulate force transmission across the amnioserosa (Goodwin et al., 2016).

In addition to generating forces for closure via contractile oscillations, cells within the amnioserosa are also required to timely exit the tissue to facilitate the advance of lateral epidermal cells (Kiehart et al., 2017). Amnioserosa ingression or extrusion was initially described as cells "dropping" out of the focal plane with early movies capturing the tendency of cells to leave the tissue. Neighboring cells then fill in for the departing members as the surface area of exposed amnioserosa continually decreases during closure (Hayes and Solon, 2017; Kiehart et al., 2000). These results were among the first to challenge older models suggesting that lateral cells simply crawl over static amnioserosa (Campos-Ortega and Hartenstein, 1997; Kiehart et al., 2000). Indeed, amnioserosa cells progressively ingress to facilitate closure with all cells eventually succumbing to apoptosis upon closure completion (Rodriguez-Diaz et al., 2008). Surprisingly, apoptosis serves both to remove cells, decreasing the distance between each side of the lateral epidermis, and actively contributes to the forces required for dorsal closure. Apoptotic cells within the amnioserosa cause deformations in neighboring cells as the apoptotic cell is cleared. Further experiments utilizing genetic modulation of the apoptotic pathway combined with laser ablation estimate that apoptosis accounts for about one-third of the force produced by the amnioserosa. Indeed, increasing the rate of apoptosis alone is sufficient to speed tissue closure (Toyama et al., 2008). Removal of apoptotic cells is essential, however, as evidenced by closure defects observed in mutants for the receptor tyrosine kinsae *Pvr*. These mutants have improper hemocyte function and visible debris associated with closure defects, suggesting inefficient clearance of apoptotic corpses (Garlena et al., 2015).

2.1.2 Actomyosin cables govern the dorsal advance of the lateral epidermis

While pulsatile contractions and apoptotic extrusion provide forces that draw flanking epidermal cells towards the dorsal midline, epidermal cells themselves must also be carefully managed for efficient closure (Fig. 1.4; Kiehart et al., 2017). At the outset of closure the dorsal opening accounts for about 40% of the circumference of the embryo when measured at the midpoint (Fig. 1.4 A; Campos-Ortega and Hartenstein, 1997). This opening is flanked by lateral epidermal cells that have a blunt interface with the amnioserosa at the anterior end and a rounded interface at the posterior (Fig. 1.4 A; Kiehart et al., 2000; Kiehart et al., 2017). While factors initiating closure are still being elucidated, closure begins when lateral epidermal sheets start moving towards the midline. Initially the leading edge the lateral epidermis is scalloped before being smoothed by actomyosin rich purse strings (Fig 1.4; Kiehart et al., 2000; Kiehart et al., 2017).

During dorsal closure, cells within the lateral epidermis elongate starting with the leading edge and extending back through further rows of cells as closure progresses (Young et al., 1993). As in the amnioserosa, proper cell shape in the lateral epidermis requires actomyosin contractility. Closure defects and misshapen cells in the leading edge are observed in *zipper* (*zip)* mutants, the *Drosophila* Myosin II, non-muscle myosin heavy chain (Young et al., 1993). Indeed, myosin localizes at the leading edge of both sheets of lateral epidermis forming contractile purse strings (Fig. 1.4 B; Kiehart et al., 2000).

How contractile actomyosin cables in the lateral epidermis contribute remains unclear. Mutants for the actin cytoskeleton protein Zasp52 fail to form actin cables in lateral epidermis, but still close as efficiently as wildtype controls (Ducuing and Vincent, 2016). These results were surprising and differ from prior reports that describe the purse strings as an essential force

generating component in closure (Hutson et al., 2003). This discrepancy may be explained by tissue robustness and the different techniques used for investigation. Laser ablation at the leading edge for instance likely influences both epidermal cells and underlying amnioserosa (Ducuing and Vincent, 2016). Another factor complicating analysis of force contribution required for closure is the likely compensatory nature of one tissue for the other. Laser ablation at the leading edge may increase contractility in amnioserosa (Hutson et al., 2003). *Zasp52* mutants that have laser ablated amnioserosa still complete closure suggesting the possibility that an additional force generating component contributes to the process (Ducuing and Vincent, 2016).

It is widely accepted however, that purse strings contribute to cell shape maintenance within the leading edge of lateral epidermal cells and an efficient zipping mechanism (Fig. 1.4 B; Ducuing and Vincent, 2016; Jacinto et al., 2002; Kiehart et al., 2017). Myosin is required to maintain cell shapes within the lateral epidermis (Young et al., 1993). Furthermore, actomyosin purse strings may be required to limit cell movement at the leading edge. Sections of epidermis with disrupted actomyosin cable contained cells that were more protrusive and gained a migration advantage over neighbors that were properly restrained by the purse string (Jacinto et al., 2002). In addition, both *zip* (myosin heavy chain) and *rho1* (a myosin regulator) mutants have puckering and segment misalignment at the completion of closure (Jacinto et al., 2002). Finally, Zasp52 was required for proper segment alignment further indicating a role for contractile purse strings in efficient closure perhaps through a coordinated cell-matching, zipping mechanism (Ducuing and Vincent, 2016).

2.1.3 Intercellular linkages ensure efficient force transmission and closure

The coordinated forces of closure require maintenance of cell-cell contacts between the amnioserosa and lateral epidermal cells as well as cell-cell adhesions between the constituent

cells of each tissue. As closure begins the amnioserosa-epidermal interface is adjusted slightly from an initial "equal" cell-cell contact perpendicular to the apical surface of the embryo to an overlap of reciprocal wedge-shaped cells with each epidermal cell at the leading edge overlaying the amnioserosa (Fig. 1.3 A; Narasimha and Brown, 2004). This tissue-tissue interaction is mediated by integrin-based adhesion. Integrin mutants fail to maintain proper contacts at the leading edge and have visible tissue rips during closure (Hutson et al., 2003; Narasimha and Brown, 2004). Similarly, E-Cadherin mutants sometimes fail to assemble actomyosin cables at the leading edge. These mutants have tears at the tissue interface and epidermal cells that fail to elongate (Gorfinkiel and Arias, 2007). Efficient closure is a marriage of tissue functions, coordinated at the leading edge, and relying on proper cell-cell contacts at the tissue interface (Ducuing and Vincent, 2016; Gorfinkiel and Arias, 2007; Hutson et al., 2003; Kiehart et al., 2017; Narasimha and Brown, 2004).

In addition to tissue-tissue interactions, cell-cell adhesions within each tissue are also of critical importance. Elegant experiments using laser ablation identify tissue-level tension in both the amnioserosa and lateral epidermal cells (Hutson et al., 2003; Kiehart et al., 2000). Tissue level tension requires efficient coupling of contractile cellular behaviors at AJs (Harris, 2012). Apoptosis in the amnioserosa contributes to efficient closure suggesting that apoptosis may be another source of local forces within the tissue (Toyama et al., 2008). Apoptotic forces facilitating closure likely require efficient coupling to neighboring cells via AJs (Harris, 2012; Toyama et al., 2008). Further efforts have uncovered some of the nuances required for force transmission across tissues that drive morphogenesis. The AJs actomyosin linker α-Catenin, for example, stabilizes E-Cadherin and regulates actomyosin dynamics in amnioserosa (Jurado et al.,

2016). Similarly, an adaptor protein, Girden, was identified as a regulator of AJs in closure (Houssin et al., 2015).

2.2 Under the sheet: centripetal follicle cell migration lays down a molecular corset constraining egg chamber growth

Heterotypic interactions that lead to shape changes in epithelial cells are not limited to the lateral epidermis of dorsal closure. Follicle cells of the *Drosophila* egg chamber are shaped by both an underlying, expanding germline and an overlying, constraining basement membrane. The *Drosophila* egg chamber is an emerging model of epithelial morphogenesis driven by tissue-tissue interactions. During oogenesis a string of progressively developing egg chambers buds off the stem-cell housing germarium. Each egg chamber consists of 16 germline cells encased in a continuous follicular epithelium. Egg chambers undergo a period of dramatic elongation during stages 5-10 of oogenesis changing from a spheroid to an ovoid shape (Fig. 1.5 A; Crest et al., 2017; Haigo and Bilder, 2011). Egg chamber elongation requires coordination of germline cell expansion along with follicle cell rotation that deposits a constricting basement membrane (Fig. 1.5; Cetera and Horne-Badovinac, 2015; Crest et al., 2017; McLaughlin and Bratu, 2015).

2.2.1 An atypical cadherin initiates cytoskeletal polarity to set up a unique, circuitous sheet migration

The *Drosophila* egg chamber has a continuous follicular epithelium that makes contact apically with the inner germline cells and basally with a basement membrane extracellular matrix (Fig. 1.5 B; Cetera and Horne-Badovinac, 2015; Cetera et al., 2014; Haigo and Bilder, 2011). Follicle cells migrate along the basal basement membrane as a continuous sheet perpendicular to the anterior-posterior axis of the egg chamber. Follicle cells maintain adhesions at the apical surface with germline cells and their migration causes the entire egg chamber to spin (Fig. 1.5 A;

Cetera and Horne-Badovinac, 2015; Cetera et al., 2014; Haigo and Bilder, 2011). Initially it was thought that follicle cell migration begins at stage 5 of oogenesis and ends at stage 9 (Haigo and Bilder, 2011). Migration begins much earlier however, starting soon after egg chamber formation at stage 1. Follicle cell migration is slow initially but speeds up at stage 6 (Cetera et al., 2014).

Follicle cells assemble both filopodia and lamellipodia which are common amongst other migrating cells (Cetera et al., 2014; Gardel et al., 2010; Ridley, 2011). Protrusions are restricted to one side of the cell with cells migrating in the direction of protrusions suggesting that follicle cell sheets have a leading edge (Cetera et al., 2014). Since follicle sheet migration can occur in both a clockwise and counterclockwise direction factors that initiate migration and contribute to its directionality are an open area of interest (Haigo and Bilder, 2011). The atypical cadherin, Fat2, is necessary to establish planar polarization of actin filaments during mid-oogenesis (Viktorinová et al., 2009). Actin polymerization, non-muscle myosin contractility, and microtubules are required for follicle cell migration and egg chamber rotation. Egg chamber rotation was dramatically perturbed by the addition of latrunculin A (actin inhibitor), Y-27632 (myosin inhibitor), or colchicine (microtubule inhibitor) (Viktorinová and Dahmann, 2013). Microtubules, similar to actin filaments align perpendicularly to the anterior-posterior axis of egg chambers during stages 4-8 and microtubule growth occurs in the opposite direction of egg chamber rotation. Furthermore, the atypical cadherin, Fat2, was required for microtubule alignment relative to the egg chamber with microtubules then helping restrict Fat2 to the lagging edge of follicle cells. These results suggest a feedback mechanism between microtubules and Fat2 controls rotation directionality (Viktorinová and Dahmann, 2013). Further analysis revealed an early alignment of microtubules in region 2b of the germarium suggesting that cytoskeletal elements are planar polarized in follicle cells before egg chamber formation and rotation (Chen

et al., 2016). Fat2 is required for microtubule growth bias and thus contributes to direction of rotation (Chen et al., 2016).

2.2.2 Follicle cell migration and secretion constructs a polarized basement membrane

The follicular epithelium is surrounded at its basal surface by a Collagen IV rich extracellular matrix that is organized into circumferentially planar polarized fibrils (Haigo and Bilder, 2011). Collagen fibrils increase in density during follicle cell migration. Clonal analysis using Collagen IV-GFP and a fluorescent follicle cell marker showed distance between source follicle cells and deposited collagen fibrils suggesting that follicle cells dispense collagen as they migrate (Haigo and Bilder, 2011). Interestingly, both actin and microtubules are planar polarized in follicle cells during migration running in the same direction as deposited collagen with rotation essential to maintaining tissue level actin alignment from stages 2-8 (Cetera et al., 2014; Chen et al., 2016; Haigo and Bilder, 2011; Viktorinová and Dahmann, 2013). Thus, follicle cell migration is linked to planar cell polarity and basement membrane deposition. Basement membranes are composed of about ~50% Collagen IV (Kalluri, 2003). Given the relationship between planar cell polarity, follicle cell migration, and Collagen IV deposition, a current area of research focuses on disentangling how follicle cell migration and planar cell polarity contribute to basement membrane deposition (Cetera et al., 2014; Chen et al., 2016; Haigo and Bilder, 2011; Viktorinová and Dahmann, 2013).

Both Collagen IV mRNAs, *Cg25C* and *vkg*, localize basally within follicle cells suggesting that basement membrane proteins are synthesized in a basal compartment of the endoplasmic reticulum (ER) (Lerner et al., 2013). The Tango1 cargo receptor facilitates Collagen IV exit from the ER with the small GTPase Rab10 helping guide protein deposition to the basal cell surface (Lerner et al., 2013). Interestingly, both Tango1 and Rab10 are planar polarized

suggesting that basement membrane deposition may be planar polarized basally as well as along the apical-basal axis (Lerner et al., 2013).

New work suggests the planar polarized microtubules that help orient follicle cell migration also play a role in basement membrane deposition (Chen et al., 2016; Viktorinová and Dahmann, 2013; Zajac and Horne-Badovinac, 2022). The polarity of microtubules along both the apical-basal and migratory axes of follicle cells make them prime candidates for basement membrane protein transport via the kinesin transport proteins Khc-73 and Khc (Zajac and Horne-Badovinac, 2022). Together these transporters move Rab10+ basement membrane protein vesicles to basal secretion sites where follicle cell migration helps integrate newly synthesized proteins into a growing basement membrane (Isabella and Horne-Badovinac, 2016; Zajac and Horne-Badovinac, 2022).

2.2.3 A basement membrane 'molecular corset' constrains germline expansion to shape the developing egg

Follicle cell migration shapes a robust basement membrane that is required for egg chamber elongation (Popkova et al., 2021). An early report comparing basement membrane laminin and F-actin distribution in wildtype egg chambers to a round egg mutant *kugel* found that *kugel* mutants had lost polarization of basement membrane components and led the authors to propose the basement membrane acts as a 'molecular corset' shaping egg chamber elongation (Gutzeit et al., 1991). Further studies have characterized many other mutants that disrupt planar cell polarity and have round egg chambers further reinforcing the link between planar polarized filaments in the basement membrane and successful egg chamber elongation (Bateman et al., 2001; Frydman and Spradling, 2001; Horne-Badovinac et al., 2012; Viktorinová et al., 2009). Not surprisingly, disrupting follicle cell migration, which is essential for basement membrane

deposition, results in egg chamber elongation defects (Cetera et al., 2014; Haigo and Bilder, 2011; Isabella and Horne-Badovinac, 2016; Viktorinová and Dahmann, 2013; Zajac and Horne-Badovinac, 2022).

Much of the dramatic egg chamber elongation observed during oogenesis takes place when the follicular epithelium is postmitotic from stages 6-9 (Fig. 1.5 A; Crest et al., 2017; Haigo and Bilder, 2011). During this period egg chamber elongation is patterned by differential basement membrane stiffness that together with isotropic germline expansion result in the transition from a spheroid to ovoid shaped egg chamber (Fig. 1.5; Crest et al., 2017). Atomic force microscopy (AFM) reveals that polar regions of basement membrane are less stiff than central regions at stages 7-8 (Fig. 1.5 C; Crest et al., 2017). Importantly, increasing basement membrane stiffness genetically resulted in more elongated egg chambers whereas decreasing stiffness produced rounder egg chambers underscoring the importance of stiffness in tissue patterning (Crest et al., 2017). Of the basement membrane components, Perlecan and Collagen IV make major contributions to elongation, while Laminin and Nidogen play more minor roles (Töpfer et al., 2022).

In addition to patterned basement membrane stiffness, regional differences in follicle cell contractility may also contribute to egg chamber elongation (Balaji et al., 2019). Main body follicle cells contacting nurse cells, for example, have increased medial myosin activity and greater junctional tension than follicle cells contacting the oocyte at stages 7 and 9 (Balaji et al., 2019). Contractility in follicle cells covering nurse cells was also critical to restrain nurse cell expansion. Reducing contractility in these cells resulted in nurse cells bulging at the basement membrane (Balaji et al., 2019). Therefore, follicle cell rotation assembles a constraining

basement membrane with regions of differential stiffness, that together with follicle cell contractility, patterns the ovoid shape of the developing egg chamber.

3. Collective cell migration: cell groups drive development and disease

Collective cell migrations are essential to major tissue remodeling events during embryogenesis, facilitate wound closure, and are a major mode of tumor metastasis (Friedl and Gilmour, 2009). Two examples of collective cell migration in *Drosophila* have already been covered in this introduction. See section 2.1 for collective migration of lateral epidermis during dorsal closure and section 2.2 for collective follicle cell migration during egg chamber elongation. Collective cell migration is highly conserved contributing to *Drosophila* embryogenesis, zebrafish lateral line development, and wound healing (Kiehart et al., 2017; Quirós and Nusrat, 2019; Thomas et al., 2015). Similarly, collective migration is a strategy utilized by a variety of cancers including breast cancer and glioblastoma (Serres et al., 2014; Wolf et al., 2007). Collective cell migration requires multicellular integration of guidance cues, coordination of force generating machinery, and maintenance of cell-cell contacts (Friedl and Gilmour 2009). This section will introduce one of the best studied in vivo models of collective cell migration, *Drosophila* border cell migration (Montell et al., 2012). This section will provide a general overview of the system, a description of signaling networks required for border cell fate specification, detachment and migration, and finish by exploring the mechanical components, including actomyosin rich protrusions and cell-cell linkages.

3.1 *Drosophila* border cells are an in vivo model of collective cell migration

Border cell migration begins after the specification and recruitment of 4-8 migratory border cells at late stage 8 to early stage 9 of oogenesis and is completed when border cells reach the oocyte boundary at stage 10 (Fig. 1.6 A; Saadin and Starz-Gaiano, 2016). For a more

complete review of *Drosophila* oogenesis see section 2.2 and McLaughlin and Bratu 2015. Once properly specified, border cells must detach from a basal lamina and migrate through a densely packed tissue microenvironment composed of germline derived nurse cells (Montell, 2003; Rørth, 2002). The border cell cluster develops front-back polarity in response to guidance cues secreted by the oocyte while maintaining apical-basal polarity characteristic of epithelial cells (Fig. 1.6; Montell, 2003; Montell et al., 2012). Cluster polarity helps restrict protrusion generation to the leading edge and encourages retraction at the lagging edge thereby ensuring efficient migration in the direction of the oocyte (Montell et al., 2012). Border cells maintain cell-cell contacts between each other, as well as with the non-motile, central polar cells they carry throughout the migration process (Fig. 1.6 B). The journey culminates at the oocyte where border cells help create the micropyle, a pore for sperm entry that is essential to fertility (Montell et al., 1992; Montell et al., 2012).

3.1.1 Specification cues and guidance signals control border cell specification, detatchment, and migration

Border cells start out identical to any of the other ~650 follicle cells in the developing egg chamber (Silver and Montell, 2001). A specialized group of cells called polar cells are formed during early during oogenesis and serve an organizer function to specify and recruit migratory border cells at stage 8 (Fig. 1.6 A; Nystul and Spradling 2010; Ruohola et al., 1991; Silver and Montell, 2001). Polar cells activate JAK/STAT signaling in neighboring cells by secreting the ligand unpaired (UPD). UPD then binds to the transmembrane receptor Domeless activating the tyrosine kinase JAK. JAK then phosphorylates both itself and Domeless, which allows STAT to bind, become phosphorylated, and dimerize. For a detailed review of JAK/STAT signaling see Herrera and Bach 2019. Activated STAT can then translocate to the nucleus and facilitate

transcription of target genes including the border cell fate determinant *slow border cells (slbo)* (Beccari et al., 2002; Ghiglione et al., 2002; Silver and Montell, 2001; Starz-Gaiano et al., 2008; Xi et al., 2003).

Selecting the appropriate number of border cells from the surrounding follicle cell population is critical as cluster size influences migration efficiency (Cai et al., 2016; Stonko et al., 2015). JAK/STAT signaling thus requires a sophisticated regulatory mechanism. The initially graded signal based upon the diffusible ligand UPD is further refined by Apontic (Apt) in conjunction with *Socs36E* and *miR-279* which together transform the graded signal into discrete on/off states in follicle cells (Monahan and Starz-Gaiano, 2013; Yoon et al., 2011). Follicle cells with high STAT activity will become migratory and leave the epithelium, while those with little to no STAT activity will stay behind (Montell et al., 2012; Saadin and Starz-Gaiano, 2016). Ectopic STAT activation is sufficient to induce extra migratory border cells (Silver and Montell 2001). Downstream of STAT and Slbo activation a suite of about 300 target genes are significantly upregulated in border cells, but further work is needed to determine the role each of these play (Borghese et al., 2006; Wang et al., 2006).

Interestingly, while border cells are fated at stage 8 via the JAK/STAT pathway, they do not begin migration until stage 9 (Montell et al., 2012, Saadin and Starz-Gaiano 2016). The insect steroid hormone Ecdysone rises during stages 8-9 and helps govern this process (Jang et al., 2009; Schwartz et al., 1989). Ecdysone activates a heterodimer of Ecdysone receptor (EcR) and Ultraspiracle (USP) that with the help of co-activator Taiman (Tai) initiate the starting signal for border cell migration (Bai et al., 2000; Montell et al., 2012; Saadin and Starz-Gaiano, 2016; Yao et al., 1993). How ecdysone signaling initiates border cell migration is still poorly understood, but one definitive target is E-Cadherin. E-Cadherin becomes abnormally elevated at

border cell-nurse cell interfaces in *tai* mutants suggesting that ecdysone signaling may be required for adhesion protein turnover important for migration (Bai et al., 2000).

Once the cluster has left the epithelium, migration is guided by external cues secreted primarily by the oocyte (Saadin and Starz-Gaiano 2016). Border cells express PVR, a receptor tyrosine kinase related to mammalian PDGF and VEGF receptors, and EGFR or epidermal growth factor receptor. PVR is activated by PVF1, PDGF and VEGF related factor 1, while EGFR is activated by Spitz, Keren, or Gurken. Gurken signal emanates specifically from the dorsal-anterior corner of the oocyte and helps to guide border cells dorsally as they complete migration (Figure 1.6 A; Duchek and Rørth, 2001; Duchek et al., 2001; McDonald et al., 2003; McDonald et al., 2006). Guidance cues help bias actin-rich protrusions, the force generating machinery of migration, toward the oocyte, but are not essential for protrusive activity (Prasad and Montell, 2007).

3.1.2 Regulated adhesion and actomyosin contractility are central to cluster locomotion

Cluster cohesion and polarity contribute to supracellular behaviors required for efficient migration (Montell et al., 2012). In addition to the leading-lagging edge polarity exhibited by the whole cluster, constituent cells of the border cell cluster maintain apical-basal polarity and cell-cell adhesions during migration (Fig. 1.6 B; Montell et al., 2012). Jun N-terminal kinase (JNK) signaling is one factor contributing to cluster cohesion during border cell migration. Loss of JNK activity in border cells resulted in migration defects with clusters that dissociated and had excess protrusive activity rather than the expected leader-follower dynamics (Llense and Martín-Blanco, 2008). Further analysis revealed that JNK depleted border cells lost polarity and had perturbed E-Cadherin enrichment (Llense and Martin-Blanco 2008). Direct inhibition of polarity determinants PAR3 and PAR6 also resulted in perturbed migration and adhesion defects

(Pinheiro and Montell, 2004). These reports underscore the importance of proper cellular polarity and adhesion in coordinated collective migration.

Cell-cell contacts are important to make sure no cells are lost along the journey, but also for organization of actomyosin rich protrusions. Cell-cell contacts are instructive for inside-outside polarity of the cluster with cell-cell adhesion molecules playing a fundamental role in the process (Montell et al., 2012). E-Cadherin is required for successful border cell migration and likely contributes to the contact dependent inhibition of protrusion observed in border cell migration (Cai et al., 2014; Niewiadomska et al., 1999). Protrusions form specifically at the border cell-nurse cell interface rather than at border cell-border cell contacts or border cell-polar cell contacts. Interestingly E-Cadherin is less enriched at the cluster cortex than in the interior and this adhesion differential may be instructive for protrusion generation (Montell et al., 2012). Furthermore, an E-Cadherin tension sensor reveals increased amounts of E-Cadherin under tension at the front of the cluster vs the rear. E-Cadherin also exhibits positive feedback on Rac that helps bias forward directed protrusions (Cai et al., 2014). Therefore, cell-cell contacts and adhesion molecules contribute to both cluster integrity and directed migration.

Actomyosin contractility contributes to robust protrusion generation. The Rho-family GTPase Rac induces protrusion formation at the leading edge of the border cell cluster (Fig. 1.6 B). This process is initiated upstream by the RTK, PVR, which when bound by PDGF/PVF1 factor activates Rac via the GFP exchange factor (GEF) Vav (Duchek et al., 2001; Fernández-Espartero et al., 2013; Saadin and Starz-Gaiano, 2016). Experiments utilizing a photoactivatable Rac (PA-Rac) revealed that Rac activation in a single cell was sufficient to generate protrusions in that cell that can steer the migration of the entire cluster (Wang et al., 2010). Myosin activity is required to limit ectopic protrusions and balance the contractile forces of the constricting nurse

cell tissue microenvironment. These roles are likely attributable to the supracellular organization of an actomyosin network that can relay information from one side of the cluster to the other (Aranjuez et al., 2016; Mishra et al., 2019; Wang et al., 2020). Efficient coupling of the actomyosin cytoskeleton to AJs is essential to the cell shape changes that typify morphogenesis (Perez-Vale and Peifer, 2020). Disrupting the AJs component E-Cadherin, or the AJs cytoskeleton linkers α-Catenin or β-Catenin all caused border cell clusters to fall apart during migration (Chen et al., 2020). Further work will be required to disentangle the complicated relationships between guidance signals that initiate cellular responses, individual cellular behaviors, and the coordination of information across all the cells in the cluster that cumulatively result in efficient migration.

4. GTPases: intracellular switches coordinating development and disease

Small GTPases are conserved molecular switches serving diverse roles in organisms ranging from budding yeast to higher mammals (Frische and Zwartkruis, 2010). GTPases benefit from a simple shared design and binary mode of activation. When bound to GTP, these molecules are active and participate in numerous downstream cellular activities but are inactive when bound by GDP. Small GTPases also possess an inherent GTP hydrolyzing activity which results in their inactivation (Bourne et al., 1991). Guanine nucleotide exchange factors (GEFs) and GTPase-activating proteins (GAPs) modulate GTPase activity. GEFs result in the exchange of GDP for GTP and thus activate GTPases. GAPs promote the fast hydrolysis of GTP to GDP and result in an inactive GTPase (Fig. 1.7; Bos et al., 2007). The Ras superfamily of GTPases can be divided into five sub-families together regulating cell behaviors including nuclear import/export, vesicle transport, cell shape changes, cell migration, and cell signaling and differentiation pathways (Bos et al., 2007). In addition to their roles in development, GTPases

contribute to tumorigenesis with Ras mutants occurring in 15% of all human tumors (Bos et al., 2007) This section will introduce the small GTPase Rap1 (Fig. 1.7), briefly cover a few examples of its activation in vivo, and discuss how common roles of Rap1 contribute to development and disease.

4.1 The small GTPase Rap1 is controlled by GAPs and GEFs

Rap1 has two isoforms with 95% identity, Rap1A and Rap1B (Wittchen et al., 2011). Rap1 has a CAAX motif at its C-terminus that accepts the posttranslational addition of a 20-carbon geranylgeranyl isoprenoid chain on the Cys residue that facilitates membrane targeting (Jaśkiewicz et al., 2018). A host of GAPs and GEFs regulate Rap1 activity and diverse downstream functions ranging from transmitting polarization cues in de novo epithelialization of murine epiblast to regulating motility of prostate cancer cells (Chinigò et al., 2022; Kim et al., 2022). GAPs and GEFs themselves are regulated upstream by a variety of signals that contribute to their activity, stability, or cellular distribution thereby enhancing or inhibiting their ability to activate Rap1 (Gloerich and Bos, 2011).

4.1.1 C3G and PDZ-GEF transmit upstream signals resulting in Rap1 function

The section will use C3G (RAPGEF1) and PDZ-GEF as examples to explore control of Rap1 function in vivo. For a more complete review of Rap1 family GAPs and GEFs see Gloerich and Bos 2011. C3G is a principle activating GEF for Rap1 contributing to functions ranging from platelet activation to T cell migration (Gutiérrez-Herrero et al., 2020; Huang et al., 2015). Like other GEFs, C3G can act as a relay mechanism between an extracellular signal and an intracellular response mediated by Rap1 activation (Gloerich and Bos 2011). In platelet activation, for example, thrombin induced ERK (extracellular-signal regulated kinase) activation results in downstream C3G phosphorylation (Gutierrez-Herrero et al., 2020). C3G activity was

essential for hemostasis with GEF inactive C3G transgenic mice having significantly longer bleeding times than sibling controls in tail-bleed assays (Gutiérrez-Herrero et al., 2012). A Rap1 activation assay in platelet-rich plasma revealed decreased Rap1-GTP levels in GEF inactive C3G platelets (Gutierrez-Herrero 2012). Together these results position C3G as a relay between extracellular thrombin activation and Rap1 activity essential for platelet function in mice (Gutierrez-Herrero et al., 2020, Gutierrez-Herrero et al., 2012). Similarly, C3G is required as a relay between cytokine activation of T cells and Rap1 activation required for adhesion-dependent chemotaxis (Huang et al., 2015). The adaptor proteins CRK/CRKL are required for C3G activation which likely promotes chemotaxis through the integrin regulatory functions of Rap1 (Huang et al., 2015).

PDZ-GEF also contributes to the diverse roles of Rap1. In zebrafish angiogenesis PDZ-GEF serves as an intermediary between Polo-like kinase 2 (PLK2) and Rap1 activation required for lamellipodia formation in endothelial tip cells (Yang et al., 2015). Many other functions of PDZ-GEF have been revealed by work in *Drosophila.* PDZ-GEF regulates Rap1 activity required for border cell migration (reviewed in section 3.1), but the factors upstream of PDZ-GEF remain unknown in this context (Sawant et al., 2018). Similarly, PDZ-GEF is required in ventral furrow formation during gastrulation and for zonula adherens formation in fly photoreceptors (Spahn et al., 2012; Walther et al., 2018). While context specific controls for GEF activity upstream are still being elucidated, GEFs are commonly regulated by secondary messengers. In addition, GEF domain architectures can promote GEF localization by specific binding activity with intracellular molecules (Gloerich and Bos 2011).

4.1.2 Rap1 dependent adhesion and motility are common contributors to many physiological roles

Adhesion regulation and cell migration are two well-known functions of Rap1 (Jaskiewicz et al., 2018). These two processes are linked, with important developmental consequences, as loss of adhesion is often a prerequisite for cell migrations including those associated with tumor dissemination (Cavallaro and Christofori, 2001; Friedl and Gilmour, 2009). Studies using invertebrate models provide the bulk of what we know about how Rap1-dependent adhesion contributes to development, including *Drosophila* ventral furrow formation and border cell migration (Chang et al., 2018; Sawant et al., 2018; Spahn et al., 2012). One of the best studied examples of how Rap1 functions in cell adhesion in higher mammals comes from studies on integrin activation in platelets and lymphocytes (Boettner and Van Aelst, 2009). Integrin alphaIIbbeta3, for example, is required in platelets for adhesion and aggregation in hemostasis (Shattil and Newman, 2004). During platelet activation Ca^{2+} signaling results in Rap1 dependent integrin activation (Franke et al., 1997; Han et al., 2006). The Rap1 effector RIAM (Rap1-GTP-interaction adaptor molecule) is thought to promote talin tethering that facilitates integrin activation (Boettner and Van Aelst 2009). Similarly, Rap1 promotes lymphocyte adhesion via RAPL dependent LFA-1 (Lymphocyte function-associated antigen 1, a lymphocyte integrin) redistribution at the leading edge (Katagiri et al., 2003).

Adhesion can be downregulated as part of the epithelial to mesenchymal transition or maintained between cells in collective migration (Canel et al., 2013; Friedl and Gilmour, 2009). Similarly, focal adhesions are critical for cell-ECM interactions in cell migrations (Doyle et al., 2022). It is difficult, therefore, to discuss functions of Rap1 in motility without partial overlap with adhesion. One role of Rap1 independent of its function in cell-substrate adhesion may be in

controlling actin-rich protrusion formation. Rap1 activity is required to form actin-rich protrusions in IGF1 (insulin-like growth factor type 1) sensitive MCF-7 cells (Guvakova et al., 2014). Cells overexpressing Rap1GAP1 had reduced Rap1 activity and failed to form actin rich stress fibers (Guvakova et al., 2014). Similarly, Rap1A knockdown reduced metastatic tumor nodules in a mouse model of esophageal squamous carcinoma (Li et al., 2019). These results point to a pro-migration role for Rap1 activity (Guvakova et al., 2014; Li et al., 2019). The opposite was observed, however, in hepatic stellate cells (HSCs) where Rap1 inhibition of RhoA was released upon TGF-β1 stimulation allowing cells to accumulate actin (Moon et al., 2019). Together these studies indicate a complex, context-specific relationship between Rap1 and cell migration with critical disease significance. How Rap1 regulates these processes as well as how Rap1 itself is regulated remains poorly understood. Current work in this field implicates Rap1 in diverse contexts ranging from wound healing to tension sensing (Freeman et al., 2017; Yoo et al., 2016).

5. Using *Drosophila* oogenesis to understand how Rap1 GTPase contributes to epithelial morphogenesis and collective cell migration

Epithelia are prevalent in the body's tissues and organs. They serve essential roles in wound healing, tissue homeostasis, and form a barrier against pathogens (Guillot and Lecuit, 2013; Leoni et al., 2015). Cells that undergo an improper epithelial-mesenchymal transition contribute to numerous types of cancer (Lai et al., 2020). It is critical therefore to understand how epithelial cells maintain connections with one another as they are challenged during development by tissue growth, cellular turnover, and insults from the microenvironment (Guillot and Lecuit 2013).

Similarly, understanding how epithelial cells break away from static environments and migrate is a challenge with clinical relevance. Collective cell migration is poorly understood relative to singly migrating cells and is a known mode of tumor dissemination (Friedl and Gilmour 2009). In this introductory Chapter I have outlined conserved epithelial behaviors during development using well known examples from *Drosophila.* The goal of this thesis is to investigate how the small GTPase Rap1 contributes to conserved cell behaviors in development and collective cell migration. Our lab typically uses the *Drosophila* model to investigate questions about collective cell migration. In this work I expand our studies of *Drosophila* oogenesis to investigate how Rap1 contributes to epithelial morphogenesis during tissue growth (Chapter 2) and perform an unbiased search for Rap1 effectors in *Drosophila* border cell migration (Chapter 3).

Key findings from this work include identifying a new role for Rap1 as a cell viability regulator required during tissue growth and three potential Rap1 effectors in border cell migration. The pro-survival function of Rap1 contributes to the proper assembly of the migratory border cell cluster. During border cell migration proper cycling of Rap1 activity states is required for efficient migration (Chang et al., 2018; Sawant et al., 2018). Making use of a constitutively active Rap1, $Rap1^{V12}$, with strong migration defects allowed for the unbiased screening of chromosomal deficiencies that suppressed Rap1 related migration defects. Here I report *sno, fz4,* and *Usp16-45* as genes genetically interacting with Rap1 in border cell migration.

Overall, these studies enhance our understanding of how Rap1 contributes to tissue integrity, cell viability, and cell migration. Tissue growth and cell migration are highly conserved features of metazoan development and make our findings relevant to other organisms. Our data support a role for Rap1 as an AJs actomyosin contractility linker that is necessary to maintain

epithelial integrity in tissues tested by dramatic growth. Moreover, our findings identify novel candidate partners for Rap1 function in border cell migration. Further work is required to fully define the mechanistic role of Rap1 at AJs and how potential Rap1 effectors coordinate migration.

6. Figures

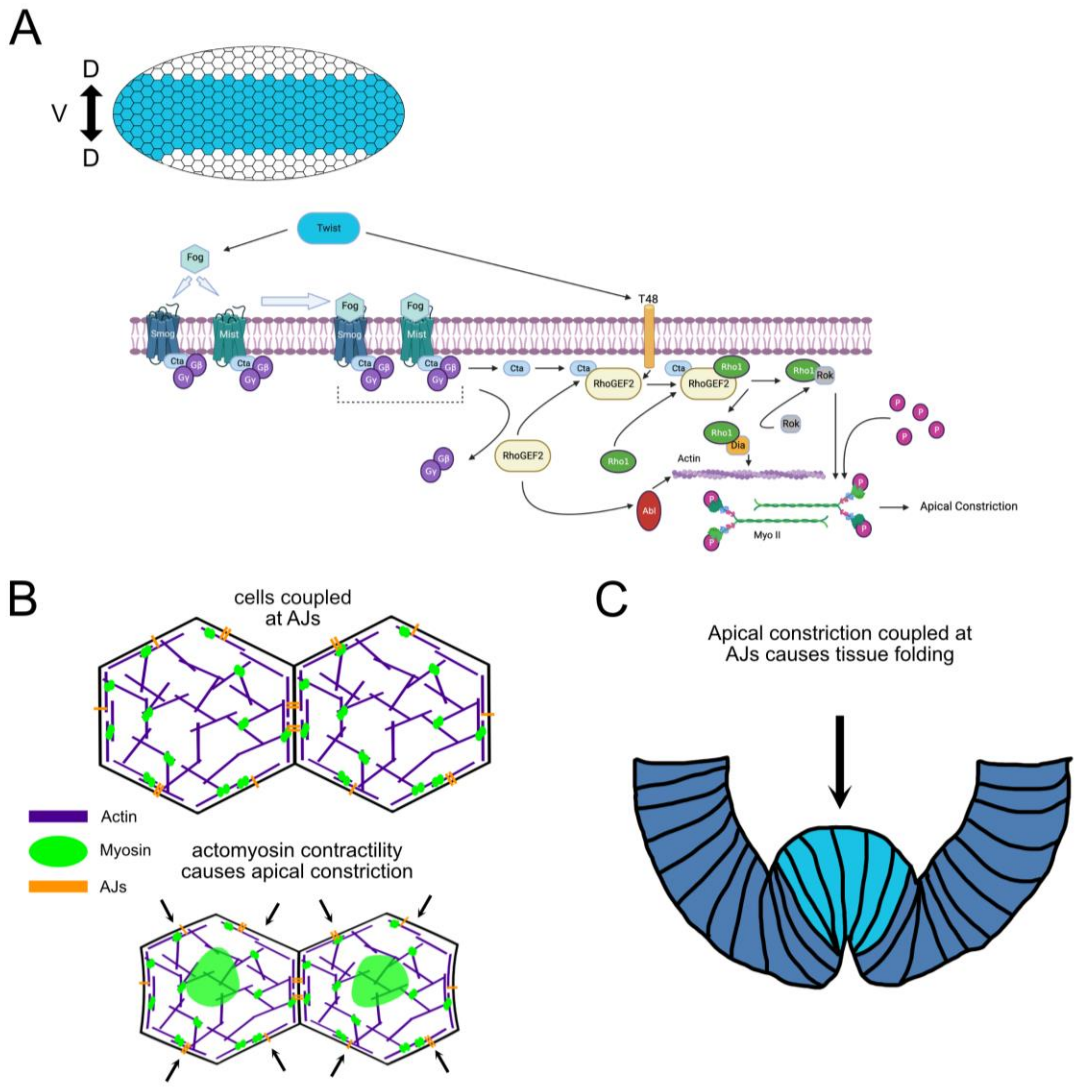

Figure 1.1 Apical constriction in *Drosophila* ventral furrow formation

A) Schematic indicating *twist* expression in the *Drosophila* embryo and the downstream signaling pathway leading to myosin activation. Signaling pathway created with Biorender.com. B) Apical constriction requires pulsatile actomyosin contractions at the medial apical cortex. Cells are linked at AJs. C) Schematic illustrating how apical constriction drives tissue bending to create the *Drosophila* ventral furrow. Apically constricting cells are colored light blue.

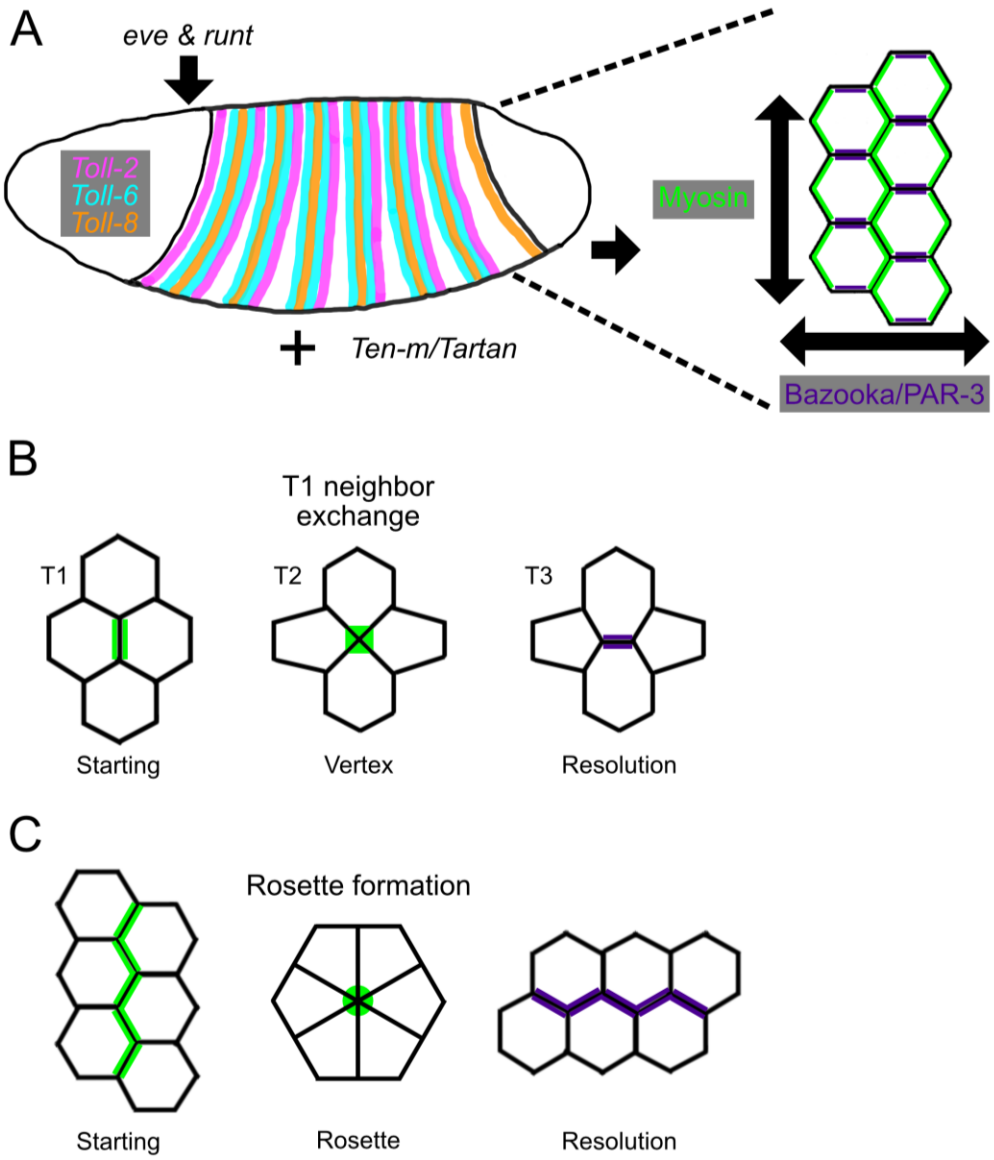

Figure 1.2 Segment polarity genes guide polarized intercalation

A) Segment polarity genes in conjunction with Toll family members and *Ten-m/Tartan* guide myosin localization at anterior posterior cell boundaries and Bazooka/PAR-3 localization at dorsoventral boundaries. Myosin in green. Bazooka/PAR-3 in purple. Right side of panel represents cell level zoom of embryo at left. B) T1 transition mode of intercalation. Cells swap neighbors extending along the anterior posterior axis. Myosin in green. Bazooka/PAR-3 in purple. C) Rosette formation mode of intercalation. Myosin contractility collapses a group of

cells into a rosette. The rosette is resolved extending the anterior posterior axis. Myosin in green. Bazooka/PAR-3 in purple.

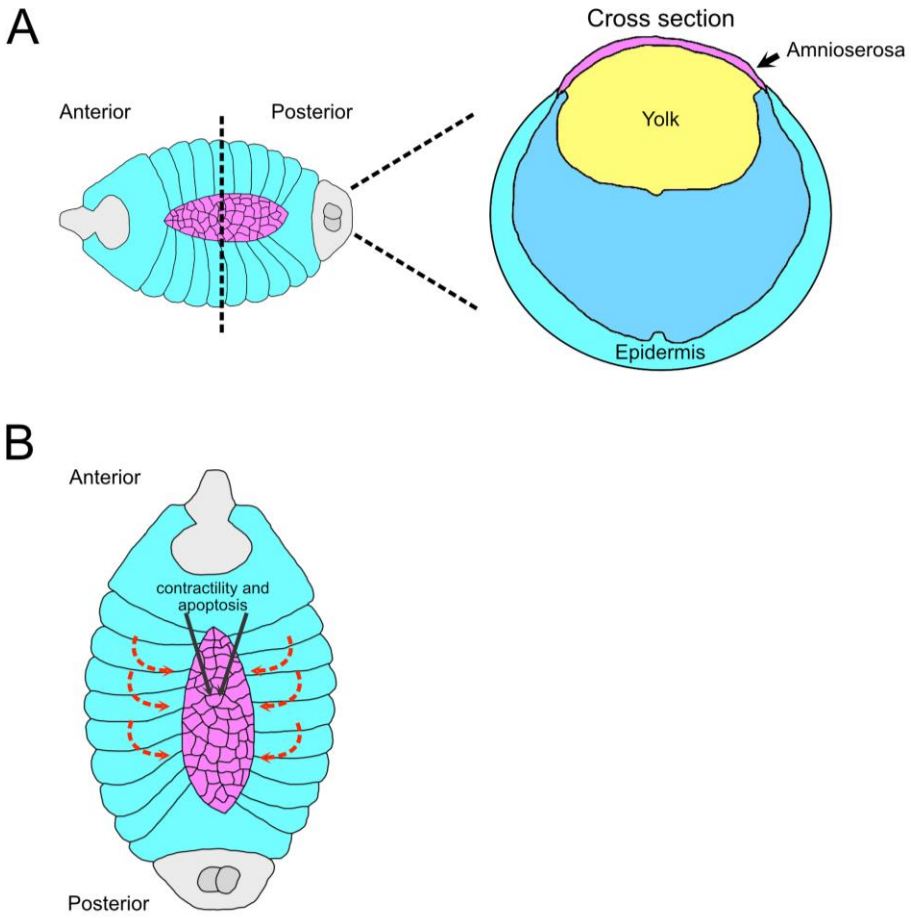

Figure 1.3 Actomyosin contractility and ingression within the aminoserosa facilitates closure

A) Embryo schematic (left) showing amnioserosa (pink) and lateral epidermis (cyan) during closure. Cross section (right) shows underlying yolk and amnioserosa-epidermis interface. B) Myosin contractility and apoptosis in amnioserosa draws lateral epidermis towards embryo center.

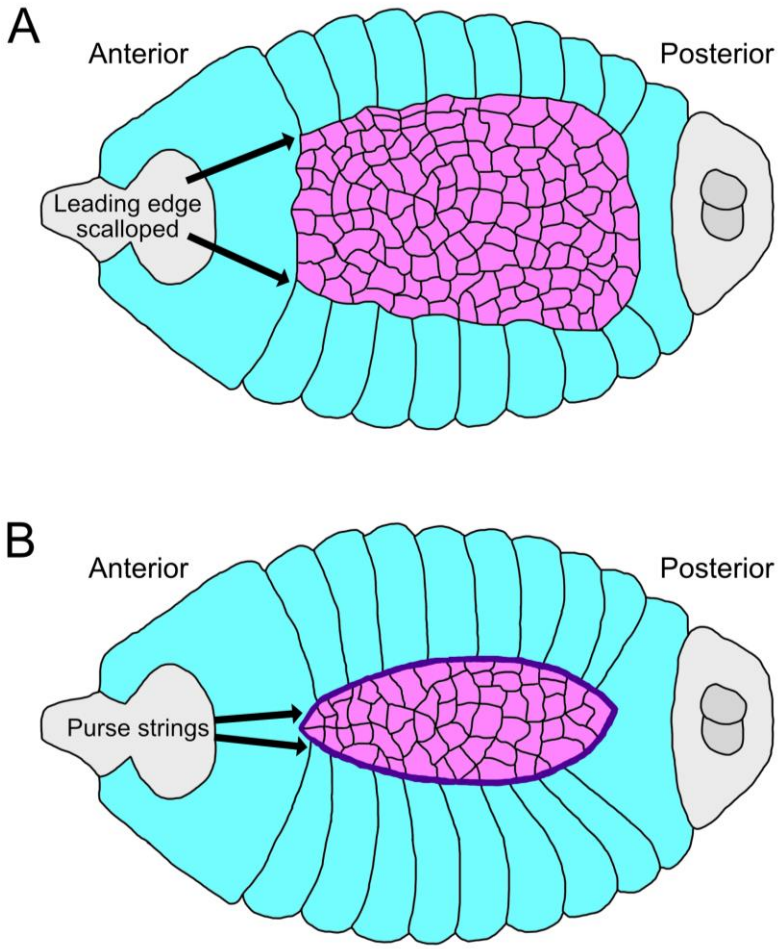

Figure 1.4 Actomyosin purse strings shape the leading edge for efficient closure

A) The lateral epidermis pictured in cyan has a scalloped leading edge at the outset of closure. Amnioserosa in pink. B) As closure progresses actomyosin purse strings (purple) are assembled that smooth the leading edge and contribute to zipping at the end stages of closure.

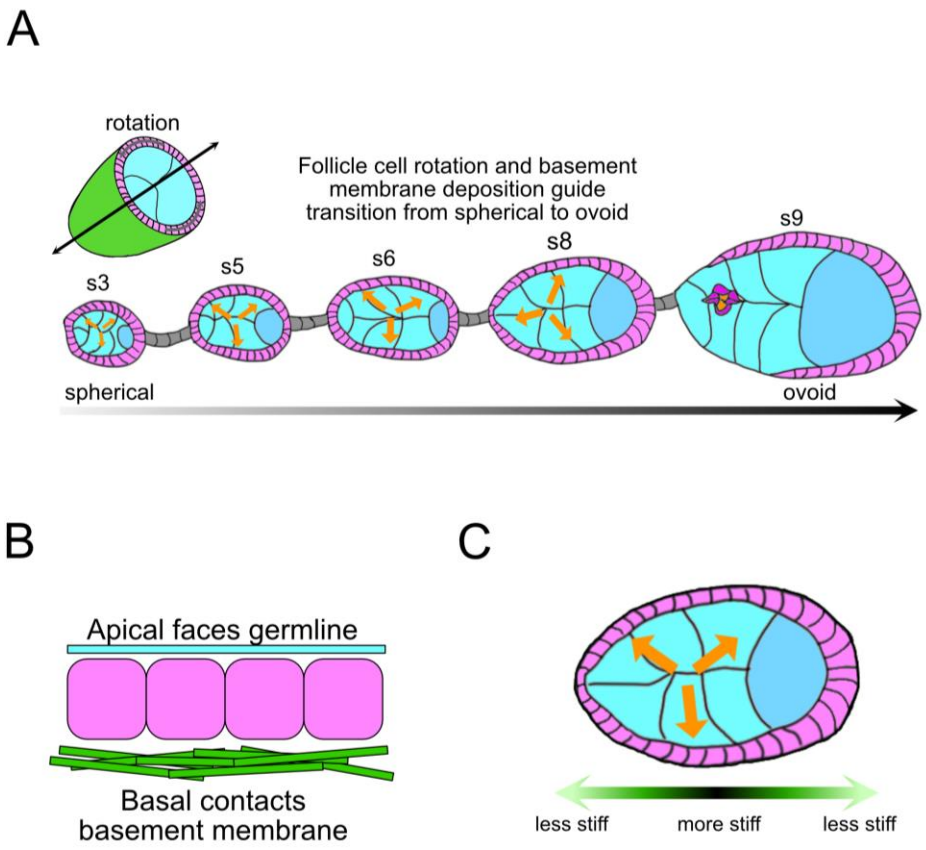

Figure 1.5 Follicle cell rotation builds a constricting basement membrane that contributes to egg chamber shape

A) Egg chamber section schematic (top). Follicle cells migrate spinning the egg chamber orthogonal to the anterior posterior axis. Follicle cells in pink. Ovariole schematic (bottom) shows the progression from spherical early-stage egg chambers to elliptical later stage egg chambers. Orange arrows indicate expansion of germline cells in cyan. B) Follicle cells in pink contact a basement membrane layer basally (green) and the germline (cyan) at the apical surface. C) Stage 8 egg chamber indicating the basement membrane stiffness gradient. Darker region of arrow near the center represents the stiffer region of basement membrane. Lighter colors at arrow ends indicate polar regions with relative lower stiffness.

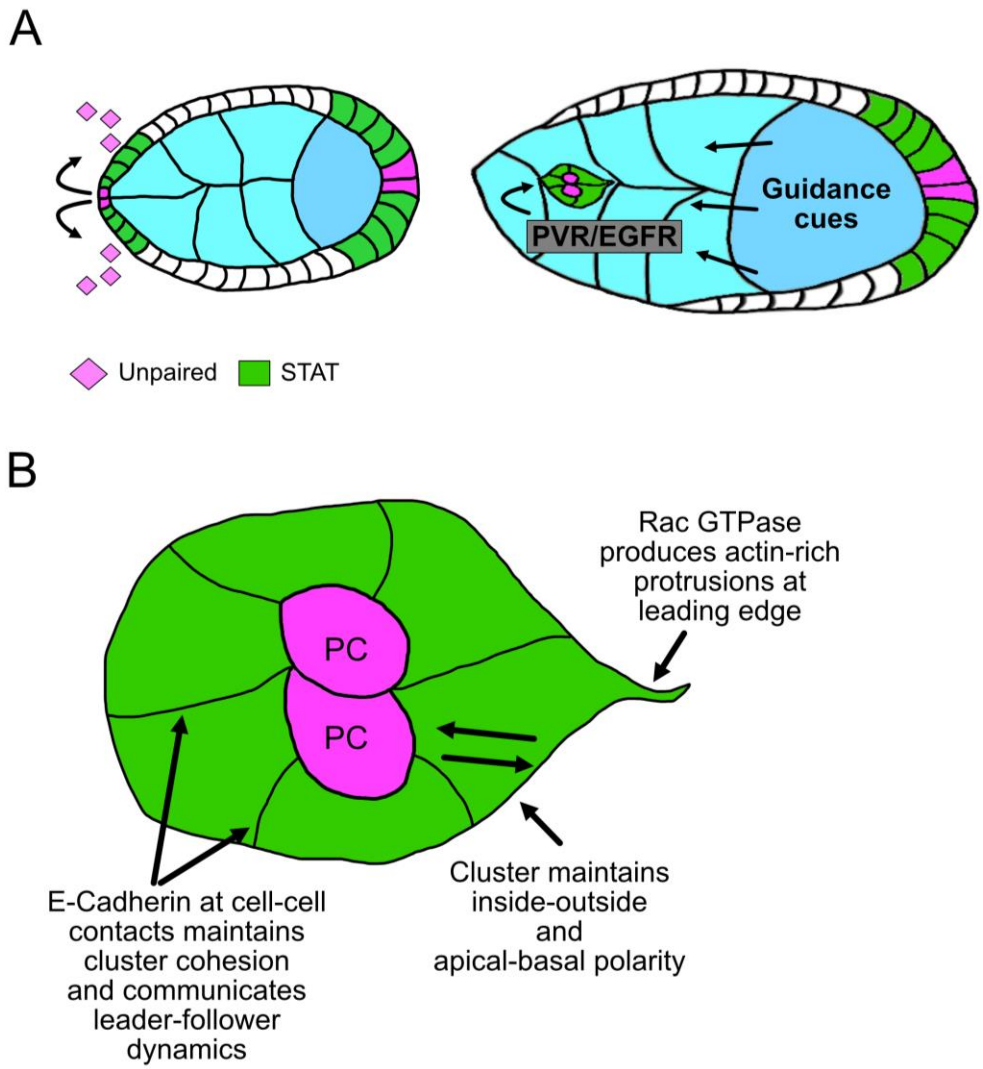

Figure 1.6 Border cell specification and migration requires the coordination of signaling pathways and cell to cell communication

A) Schematic depicting border cell fate specification and migration. Border cells are fated by JAK/STAT signaling. The polar cells (pink) secrete the ligand Unpaired (pink triangles) which results in local STAT activation (green). Once specified border cells rely on guidance cues secreted by germline cells to migrate towards the oocyte. B) Schematic of a migrating border cell cluster. Border cells (green) carry along non-motile polar cells (pink). Border cells generate actin

rich protrusions in the direction of migration, maintain apical-basal and inside-out polarity, and communicate leader-follower dynamics through E-Cadherin rich cell-cell adhesions.

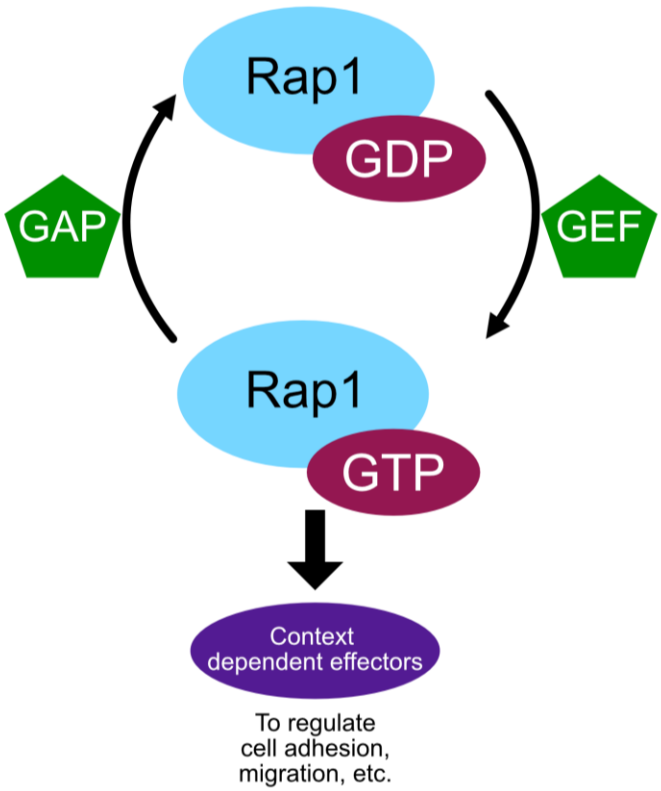

Figure 1.7 Rap1 GTPase activity contributes to cellular behaviors through unknown effectors

A) Schematic indicating the cyclical activity of Rap1 and other GTPases. GAPs result in the inactive GDP bound form, while GEFs result in the active GTP bound form. Once active Rap1 contributes to cell adhesion and migration through context dependent effector molecules.

7. References

Aranjuez, G., Burtscher, A., Sawant, K., Majumder, P. and McDonald, J. A. (2016). Dynamic myosin activation promotes collective morphology and migration by locally balancing oppositional forces from surrounding tissue. *Mol Biol Cell* **27**, 1898–1910.

Bai, J., Uehara, Y. and Montell, D. J. (2000). Regulation of Invasive Cell Behavior by Taiman, a Drosophila Protein Related to AIB1, a Steroid Receptor Coactivator Amplified in Breast Cancer. *Cell* **103**, 1047–1058.

Balaji, R., Weichselberger, V. and Classen, A.-K. (2019). Response of epithelial cell and tissue shape to external forces in vivo. *Development* dev.171256.

Barrett, K., Leptin, M. and Settleman, J. (1997). The Rho GTPase and a putative RhoGEF mediate a signaling pathway for the cell shape changes in Drosophila gastrulation. *Cell* **91**, 905–15.

Bateman, J., Reddy, R. S., Saito, H. and Van Vactor, D. (2001). The receptor tyrosine phosphatase Dlar and integrins organize actin filaments in the Drosophila follicular epithelium. *Current Biology* **11**, 1317–1327.

Beccari, S., Teixeira, L. and Rørth, P. (2002). The JAK/STAT pathway is required for border cell migration during Drosophila oogenesis. *Mechanisms of Development* **111**, 115–123.

Behrndt, M., Salbreux, G., Campinho, P., Hauschild, R., Oswald, F., Roensch, J., Grill, S. W. and Heisenberg, C.-P. (2012). Forces Driving Epithelial Spreading in Zebrafish Gastrulation. *Science* **338**, 257–260.

Bertet, C., Sulak, L. and Lecuit, T. (2004). Myosin-dependent junction remodelling controls planar cell intercalation and axis elongation. *Nature* **429**, 667–71.

Blanchard, G. B., Murugesu, S., Adams, R. J., Martinez-Arias, A. and Gorfinkiel, N. (2010). Cytoskeletal dynamics and supracellular organisation of cell shape fluctuations during dorsal closure. *Development* **137**, 2743–2752.

Blankenship, J. T., Backovic, S. T., Sanny, J. S. P., Weitz, O. and Zallen, J. A. (2006). Multicellular Rosette Formation Links Planar Cell Polarity to Tissue Morphogenesis. *Developmental Cell* **11**, 459–470.

Blanpain, C. and Fuchs, E. (2009). Epidermal homeostasis: a balancing act of stem cells in the skin. *Nature reviews. Molecular cell biology* **10**, 207–17.

Boettner, B. and Van Aelst, L. (2009). Control of cell adhesion dynamics by Rap1 signaling. *Curr Opin Cell Biol* **21**, 684–693.

Borghese, L., Fletcher, G., Mathieu, J., Atzberger, A., Eades, W. C., Cagan, R. L. and Rørth, P. (2006). Systematic analysis of the transcriptional switch inducing migration of border cells. *Developmental cell* **10**, 497–508.

Bos, J. L., Rehmann, H. and Wittinghofer, A. (2007). GEFs and GAPs: critical elements in the control of small G proteins. *Cell* **129**, 865–877.

Bourne, H. R., Sanders, D. A. and McCormick, F. (1991). The GTPase superfamily: conserved structure and molecular mechanism. *Nature* **349**, 117–127.

Broussard, J. A., Jaiganesh, A., Zarkoob, H., Conway, D. E., Dunn, A. R., Espinosa, H. D., Janmey, P. A. and Green, K. J. (2020). Scaling up single-cell mechanics to multicellular tissues - the role of the intermediate filament-desmosome network. *J Cell Sci* **133**, jcs228031.

Bruce, A. E. E. (2016). Zebrafish epiboly: Spreading thin over the yolk. *Developmental Dynamics* **245**, 244–258.

Buckley, C. E. and St Johnston, D. (2022). Apical–basal polarity and the control of epithelial form and function. *Nature Reviews Molecular Cell Biology* **23**, 559–577.

Cai, D., Chen, S. C., Prasad, M., He, L., Wang, X., Choesmel-Cadamuro, V., Sawyer, J. K., Danuser, G. and Montell, D. J. (2014). Mechanical feedback through E-cadherin promotes direction sensing during collective cell migration. *Cell* **157**,.

Cai, D., Dai, W., Prasad, M., Luo, J., Gov, N. S. and Montell, D. J. (2016). Modeling and analysis of collective cell migration in an in vivo three-dimensional environment. *Proceedings of the National Academy of Sciences of the United States of America* **113**, E2134–E2141.

Campos-Ortega, J. A. and Hartenstein, V. (1997). *The Embryonic Development of Drosophila melanogaster*. Berlin, Heidelberg: Springer Berlin Heidelberg.

Canel, M., Serrels, A., Frame, M. C. and Brunton, V. G. (2013). E-cadherin-integrin crosstalk in cancer invasion and metastasis. *J Cell Sci* **126**, 393–401.

Cavallaro, U. and Christofori, G. (2001). Cell adhesion in tumor invasion and metastasis: loss of the glue is not enough. *Biochimica et Biophysica Acta (BBA) - Reviews on Cancer* **1552**, 39–45.

Cetera, M. and Horne-Badovinac, S. (2015). Round and round gets you somewhere: collective cell migration and planar polarity in elongating Drosophila egg chambers. *Current Opinion in Genetics & Development* **32**, 10–15.

Cetera, M., Ramirez-San Juan, G. R., Oakes, P. W., Lewellyn, L., Fairchild, M. J., Tanentzapf, G., Gardel, M. L. and Horne-Badovinac, S. (2014). Epithelial rotation promotes the global alignment of contractile actin bundles during Drosophila egg chamber elongation. *Nature Communications* **5**, 5511–5511.

Chang, Y. C., Wu, J. W., Hsieh, Y. C., Huang, T. H., Liao, Z. M., Huang, Y. S., Mondo, J. A., Montell, D. and Jang, A. C. C. (2018). Rap1 Negatively Regulates the Hippo

Pathway to Polarize Directional Protrusions in Collective Cell Migration. *Cell Reports* **22**, 2160–2175.

Chen, D.-Y., Lipari, K. R., Dehghan, Y., Streichan, S. J. and Bilder, D. (2016). Symmetry Breaking in an Edgeless Epithelium by Fat2-Regulated Microtubule Polarity. *Cell reports* **15**, 1125–33.

Chen, Y., Kotian, N., Aranjuez, G., Chen, L., Messer, C. L., Burtscher, A., Sawant, K., Ramel, D., Wang, X. and McDonald, J. A. (2020). Protein phosphatase 1 activity controls a balance between collective and single cell modes of migration. *eLife* **9**,.

Chinigò, G., Grolez, G. P., Audero, M., Bokhobza, A., Bernardini, M., Cicero, J., Toillon, R.-A., Bailleul, Q., Visentin, L., Ruffinatti, F. A., et al. (2022). TRPM8-Rap1A Interaction Sites as Critical Determinants for Adhesion and Migration of Prostate and Other Epithelial Cancer Cells. *Cancers (Basel)* **14**, 2261.

Chisholm, A. D. and Hardin, J. (2005). Epidermal morphogenesis. *WormBook : the online review of C. elegans biology* 1–22.

Collinet, C., Rauzi, M., Lenne, P.-F. and Lecuit, T. (2015). Local and tissue-scale forces drive oriented junction growth during tissue extension. *Nature cell biology* **17**, 1247–58.

Crest, J., Diz-Muñoz, A., Chen, D.-Y., Fletcher, D. A. and Bilder, D. (2017). Organ sculpting by patterned extracellular matrix stiffness. *eLife* **6**,.

Davidson, L. A., Ezin, A. M. and Keller, R. (2002). Embryonic wound healing by apical contraction and ingression in Xenopus laevis. *Cell Motil Cytoskeleton* **53**, 163–176.

Dawes-Hoang, R. E., Parmar, K. M., Christiansen, A. E., Phelps, C. B., Brand, A. H. and Wieschaus, E. F. (2005). folded gastrulation , cell shape change and the control of myosin localization. *Development* **132**, 4165–4178.

Doyle, A. D., Nazari, S. S. and Yamada, K. M. (2022). Cell–extracellular matrix dynamics. *Phys. Biol.* **19**, 021002.

Duchek, P. and Rørth, P. (2001). Guidance of Cell Migration by EGF Receptor Signaling During Drosophila Oogenesis. *Science* **291**, 131–133.

Duchek, P., Somogyi, K., Jékely, G., Beccari, S. and Rørth, P. (2001). Guidance of Cell Migration by the Drosophila PDGF/VEGF Receptor. *Cell* **107**, 17–26.

Ducuing, A. and Vincent, S. (2016). The actin cable is dispensable in directing dorsal closure dynamics but neutralizes mechanical stress to prevent scarring in the Drosophila embryo. *Nature Cell Biology* **18**, 1149–1160.

Fernández-Espartero, C. H., Ramel, D., Farago, M., Malartre, M., Luque, C. M., Limanovich, S., Katzav, S., Emery, G. and Martín-Bermudo, M. D. (2013). GTP

exchange factor Vav regulates guided cell migration by coupling guidance receptor signalling to local Rac activation. *J Cell Sci* **126**, 2285–2293.

Fernandez-Gonzalez, R. and Peifer, M. (2022). Powering morphogenesis: multiscale challenges at the interface of cell adhesion and the cytoskeleton. *Molecular Biology of the Cell* **33**,.

Fernandez-Gonzalez, R., Simoes, S. de M., Röper, J.-C., Eaton, S. and Zallen, J. A. (2009). Myosin II dynamics are regulated by tension in intercalating cells. *Developmental cell* **17**, 736–43.

Fox, D. T. and Peifer, M. (2007). Abelson kinase (Abl) and RhoGEF2 regulate actin organization during cell constriction in Drosophila. *Development* **134**, 567–578.

Franke, B., Akkerman, J. W. and Bos, J. L. (1997). Rapid Ca2+-mediated activation of Rap1 in human platelets. *EMBO J* **16**, 252–259.

Freeman, S. A., Christian, S., Austin, P., Iu, I., Graves, M. L., Huang, L., Tang, S., Coombs, D., Gold, M. R. and Roskelley, C. D. (2017). Applied stretch initiates directional invasion through the action of Rap1 GTPase as a tension sensor. *J Cell Sci* **130**, 152–163.

Friedl, P. and Gilmour, D. (2009). Collective cell migration in morphogenesis, regeneration and cancer. *Nature Reviews Molecular Cell Biology* **10**, 445–457.

Frische, E. W. and Zwartkruis, F. J. T. (2010). Rap1, a mercenary among the Ras-like GTPases. *Dev Biol* **340**, 1–9.

Frydman, H. M. and Spradling, A. C. (2001). The receptor-like tyrosine phosphatase Lar is required for epithelial planar polarity and for axis determination with Drosophila ovarian follicles. *Development* **128**, 3209–3220.

Fuse, N., Yu, F. and Hirose, S. (2013). Gprk2 adjusts Fog signaling to organize cell movements in Drosophila gastrulation. *Development (Cambridge, England)* **140**, 4246–55.

Garcia De Las Bayonas, A., Philippe, J.-M., Lellouch, A. C. and Lecuit, T. (2019). Distinct RhoGEFs Activate Apical and Junctional Contractility under Control of G Proteins during Epithelial Morphogenesis. *Current Biology* **29**, 3370-3385.e7.

Gardel, M. L., Schneider, I. C., Aratyn-Schaus, Yvonne and Waterman, C. M. (2010). Mechanical Integration of Actin and Adhesion Dynamics in Cell Migration. *Annual Review of Cell and Developmental Biology* **26**, 315–333.

Garlena, R. A., Lennox, A. L., Baker, L. R., Parsons, T. E., Weinberg, S. M. and Stronach, B. E. (2015). The receptor tyrosine kinase Pvr promotes tissue closure by coordinating corpse removal and epidermal zippering. *Development (Cambridge, England)* **142**, 3403–15.

Gheisari, E., Aakhte, M. and Müller, H.-A. J. (2020). Gastrulation in Drosophila melanogaster: Genetic control, cellular basis and biomechanics. *Mechanisms of development* **163**, 103629–103629.

Ghiglione, C., Devergne, O., Georgenthum, E., Carballès, F., Médioni, C., Cerezo, D. and Noselli, S. (2002). The Drosophila cytokine receptor Domeless controls border cell migration and epithelial polarization during oogenesis. *Development* **129**, 5437–5447.

Gloerich, M. and Bos, J. L. (2011). Regulating Rap small G-proteins in time and space. *Trends in Cell Biology* **21**, 615–623.

Goodenough, D. A. and Paul, D. L. (2009). Gap junctions. *Cold Spring Harb Perspect Biol* **1**, a002576.

Goodwin, K., Ellis, S. J., Lostchuck, E., Zulueta-Coarasa, T., Fernandez-Gonzalez, R. and Tanentzapf, G. (2016). Basal Cell-Extracellular Matrix Adhesion Regulates Force Transmission during Tissue Morphogenesis. *Developmental Cell* **39**, 611–625.

Gorfinkiel, N. and Arias, A. M. (2007). Requirements for adherens junction components in the interaction between epithelial tissues during dorsal closure in Drosophila. *Journal of Cell Science* **120**, 3289–3298.

Guillot, C. and Lecuit, T. (2013). Mechanics of epithelial tissue homeostasis and morphogenesis. *Science (New York, N.Y.)* **340**, 1185–9.

Gutiérrez-Herrero, S., Maia, V., Gutiérrez-Berzal, J., Calzada, N., Sanz, M., González-Manchón, C., Pericacho, M., Ortiz-Rivero, S., González-Porras, J. R., Arechederra, M., et al. (2012). C3G transgenic mouse models with specific expression in platelets reveal a new role for C3G in platelet clotting through its GEF activity. *Biochim Biophys Acta* **1823**, 1366–1377.

Gutiérrez-Herrero, S., Fernández-Infante, C., Hernández-Cano, L., Ortiz-Rivero, S., Guijas, C., Martín-Granado, V., González-Porras, J. R., Balsinde, J., Porras, A. and Guerrero, C. (2020). C3G contributes to platelet activation and aggregation by regulating major signaling pathways. *Signal Transduct Target Ther* **5**, 29.

Gutzeit, H. O., Eberhardt, W. and Gratwohl, E. (1991). Laminin and basement membrane-associated microfilaments in wild-type and mutant Drosophila ovarian follicles. *Journal of Cell Science* **100**, 781–788.

Guvakova, M. A., Lee, W. S. Y., Furstenau, D. K., Prabakaran, I., Li, D. C., Hung, R. and Kushnir, N. (2014). The small GTPase Rap1 promotes cell movement rather than stabilizes adhesion in epithelial cells responding to insulin-like growth factor I. *Biochem J* **463**, 257–270.

Haigo, S. L. and Bilder, D. (2011). Global Tissue Revolutions in a Morphogenetic Movement Controlling Elongation. *Science* **331**, 1071–1074.

Han, J., Lim, C. J., Watanabe, N., Soriani, A., Ratnikov, B., Calderwood, D. A., Puzon-McLaughlin, W., Lafuente, E. M., Boussiotis, V. A., Shattil, S. J., et al. (2006). Reconstructing and deconstructing agonist-induced activation of integrin alphaIIbbeta3. *Curr Biol* **16**, 1796–1806.

Harris, T. J. C. (2012). Adherens junction assembly and function in the Drosophila embryo. *International review of cell and molecular biology* **293**, 45–83.

Hayes, P. and Solon, J. (2017). Drosophila dorsal closure: An orchestra of forces to zip shut the embryo. *Mechanisms of Development* **144**, 2–10.

Heer, N. C., Miller, P. W., Chanet, S., Stoop, N., Dunkel, J. and Martin, A. C. (2017). Actomyosin-based tissue folding requires a multicellular myosin gradient. *Development (Cambridge, England)* **144**, 1876–1886.

Herrera, S. C. and Bach, E. A. (2019). JAK/STAT signaling in stem cells and regeneration: from Drosophila to vertebrates. *Development* **146**, dev167643.

Honda, H. (2017). The world of epithelial sheets. *Develop. Growth Differ.* **59**, 306–316.

Horne-Badovinac, S., Hill, J., Gerlach, G., Menegas, W. and Bilder, D. (2012). A Screen for Round Egg Mutants in Drosophila Identifies Tricornered, Furry, and Misshapen as Regulators of Egg Chamber Elongation. *G3 Genes|Genomes|Genetics* **2**, 371–378.

Houssin, E., Tepass, U. and Laprise, P. (2015). Girdin-mediated interactions between cadherin and the actin cytoskeleton are required for epithelial morphogenesis in Drosophila. *Development (Cambridge, England)* **142**, 1777–84.

Huang, Y., Clarke, F., Karimi, M., Roy, N. H., Williamson, E. K., Okumura, M., Mochizuki, K., Chen, E. J. H., Park, T.-J., Debes, G. F., et al. (2015). CRK proteins selectively regulate T cell migration into inflamed tissues. *J Clin Invest* **125**, 1019–1032.

Hunter, M. V. and Fernandez-Gonzalez, R. (2017). Coordinating cell movements in vivo: junctional and cytoskeletal dynamics lead the way. *Curr Opin Cell Biol* **48**, 54–62.

Hutson, M. S., Tokutake, Y., Chang, M.-S., Bloor, J. W., Venakides, S., Kiehart, D. P. and Edwards, G. S. (2003). Forces for Morphogenesis Investigated with Laser Microsurgery and Quantitative Modeling. *Science* **300**, 145–149.

Irvine, K. D. and Wieschaus, E. (1994). Cell intercalation during Drosophila germband extension and its regulation by pair-rule segmentation genes. *Development (Cambridge, England)* **120**, 827–41.

Isabella, A. J. and Horne-Badovinac, S. (2016). Rab10-Mediated Secretion Synergizes with Tissue Movement to Build a Polarized Basement Membrane Architecture for Organ Morphogenesis. *Developmental Cell* **38**, 47–60.

Jacinto, A., Wood, W., Woolner, S., Hiley, C., Turner, L., Wilson, C., Martinez-Arias, A. and Martin, P. (2002). Dynamic Analysis of Actin Cable Function during Drosophila Dorsal Closure. *Current Biology* **12**, 1245–1250.

Jang, A. C.-C., Chang, Y.-C., Bai, J. and Montell, D. (2009). Border-cell migration requires integration of spatial and temporal signals by the BTB protein Abrupt. *Nature cell biology* **11**, 569–79.

Jaśkiewicz, A., Pająk, B. and Orzechowski, A. (2018). The Many Faces of Rap1 GTPase. *Int J Mol Sci* **19**, E2848.

Jewett, C. E., Vanderleest, T. E., Miao, H., Xie, Y., Madhu, R., Loerke, D. and Blankenship, J. T. (2017). Planar polarized Rab35 functions as an oscillatory ratchet during cell intercalation in the Drosophila epithelium. *Nature communications* **8**, 476–476.

Jodoin, J. N., Coravos, J. S., Chanet, S., Vasquez, C. G., Tworoger, M., Kingston, E. R., Perkins, L. A., Perrimon, N. and Martin, A. C. (2015). Stable Force Balance between Epithelial Cells Arises from F-Actin Turnover. *Developmental cell* **35**, 685–97.

Jurado, J., de Navascués, J. and Gorfinkiel, N. (2016). α-Catenin stabilises Cadherin-Catenin complexes and modulates actomyosin dynamics to allow pulsatile apical contraction. *Journal of Cell Science*.

Kalluri, R. (2003). Basement membranes: structure, assembly and role in tumour angiogenesis. *Nature Reviews Cancer* **3**, 422–433.

Katagiri, K., Maeda, A., Shimonaka, M. and Kinashi, T. (2003). RAPL, a Rap1-binding molecule that mediates Rap1-induced adhesion through spatial regulation of LFA-1. *Nat Immunol* **4**, 741–748.

Keller, R. and Sutherland, A. (2020). Convergent extension in the amphibian, Xenopus laevis. *Current topics in developmental biology* **136**, 271–317.

Kerridge, S., Munjal, A., Philippe, J.-M., Jha, A., de las Bayonas, A. G., Saurin, A. J. and Lecuit, T. (2016). Modular activation of Rho1 by GPCR signalling imparts polarized myosin II activation during morphogenesis. *Nature Cell Biology* **18**, 261–270.

Kiehart, D. P., Galbraith, C. G., Edwards, K. A., Rickoll, W. L. and Montague, R. A. (2000). Multiple Forces Contribute to Cell Sheet Morphogenesis for Dorsal Closure in Drosophila. *Journal of Cell Biology* **149**, 471–490.

Kiehart, D. P., Crawford, J. M., Aristotelous, A., Venakides, S. and Edwards, G. S. (2017). Cell Sheet Morphogenesis: Dorsal Closure in Drosophila melanogaster as a Model System. *Annual review of cell and developmental biology* **33**, 169–202.

Kim, Y. S., Fan, R., Lith, S. C., Dicke, A.-K., Drexler, H. C. A., Kremer, L., Kuempel-Rink, N., Hekking, L., Stehling, M. and Bedzhov, I. (2022). Rap1 controls epiblast

morphogenesis in sync with the pluripotency states transition. *Dev Cell* **57**, 1937-1956.e8.

Kölsch, V., Seher, T., Fernandez-Ballester, G. J., Serrano, L. and Leptin, M. (2007). Control of Drosophila gastrulation by apical localization of adherens junctions and RhoGEF2. *Science (New York, N.Y.)* **315**, 384–6.

Labernadie, A. and Trepat, X. (2018). Sticking, steering, squeezing and shearing: cell movements driven by heterotypic mechanical forces. *Current Opinion in Cell Biology* **54**, 57–65.

Lai, X., Li, Q., Wu, F., Lin, J., Chen, J., Zheng, H. and Guo, L. (2020). Epithelial-Mesenchymal Transition and Metabolic Switching in Cancer: Lessons From Somatic Cell Reprogramming. *Frontiers in Cell and Developmental Biology* **8**,.

Leoni, G., Neumann, P.-A., Sumagin, R., Denning, T. L. and Nusrat, A. (2015). Wound repair: role of immune–epithelial interactions. *Mucosal Immunology* **8**, 959–968.

Leptin, M. (1999). Gastrulation in Drosophila: the logic and the cellular mechanisms. *The EMBO journal* **18**, 3187–92.

Leptin, M. and Grunewald, B. (1990). Cell shape changes during gastrulation in Drosophila. *Development (Cambridge, England)* **110**, 73–84.

Lerner, D. W., McCoy, D., Isabella, A. J., Mahowald, A. P., Gerlach, G. F., Chaudhry, T. A. and Horne-Badovinac, S. (2013). A Rab10-Dependent Mechanism for Polarized Basement Membrane Secretion during Organ Morphogenesis. *Developmental Cell* **24**, 159–168.

Levayer, R., Pelissier-Monier, A. and Lecuit, T. (2011). Spatial regulation of Dia and Myosin-II by RhoGEF2 controls initiation of E-cadherin endocytosis during epithelial morphogenesis. *Nature cell biology* **13**, 529–40.

Li, Q., Xu, A., Chu, Y., Chen, T., Li, H., Yao, L., Zhou, P. and Xu, M. (2019). Rap1A promotes esophageal squamous cell carcinoma metastasis through the AKT signaling pathway. *Oncol Rep* **42**, 1815–1824.

Lim, B., Levine, M. and Yamazaki, Y. (2017). Transcriptional Pre-patterning of Drosophila Gastrulation. *Current biology : CB* **27**, 286–290.

Llense, F. and Martín-Blanco, E. (2008). JNK Signaling Controls Border Cell Cluster Integrity and Collective Cell Migration. *Current Biology* **18**, 538–544.

Ma, X., Lynch, H. E., Scully, P. C. and Hutson, M. S. (2009). Probing embryonic tissue mechanics with laser hole drilling. *Physical Biology* **6**, 036004–036004.

Manning, A. J., Peters, K. A., Peifer, M. and Rogers, S. L. (2013). Regulation of epithelial morphogenesis by the G protein-coupled receptor mist and its ligand fog. *Science signaling* **6**, ra98–ra98.

Martin, A. C. and Goldstein, B. (2014). Apical constriction: themes and variations on a cellular mechanism driving morphogenesis. *Development* **141**, 1987–1998.

Martin, A. C., Kaschube, M. and Wieschaus, E. F. (2009). Pulsed contractions of an actin-myosin network drive apical constriction. *Nature* **457**, 495–9.

Martin, A. C., Gelbart, M., Fernandez-Gonzalez, R., Kaschube, M. and Wieschaus, E. F. (2010). Integration of contractile forces during tissue invagination. *The Journal of cell biology* **188**, 735–49.

McDonald, J. A., Pinheiro, E. M. and Montell, D. J. (2003). PVF1, a PDGF/VEGF homolog, is sufficient to guide border cells and interacts genetically with Taiman. *Development* **130**, 3469–3478.

McDonald, J. A., Pinheiro, E. M., Kadlec, L., Schupbach, T. and Montell, D. J. (2006). Multiple EGFR ligands participate in guiding migrating border cells. *Developmental Biology* **296**, 94–103.

McLaughlin, J. M. and Bratu, D. P. (2015). Drosophila melanogaster Oogenesis: An Overview.pp. 1–20.

Miao, H., Vanderleest, T. E., Jewett, C. E., Loerke, D. and Blankenship, J. T. (2019). Cell ratcheting through the Sbf RabGEF directs force balancing and stepped apical constriction. *The Journal of cell biology* **218**, 3845–3860.

Mishra, A. K., Mondo, J. A., Campanale, J. P. and Montell, D. J. (2019). Coordination of protrusion dynamics within and between collectively migrating border cells by myosin II. *MBoC* **30**, 2490–2502.

Monahan, A. J. and Starz-Gaiano, M. (2013). Socs36E attenuates STAT signaling to optimize motile cell specification in the Drosophila ovary. *Developmental biology* **379**, 152–66.

Montell, D. J. (2003). Border-cell migration: the race is on. *Nature Reviews Molecular Cell Biology* **4**, 13–24.

Montell, D. J., Rorth, P. and Spradling, A. C. (1992). slow border cells, a locus required for a developmentally regulated cell migration during oogenesis, encodes Drosophila CEBP. *Cell* **71**, 51–62.

Montell, D. J., Yoon, W. H. and Starz-Gaiano, M. (2012). Group choreography: mechanisms orchestrating the collective movement of border cells. *Nature reviews. Molecular cell biology* **13**, 631–45.

Moon, M.-Y., Kim, H.-J., Kim, M.-J., Uhm, S., Park, J.-W., Suk, K.-T., Park, J.-B., Kim, D.-J. and Kim, S.-E. (2019). Rap1 regulates hepatic stellate cell migration through the modulation of RhoA activity in response to TGF-β1. *Int J Mol Med* **44**, 491–502.

Narasimha, M. and Brown, N. H. (2004). Novel Functions for Integrins in Epithelial Morphogenesis. *Current Biology* **14**, 381–385.

Niewiadomska, P., Godt, D. and Tepass, U. (1999). DE-Cadherin Is Required for Intercellular Motility during Drosophila Oogenesis. *Journal of Cell Biology* **144**, 533–547.

Nystul, T. and Spradling, A. (2010). Regulation of Epithelial Stem Cell Replacement and Follicle Formation in the Drosophila Ovary. *Genetics* **184**, 503–515.

Paré, A. C., Vichas, A., Fincher, C. T., Mirman, Z., Farrell, D. L., Mainieri, A. and Zallen, J. A. (2014). A positional Toll receptor code directs convergent extension in Drosophila. *Nature* **515**, 523–7.

Paré, A. C., Naik, P., Shi, J., Mirman, Z., Palmquist, K. H. and Zallen, J. A. (2019). An LRR Receptor-Teneurin System Directs Planar Polarity at Compartment Boundaries. *Developmental cell* **51**, 208-221.e6.

Parks, S. and Wieschaus, E. (1991). The drosophila gastrulation gene concertina encodes a Gα-like protein. *Cell* **64**, 447–458.

Perez-Vale, K. Z. and Peifer, M. (2020). Orchestrating morphogenesis: building the body plan by cell shape changes and movements. *Development* **147**,.

Pinheiro, D. and Bellaïche, Y. (2018). Mechanical Force-Driven Adherens Junction Remodeling and Epithelial Dynamics. *Developmental Cell* **47**, 3–19.

Pinheiro, E. M. and Montell, D. J. (2004). Requirement for Par-6 and Bazooka in Drosophila border cell migration. *Development* **131**, 5243–5251.

Popkova, A., Rauzi, M. and Wang, X. (2021). Cellular and Supracellular Planar Polarity: A Multiscale Cue to Elongate the Drosophila Egg Chamber. *Frontiers in Cell and Developmental Biology* **9**,.

Pouille, P.-A., Ahmadi, P., Brunet, A.-C. and Farge, E. (2009). Mechanical signals trigger Myosin II redistribution and mesoderm invagination in Drosophila embryos. *Science signaling* **2**, ra16–ra16.

Prasad, M. and Montell, D. J. (2007). Cellular and Molecular Mechanisms of Border Cell Migration Analyzed Using Time-Lapse Live-Cell Imaging. *Developmental Cell* **12**, 997–1005.

Quirós, M. and Nusrat, A. (2019). Contribution of Wound-Associated Cells and Mediators in Orchestrating Gastrointestinal Mucosal Wound Repair. *Annual review of physiology* **81**, 189–209.

Rauzi, M., Lenne, P.-F. and Lecuit, T. (2010). Planar polarized actomyosin contractile flows control epithelial junction remodelling. *Nature* **468**, 1110–4.

Rauzi, M., Krzic, U., Saunders, T. E., Krajnc, M., Ziherl, P., Hufnagel, L. and Leptin, M. (2015). Embryo-scale tissue mechanics during Drosophila gastrulation movements. *Nature communications* **6**, 8677–8677.

Ridley, A. J. (2011). Life at the Leading Edge. *Cell* **145**, 1012–1022.

Rodriguez-Diaz, A., Toyama, Y., Abravanel, D. L., Wiemann, J. M., Wells, A. R., Tulu, U. S., Edwards, G. S. and Kiehart, D. P. (2008). Actomyosin purse strings: Renewable resources that make morphogenesis robust and resilient. *HFSP Journal* **2**, 220–237.

Rørth, P. (2002). Initiating and guiding migration: lessons from border cells. *Trends in Cell Biology* **12**, 325–331.

Ruohola, H., Bremer, K. A., Baker, D., Swedlow, J. R., Jan, L. Y. and Jan, Y. N. (1991). Role of neurogenic genes in establishment of follicle cell fate and oocyte polarity during oogenesis in Drosophila. *Cell* **66**, 433–449.

Saadin, A. and Starz-Gaiano, M. (2016). Circuitous Genetic Regulation Governs a Straightforward Cell Migration. *Trends in Genetics* **32**, 660–673.

Salazar-Ciudad, I. (2010). Morphological evolution and embryonic developmental diversity in metazoa. *Development* **137**, 531–539.

Sawant, K., Chen, Y., Kotian, N., Preuss, K. M. and McDonald, J. A. (2018). Rap1 GTPase promotes coordinated collective cell migration in vivo. *Molecular Biology of the Cell* **29**, 2656–2673.

Sawyer, J. M., Harrell, J. R., Shemer, G., Sullivan-Brown, J., Roh-Johnson, M. and Goldstein, B. (2010). Apical constriction: a cell shape change that can drive morphogenesis. *Dev Biol* **341**, 5–19.

Schwartz, M. B., Kelly, T. J., Woods, C. W. and Imberski, R. B. (1989). Ecdysteroid fluctuations in adult Drosophila melanogaster caused by elimination of pupal reserves and synthesis by early vitellogenic ovarian follicles. *Insect biochemistry (USA)*.

Serres, E., Debarbieux, F., Stanchi, F., Maggiorella, L., Grall, D., Turchi, L., Burel-Vandenbos, F., Figarella-Branger, D., Virolle, T., Rougon, G., et al. (2014). Fibronectin expression in glioblastomas promotes cell cohesion, collective invasion of basement membrane in vitro and orthotopic tumor growth in mice. *Oncogene* **33**, 3451–3462.

Shattil, S. J. and Newman, P. J. (2004). Integrins: dynamic scaffolds for adhesion and signaling in platelets. *Blood* **104**, 1606–1615.

Silver, D. L. and Montell, D. J. (2001). Paracrine Signaling through the JAK/STAT Pathway Activates Invasive Behavior of Ovarian Epithelial Cells in Drosophila. *Cell* **107**, 831–841.

Slattum, G., McGee, K. M. and Rosenblatt, J. (2009). P115 RhoGEF and microtubules decide the direction apoptotic cells extrude from an epithelium. *J Cell Biol* **186**, 693–702.

Spahn, P., Ott, A. and Reuter, R. (2012). The PDZ-GEF protein Dizzy regulates the establishment of adherens junctions required for ventral furrow formation in Drosophila. *Journal of cell science* **125**, 3801–12.

Starz-Gaiano, M., Melani, M., Wang, X., Meinhardt, H. and Montell, D. J. (2008). Feedback Inhibition of JAK/STAT Signaling by Apontic Is Required to Limit an Invasive Cell Population. *Developmental Cell* **14**, 726–738.

Stonko, D. P., Manning, L., Starz-Gaiano, M. and Peercy, B. E. (2015). A mathematical model of collective cell migration in a three-dimensional, heterogeneous environment. *PLoS ONE* **10**,.

Sweeton, D., Parks, S., Costa, M. and Wieschaus, E. (1991). Gastrulation in Drosophila: the formation of the ventral furrow and posterior midgut invaginations. *Development (Cambridge, England)* **112**, 775–89.

Tai, K., Cockburn, K. and Greco, V. (2019). Flexibility sustains epithelial tissue homeostasis. *Current opinion in cell biology* **60**, 84–91.

Thomas, E. D., Cruz, I. A., Hailey, D. W. and Raible, D. W. (2015). There and back again: development and regeneration of the zebrafish lateral line system. *Wiley Interdisciplinary Reviews: Developmental Biology* **4**, 1–16.

Töpfer, U., Guerra Santillán, K. Y., Fischer-Friedrich, E. and Dahmann, C. (2022). Distinct contributions of ECM proteins to basement membrane mechanical properties in Drosophila. *Development* **149**,.

Toyama, Y., Peralta, X. G., Wells, A. R., Kiehart, D. P. and Edwards, G. S. (2008). Apoptotic force and tissue dynamics during Drosophila embryogenesis. *Science (New York, N.Y.)* **321**, 1683–6.

Vasquez, C. G., de la Serna, E. L. and Dunn, A. R. (2021). How cells tell up from down and stick together to construct multicellular tissues - interplay between apicobasal polarity and cell-cell adhesion. *J Cell Sci* **134**, jcs248757.

Viktorinová, I. and Dahmann, C. (2013). Microtubule Polarity Predicts Direction of Egg Chamber Rotation in Drosophila. *Current Biology* **23**, 1472–1477.

Viktorinová, I., König, T., Schlichting, K. and Dahmann, C. (2009). The cadherin Fat2 is required for planar cell polarity in the Drosophila ovary. *Development* **136**, 4123–4132.

Walck-Shannon, E. and Hardin, J. (2014). Cell intercalation from top to bottom. *Nature reviews. Molecular cell biology* **15**, 34–48.

Walther, R. F., Burki, M., Pinal, N., Rogerson, C. and Pichaud, F. (2018). Rap1, Canoe and Mbt cooperate with Bazooka to promote zonula adherens assembly in the fly photoreceptor. *Journal of cell science* **131**,.

Wang, X., Bo, J., Bridges, T., Dugan, K. D., Pan, T., Chodosh, L. A. and Montell, D. J. (2006). Analysis of cell migration using whole-genome expression profiling of migratory cells in the Drosophila ovary. *Dev Cell* **10**, 483–495.

Wang, X., He, L., Wu, Y. I., Hahn, K. M. and Montell, D. J. (2010). Light-mediated activation reveals a key role for Rac in collective guidance of cell movement in vivo. *Nat Cell Biol* **12**, 591–597.

Wang, H., Guo, X., Wang, X., Wang, X. and Chen, J. (2020). Supracellular Actomyosin Mediates Cell-Cell Communication and Shapes Collective Migratory Morphology. *iScience* **23**, 101204.

Williams, M., Burdsal, C., Periasamy, A., Lewandoski, M. and Sutherland, A. (2012). Mouse primitive streak forms in situ by initiation of epithelial to mesenchymal transition without migration of a cell population. *Dev Dyn* **241**, 270–283.

Williams-Masson, E. M., Malik, A. N. and Hardin, J. (1997). An actin-mediated two-step mechanism is required for ventral enclosure of the C. elegans hypodermis. *Development* **124**, 2889–2901.

Wittchen, E. S., Aghajanian, A. and Burridge, K. (2011). Isoform-specific differences between Rap1A and Rap1B GTPases in the formation of endothelial cell junctions. *Small GTPases* **2**, 65–76.

Wolf, K., Wu, Y. I., Liu, Y., Geiger, J., Tam, E., Overall, C., Stack, M. S. and Friedl, P. (2007). Multi-step pericellular proteolysis controls the transition from individual to collective cancer cell invasion. *Nature Cell Biology* **9**, 893–904.

Wong, M.-C., Dobi, K. C. and Baylies, M. K. (2014). Discrete levels of Twist activity are required to direct distinct cell functions during gastrulation and somatic myogenesis. *PloS one* **9**, e99553–e99553.

Xi, R., McGregor, J. R. and Harrison, D. A. (2003). A Gradient of JAK Pathway Activity Patterns the Anterior-Posterior Axis of the Follicular Epithelium. *Developmental Cell* **4**, 167–177.

Yang, H., Fang, L., Zhan, R., Hegarty, J. M., Ren, J., Hsiai, T. K., Gleeson, J. G., Miller, Y. I., Trejo, J. and Chi, N. C. (2015). Polo-like kinase 2 regulates angiogenic sprouting and blood vessel development. *Developmental Biology* **404**, 49–60.

Yao, T.-P., Forman, B. M., Jiang, Z., Cherbas, L., Chen, J.-D., McKeown, M., Cherbas, P. and Evans, R. M. (1993). Functional ecdysone receptor is the product of EcR and Ultraspiracle genes. *Nature* **366**, 476–479.

Yoo, S. K., Pascoe, H. G., Pereira, T., Kondo, S., Jacinto, A., Zhang, X. and Hariharan, I. K. (2016). Plexins function in epithelial repair in both Drosophila and zebrafish. *Nat Commun* **7**, 12282.

Yoon, W. H., Meinhardt, H. and Montell, D. J. (2011). miRNA-mediated feedback inhibition of JAK/STAT morphogen signalling establishes a cell fate threshold. *Nature cell biology* **13**, 1062–9.

Young, P. E., Richman, A. M., Ketchum, A. S. and Kiehart, D. P. (1993). Morphogenesis in Drosophila requires nonmuscle myosin heavy chain function. *Genes & Development* **7**, 29–41.

Yu, J. C. and Fernandez-Gonzalez, R. (2016). Local mechanical forces promote polarized junctional assembly and axis elongation in Drosophila. *eLife* **5**,.

Zajac, A. L. and Horne-Badovinac, S. (2022). Kinesin-directed secretion of basement membrane proteins to a subdomain of the basolateral surface in Drosophila epithelial cells. *Current Biology* **32**, 735-748.e10.

Zallen, J. A. and Wieschaus, E. (2004). Patterned Gene Expression Directs Bipolar Planar Polarity in Drosophila. *Developmental Cell* **6**, 343–355.

Chapter 2 - Rap1 promotes epithelial integrity and cell viability in a growing tissue

C. Luke Messer and Jocelyn A. McDonald*

Division of Biology, Kansas State University, Manhattan, KS 66506

In revision at *Developmental Biology*

2.1 Abstract

Having intact epithelial tissues is critical for embryonic development and adult homeostasis. How epithelia respond to damaging insults or tissue growth while still maintaining intercellular connections and barrier integrity during development is poorly understood. The conserved small GTPase Rap1 is critical for establishing cell polarity and regulating cadherin-catenin cell junctions. Here, we identified a new role for Rap1 in maintaining epithelial integrity and tissue shape during *Drosophila* oogenesis. Loss of Rap1 activity disrupted the follicle cell epithelium and the shape of egg chambers during a period of major growth. Rap1 was required for proper E-Cadherin localization in the anterior epithelium and for epithelial cell survival. Both Myo-II and the adherens junction-cytoskeletal linker protein α-Catenin were required for normal egg chamber shape but did not strongly affect cell viability. Blocking the apoptotic cascade failed to rescue the cell shape defects caused by Rap1 inhibition. One consequence of increased cell death caused by Rap1 inhibition was the preferential loss of the polar cells, which later in development led to fewer cells forming a properly migrating border cell cluster. Our results thus indicate dual roles for Rap1 in maintaining epithelia and cell survival in a growing tissue during development.

2.2 Introduction

Epithelia serve critical functions throughout the body's tissues and organs. For proper homeostasis, epithelia must remain a cohesive unit while being amenable to essential remodeling events. This allows critical epithelial functions such as forming a barrier to pathogens, absorption of nutrients, wound healing, and other important roles (Abramson and Anderson, 2017; Blanpain and Fuchs, 2009; Bröer, 2008; Guillot and Lecuit, 2013; Tai et al., 2019). During development, epithelial tissues undergo dramatic tissue rearrangements. Example include convergent extension in *Drosophila* (Irvine and Wieschaus, 1994), ventral enclosure in *C. elegans* (Williams-Masson et al., 1997), and bottle cell invagination in *Xenopus* (Keller, 1981). Once formed, cells in epithelia must maintain polarity, stay connected through cell-cell contacts, and survive insults imposed by the tissue environment. Epithelial tissues are challenged by cell turnover, cellular rearrangements, and apoptosis in response to normal tissue growth and homeostasis (Duszyc et al., 2017; Guillot and Lecuit, 2013). Because dysregulation of epithelia shape and cell survival can lead to diseases such as cancer, it is important to understand the mechanisms required for epithelial maintenance.

Here we report a requirement for the conserved small GTPase Rap1 in epithelial maintenance, where it contributes both to cell and tissue shape and to cell viability. The *Drosophila* ovary is an excellent model system to investigate how epithelial cells and tissues respond to challenges such as growth and shape changes during development. The ovary is made up of a series of continuously developing egg chambers. Each egg chamber consists of an inner population of germline derived cells enveloped in a continuous, polarized somatic cell epithelium made of follicle cells. Follicle cells continue to divide until stage 6, when mitosis ceases, resulting in a monolayer of ~650 cells. The follicle cells undergo a unique rotational

migration that helps assemble a basement membrane layer. The basement membrane provides resistance to tissue growth and contributes to egg chamber shape (Duhart et al., 2017). The egg chamber starts out round but eventually grows and elongates to an ellipsoid shape starting in mid-oogenesis. During this process, the inner germline cells expand and press against the follicle cell layer, contributing to the characteristic ovoid shape of the egg. It is critical that the epithelium stays intact to allow successful oogenesis and proper development of a mature, fertilizable egg.

Rap1 plays key roles in epithelial morphogenesis during development, particularly in the establishment of tissue polarity and cell-cell adhesions. In *Drosophila*, Rap1 helps polarize epithelial cells by positioning Bazooka/Par3 (Bonello et al., 2018; Choi et al., 2013) and promotes proper cell-cell adhesion by regulating E-Cadherin-rich adherens junctions (Knox and Brown, 2002). In human podocytes, as well as other cell types, Rap1 regulates integrin mediated adhesion to the basement membrane (Potla et al., 2014). Rap1 also promotes dynamic cell shape changes during development, including the elongation of cells at the leading edge of the lateral epidermis during *Drosophila* dorsal closure (Boettner and Van Aelst, 2007; Boettner et al., 2003).

Here we show that Rap1 GTPase maintains cell and epithelial shapes and promotes follicle cell survival during oogenesis. Loss of Rap1 altered the shape of follicle cells and the egg chamber itself. We find that Rap1 contributes to cell and tissue morphogenesis during mid-oogenesis by ensuring successful actomyosin contractility through the α-Catenin/E-Cadherin adherens junctions in epithelial cells. Notably, inhibition of Rap1 also induced abnormal apoptosis of follicle cells. The pro-survival function of Rap1 was especially important in a specialized pair of epithelial follicle cells, the polar cells, during mid-oogenesis. When Rap1 was

inhibited, polar cells failed to maintain Death-associated inhibitor of apoptosis 1 (DIAP1), leading to loss of one or both polar cells. This subsequently led to fewer cells assembling into the migratory border cell cluster. Together, our results reveal dual roles for Rap1 in cell and epithelial morphogenesis and promoting cell viability within a developing tissue.

2.3 Results

Rap1 GTPase is required for proper egg chamber and epithelial shapes in mid-oogenesis

To better understand the role of Rap1 in epithelial maintenance, we first analyzed the localization of Rap1 using a functional GFP-Rap1 fusion protein expressed under the control of the endogenous *Rap1* promoter (Knox and Brown, 2002). Rap1 is expressed ubiquitously in all cells of the ovary, with highest enrichment at the apical cell cortex of follicle cells, including the polar cells (Fig. 2.1 A). While Rap1 has known roles in the morphogenesis of diverse epithelia (Kim et al., 2022; Knox and Brown, 2002; Wang et al., 2013), few studies have analyzed how Rap1 maintains epithelia during tissue growth. To address this, we inhibited Rap1 activity in the follicle cells using a validated dominant negative Rap1 construct, UAS-DN-Rap1^{N17} (DN-Rap1^{N17}), whose expression causes phenotypes that strongly resemble loss of *Rap1* or Rap1 RNAi knockdown phenotypes in the embryo and ovary (Boettner et al., 2003; Perez-Vale et al., 2022; Sawant et al., 2018). DN-Rap1^{N17} was driven by an epithelial-specific GAL4 driver, *c306*-GAL4 (Fig. 2.1 B). Expression of *c306*-GAL4 begins early during oogenesis in anterior and posterior follicle cells, but the highest expression occurs at mid-oogenesis (~stages 4-8). These stages coincide with a major egg chamber growth phase that requires the follicular epithelium to stretch and challenges epithelial cell cohesion (Balaji et al., 2019; Crest et al., 2017; Haigo and Bilder, 2011; Spradling 1993).

The shape of egg chambers at stages 4-to-6 appeared to be normal in both control and DN-Rap1^{N17} egg chambers (Fig. 2.1 C-D). However, by stages 7-8, the tissue shape of DN-Rap1^{N17}-expressing egg chambers was no longer normal, particularly at the anterior end (Fig. 2.1 D). The anterior of DN-Rap1^{N17} egg chambers was wider and flatter compared to controls (Fig. 2.1 C-D). Closer inspection revealed altered anterior epithelial follicle cell shapes specifically in the *c306*-GAL4 expression region (Fig. 2.1 B, D). DN-Rap1^{N17} follicle cells appeared to be stretched, rather than the expected cuboidal follicle cell shapes in control egg chambers at these stages (Fig. 2.1 E-F). We further quantified the observed differences in anterior egg chamber shape, which we termed "local deformation". To do this, we measured the width of the anterior egg chamber at 20% of the total egg chamber length from the anterior end (*see* Materials and Methods). Control egg chambers retained a characteristic "wedge" shape in this anterior region (mean of 37.49μm). DN-Rap1^{N17} inhibited egg chambers, however, were wider and more "cup" shaped (mean of 47.37μm; Fig. 2.1 G). These data together suggest that Rap1 promotes tissue and epithelial cell shapes during mid-oogenesis.

Rap1 promotes polar cell shape and apical E-Cadherin accumulation

In addition to the overall distorted anterior follicular epithelial cell shapes in DN-Rap1^{N17} egg chambers, we observed particularly misshapen anterior polar cells compared to controls (Fig. 2.1 E-F; 2.2 A-B"). Polar cells are a specialized pair of follicle cells found at each pole of the egg chamber. Polar cells are one of the first specified follicle cells in the ovary and express unique cell markers such as the adhesion protein Fasciclin III (Fas III) (Ruohola et al., 1991). Because anterior egg chamber shape was most impacted by Rap1 inhibition, we focused on the anterior polar cells. We asked when and how polar cell shape was altered by loss of Rap1 activity. To do

this, we quantified anterior polar cell shapes by defining their aspect ratio (AR). We measured the width of each polar cell along their dorsoventral (DV) axis and divided by their length along the anterior-posterior (AP) axis (Fig. 2.2 C). Control polar cells at stages 4-6 were typically longer along the AP axis than they were wide along the DV axis (AR=0.61; Fig. 2.2 A, A', C). At stages 4-6, DN-Rap1^{N17} polar cell shape resembled control (AR=0.65; Fig. 2.2 B, B', C). Control polar cells maintained their earlier ellipsoid shape at stages 7-8, although they lengthened slightly along the AP axis (AR=0.56; Fig. 2.2 A, A", C). In contrast, Rap1 inhibited polar cells at stages 7-8 frequently lost this elliptical shape and were now extended along the DV axis, with more spherical shapes (AR=1.02; Fig. 2.2 B, B", C). Rap1-inhibited egg chambers also had more extreme cases of abnormal polar cell morphology, with either one polar cell that appeared to be missing (Fig. 2.8 Sup. 1 A) or a distortion of the polar cell pair, such as pulling apart into "dumbbell" type shapes (Fig. 2.8 Sup. 1 B).

The defective polar cell shapes combined with examples that appeared to split apart prompted us to ask if polar cells in DN-Rap1^{N17} egg chambers were less adhesive. The homophilic cell-cell adhesion protein E-Cadherin accumulates at high levels in polar cells (Niewiadomska et al., 1999). E-Cadherin, as well as the associated cadherin-catenin complex member β-Catenin, highly localizes to the apical side of polar cells, particularly in the region where the polar cell pair is apically constricted (Niewiadomska et al., 1999; Peifer et al., 1993). Therefore, we next investigated if DN-Rap1^{N17} egg chambers accumulated E-Cadherin normally in polar cells (Fig. 2.3). We measured the apical E-Cadherin fluorescence intensity in stages 7-8 egg chambers along a line drawn starting over the anterior-most nurse cell ("1"; Fig. 2.3 A', B') that extended through the apical polar cell-polar cell interface to the lateral interface ("2"; Fig. 2.3 A', B', C). In control egg chambers, we observed a peak in fluorescence signal as the line

passed through the apical polar cell-polar cell interface (Fig. 2.3 A-A", C, D). Strikingly, in DN-Rap1^{N17} egg chambers the apical fluorescence enrichment is severely decreased and resembled the intensity values for the portion of the line that extended along the lateral interface (Fig. 2.3 B-B", C, D). These results indicated that Rap1 controls the localized enrichment of E-Cadherin to the apical interface between polar cells, which in turn may promote the normal shape of the polar cell pair.

Non-muscle myosin II (Myo-II), as visualized with a functionally-tagged regulatory light chain, Spaghetti Squash-GFP, Sqh::GFP (Royou et al., 2004), is enriched across the entire apical surface of the anterior polar cell pair as well as other follicle cells (Fig. 2.9 Sup. 2 A-A''). However, we did not observe any obvious differences in the accumulation of Sqh:GFP at the apical surface of DN-Rap1^{N17} polar cells (Fig. 2.9 Sup. 2 B-B"). To confirm this, we quantified Sqh::GFP accumulation by drawing a line across the apical surface of the polar cell pair. We then plotted the profiles of the fluorescent intensity values from at least 8 polar cell pairs per genotype. These data indicated no major differences in the Myo-II levels or patterns between control and DN-Rap1^{N17} polar cells (Fig. 2.9 Sup. 2 C). Together, our results indicate that Rap1 is dispensable for accumulation of Myo-II but is required for E-Cadherin apical enrichment in polar cells at mid-oogenesis.

Myo-II and α-Catenin are required for egg chamber morphogenesis

Actomyosin contractility and adhesion both contribute to the shape and integrity of various tissues and organs during development (Harris and Tepass, 2010; Munjal and Lecuit, 2014). Therefore, we wanted to assess whether actomyosin contractility was required for local tissue morphogenesis, similar to what we observed for Rap1 (Fig. 2.4 A-E). We targeted the Myo-II

regulatory light chain with RNAi-mediated knockdown (Sqh RNAi) and measured local (anterior) tissue deformation. Myo-II deficient staged 7-8 egg chambers resembled what we observed in DN-Rap1^{N17} inhibited egg chambers; the anterior tissue shape was wide and flat (compare Fig. 2.4 B, E to Fig. 2.1 F, G). These results were unexpected given that Rap1 inhibition did not affect apical Myo-II accumulation, at least in polar cells. Therefore, we reasoned that Rap1 may couple actomyosin contractility to the adherens junctions in the anterior epithelium, as has been described in other tissues (Sawyer et al., 2009).

To test this hypothesis, we next performed RNAi knockdown of E-Cadherin and α-Catenin, members of the adherens junction complex. Surprisingly, E-Cadherin knockdown had no effect on egg chamber morphogenesis. Anterior width measurements were no different in E-Cadherin deficient egg chambers when compared to GFP RNAi controls (Fig. 2.4 A, C, E). However, N-cadherin is expressed during these stages and has been shown to undergo compensatory upregulation due to loss of E-Cadherin (Loyer et al., 2015). Thus, we next knocked down α-Catenin (α-Cat), the linker protein that connects cadherin complex members to the cellular F-actin cytoskeleton (Wang et al., 2022; Yonemura et al., 2010). Indeed, downregulation of α-Catenin by RNAi resulted in a wider anterior egg chamber, resembling the tissue shape defects observed with Sqh RNAi and inhibition of Rap1 activity (Fig. 2.4 B, D-E; Fig. 2.1 F-G). Thus, adhesion and actomyosin are required to maintain tissue shapes at mid-oogenesis stages.

We next examined the shape of epithelial follicle cells at the anterior end of the egg chamber when Myo-II or α-Catenin were knocked down by RNAi (Fig. 2.4 F-I'). Close inspection revealed altered individual cell shapes resembling DN-Rap1^{N17} egg chambers only for α-Catenin RNAi (Fig. 2.4 H-I') but not Sqh RNAi (Fig. 2.4 G, G'). Notably, we observed a mix

of "stretched" or "flattened" follicle cells in α-Catenin RNAi egg chambers along the lateral sides of the egg chamber that looked like the cells in the anterior region of DN-Rap1^{N17} egg chambers (Fig. 2.4 H-I'; compare to Fig. 2.1 F). In the most-affected α-Catenin RNAi egg chambers (Fig. 2.4 I, I'), clumping of cells was observed at the most anterior end and closely resembled the cell shapes reported for *α-Catenin* null mutant follicle cells (Sarpal et al., 2012). The similarities in the tissue and epithelial cell shape phenotypes caused by loss of α-Catenin and Rap1 activity suggested that Rap1 modulates α-Catenin-containing adherens junctions as was observed during dorsal fold formation in the *Drosophila* embryo (Wang et al., 2013).

Rap1 promotes the viability of epithelial follicle cells during oogenesis

Our analysis of DN-Rap1^{N17} egg chambers at stages 7-8 revealed not only cases of extremely distorted polar cells, but also examples where one polar cell was missing from the required pair (Fig. 2.8 Sup. 1 A). These data suggested that Rap1 contributes to cell survival. To test this idea, we first analyzed a marker of apoptosis during oogenesis in control and Rap1 mutant ovaries. We stained egg chambers for antibodies to cleaved death caspase-1 (cDcp-1), which recognizes both *Drosophila* effector caspases, Death caspase-1 (Dcp-1) and Death related ICE-like caspase (Drice) (Li et al., 2019). During early oogenesis, excess polar cells ("supernumerary" polar cells) and excess stalk cells form but are eliminated by apoptosis during stages 3-6, whereas in healthy ovarioles other follicle cells do not undergo cell death (Borensztejn et al., 2013; Borensztejn et al., 2018; Khammari et al., 2011; Lebo and McCall, 2021; cDCp-1+ cells; Fig. 2.5 A). However, in DN-Rap1^{N17} ovarioles, in addition to the normal pattern of early polar cell and stalk cell apoptosis, we observed additional caspase activity in follicle cells during stages 2 through 8 of oogenesis (cDCp-1+ cells; Fig. 2.5 B). We quantified the number of cDcp-1 cells in control and

DN-Rap1^{N17} ovarioles and saw a significant increase in apoptotic cells only when Rap1 activity was inhibited (Fig. 2.5 C). Activation of Rap1, through expression of constitutively active CA-Rap1^{V12} did not decrease apoptotic cells during any stage of oogenesis (Fig. 2.5 C). These data suggest that Rap1 is required for follicle cell survival during oogenesis but is not sufficient to block normal developmental apoptosis.

Because Rap1 promotes both follicle cell survival and epithelial and tissue morphogenesis during oogenesis, we next asked if Myo-II or α-Catenin were also similarly required for follicle cell viability. We analyzed cell death during oogenesis using cDcp-1 in Sqh RNAi, α-Catenin RNAi, and matched control (GFP RNAi) ovarioles. We observed minimal cell death in Sqh RNAi and GFP RNAi controls (Fig. 2.5 D, E, G). However, there was a significant increase in cDcp-1 positive cells for α-Catenin RNAi ovarioles (Fig. 2.5 F, G). These results suggest that while both Myo-II and α-Catenin regulate egg chamber morphogenesis, only α-Catenin is required for viability of the follicle cells. Notably, although α-Catenin RNAi results in an increase in cDcp-1 positive cells, fewer cells per ovariole were cDcp-1 positive than when Rap1 was inhibited (2.6 cDcp-1-positive cells for α-Catenin RNAi, Fig. 2.5 G, compared to 8.8 cDcp-1-positive cells per ovariole for DN-Rap1^{N17}, Fig. 2.5 C). These findings suggest that cell adhesion via α-Catenin is required for cell viability, though Rap1 may have a greater role in promoting cell survival.

Rap1 promotes polar cell survival by suppressing apoptosis, but polar cell shape defects are not apoptosis-dependent

As described above, loss of Rap1 activity causes death of follicle cells and loss of polar cells (Fig. 2.5 B-C; Fig. 2.8 Sup. 1 A), in addition to defects in polar cell shape (Fig. 2.2 B-C; Fig. 2.8

Sup. 1 B). Therefore, we wanted to determine if Rap1 was required to manage elimination of supernumerary polar cells that form at each pole of early egg chambers (Besse and Pret, 2003; Borensztejn et al., 2013; Khammari et al., 2011). Removal of the extra polar cells by apoptosis ensures that only two "mature" polar cells remain at anterior and posterior egg chamber poles by stages 5/6 (Besse and Pret, 2003; Borensztejn et al., 2013; Khammari et al., 2011). One possibility for the absence of polar cells in later staged DN-Rap1^{N17} egg chambers could be a requirement for Rap1 in early polar cell development and elimination. Alternatively, Rap1 could promote the survival of mature polar cells later in oogenesis after these cells are specified.

We examined anterior and posterior polar cells in egg chambers from stages 3-10 of oogenesis using Eyes Absent (Eya) and FasIII (Fig. 2.10 Sup. 3 A). Eya suppresses polar cell fate and is present in all follicle cells except polar cells (Bai and Montell, 2002) and FasIII specifically marks the polar cell pair (Ruohola et al., 1991). We observed similar numbers of supernumerary polar cells at early stages of development (e.g., stages 3-4 and stages 5-6) in control and DN-Rap1^{N17} (Fig. 2.10 Sup. 3 A). Using CA-Rap1^{V12}, we next asked if increased Rap1 activity resulted in extra polar cells being maintained until maturity. At each stage examined, we observed similar numbers of polar cells for CA-Rap1^{V12} and controls (Fig. 2.10 Sup. 3 A). Moreover, in all genotypes, in agreement with other studies, there was an overall decrease in the number of polar cells as oogenesis progressed (Fig. 2.10 Sup. 3 A; Borensztejn et al., 2013; Khammari et al., 2011).

Since early polar cell development appeared normal in Rap1-deficient egg chambers, we next asked if Rap1 regulated the survival of mature polar cells later in oogenesis. We tracked polar cell-specific accumulation of cDcp-1. Control "mature" polar cells at stages 7-8 rarely died (Fig. 2.6 A-A";1 out of 66 egg chambers). In contrast, we observed an increased frequency in the

accumulation of cDcp-1 in staged 7-8 DN-Rap1^{N17} polar cells, well after the conclusion of normal developmental apoptosis (Fig. 2.6 B-B"; 7 out of 61 egg chambers). These polar cells were frequently pyknotic as visualized by DAPI staining (Fig. 2.6 B'). These data together indicate that Rap1 promotes the survival of both follicle cells and mature polar cells during oogenesis.

To further characterize this increase in polar cell death when Rap1 was inhibited, we next examined the apoptotic cascade. Death-associated inhibitor of apoptosis 1 (DIAP1) blocks caspase activity and thus prevents cells from undergoing apoptosis (Hay et al., 1995; Yan et al., 2004). DIAP1 specifically accumulates in the two mature polar cells and promotes their survival, whereas DIAP1 is downregulated in the supernumerary polar cells leading to their developmental apoptosis (Borensztejn et al., 2013; Khammari et al., 2011). We reasoned that a decrease in DIAP1 might precede the death of mature polar cells observed in DN-Rap1^{N17} egg chambers. Therefore, we analyzed DIAP1 accumulation in polar cells relative to their most adjacent follicle cell neighbors at both stages 4 to 6 and at stages 7 to 8. At the earlier stages (stages 4-6), we observed normal accumulation of DIAP1 in 13 out of 14 control polar cells (Fig. 2.6 C-C"). However, DIAP1 accumulated in only 6 out of 23 DN-Rap1^{N17} polar cells (Fig. 2.6 E-E"). Similarly, at later stages, DIAP1 accumulation was lower in DN-Rap1^{N17} inhibited polar cells, with only 8 out of 19 egg chambers having normal DIAP1 accumulation (Fig. 2.6 F-F"), compared to 10 out of 14 for control egg chambers (Fig. 2.6 D-D"). Interestingly, DIAP1 levels were altered at a greater frequency in DN-Rap1^{N17} egg chambers (Fig. 2.6 E-F") than the observed frequency of polar cell death (Fig. 2.6 B"). One possibility is that not all cells that lose DIAP1 accumulation undergo cell death. Alternatively, the threshold for DIAP1 protein depletion may need to be relatively severe for apoptosis to occur. Taken together, our results

favor a role for Rap1 in suppressing the apoptotic cascade through regulating the levels of DIAP1 in mature polar cells.

We next asked if the polar cell morphology defects caused by loss of Rap1 activity were due to apoptosis. To test this, we asked if blocking the apoptotic cascade could rescue polar cell shape defects caused by loss of Rap1 activity (Fig. 2.10 Sup. 3 B-D). We performed polar cell aspect ratio measurements in egg chambers that co-expressed DN-Rap1^{N17} with either a LacZ control or with the apoptosis inhibitor, baculoviral p35 (Clem et al., 1991; Hay et al., 1994). We found that co-expression of p35 along with DN-Rap1^{N17} failed to rescue the polar cell aspect ratio defects compared to co-expression with LacZ (Fig. 2.10 Sup. 3 B-D). There was no statistical difference in the aspect ratios of DN-Rap1^{N17} polar cells either co-expressing the LacZ control or p35 (AR=0.84, DN-Rap1^{N17} + LacZ; AR=0.85, DN-Rap1^{N17} + p35; Fig. 2.10 Sup. 3 D). These results provide further evidence that Rap1 likely controls polar cell morphogenesis independently of its function in promoting cell survival.

Rap1 requirement for polar cell survival supports formation of border cell clusters with optimal cell numbers

The role for Rap1 in promoting polar cell survival prompted us to ask what the developmental consequences were later in oogenesis. During late stage 8, the anterior pair of polar cells specifies which follicle cell neighbors become the migratory border cells through the secretion of the JAK/STAT ligand Unpaired (Beccari et al., 2002; Silver and Montell, 2001). Between 4-8 follicle cells activate high levels of JAK/STAT and subsequently surround the polar cells to produce a border cell cluster with a total of 6 to 10 cells (Silver and Montell, 2001). Having an

optimal number of cells helps the border cell cluster efficiently reach the oocyte at the correct time (Cai et al., 2016; Starz-Gaiano et al., 2008; Stonko et al., 2015)

Because inhibition of Rap1 caused a frequent loss of mature polar cells, we determined how this impacted the size of the migratory border cell cluster. We reasoned that losing a polar cell might decrease the number of cells found in border cell clusters. We quantified the total number of cells found within control (UAS-LacZ) versus Rap1-deficient (UAS-Rap1^{N17} or UAS-Rap1 RNAi) border cell clusters (Fig. 2.7 A-C). When Rap1 was inhibited using with DN-Rap1^{N17} driven by *c306*-GAL4, we found a strong reduction in the average number of cells per cluster compared to control (Fig. 2.7 A', B'; average of 6.1 cells in control compared to 4.6 cells in DN-Rap1^{N17}). *c306*-GAL4-driven *Rap1* RNAi also reduced the number of cells per cluster to an average of 5.2 cells compared to 6.1 cells in *mCherry* RNAi controls (Fig. 2.7 C). We analyzed the number of cells in border cell clusters using a different GAL4, *slbo*-GAL4, which is expressed later than *c306*-GAL4 and in a more restricted pattern (Fig. 2.11 Sup. 4 A). The overall number of cells in *slbo*-GAL4 control egg chambers is higher than that observed for *c306*-GAL4 controls (average of 8.2 cells; Fig. 2.11 Sup. 4 B, B', D). Nonetheless, we observed a significant reduction in the number of DN-Rap1^{N17} cells within the border cell cluster (Fig. 2.11 Sup. 4 C-D; average 6.7 cells). Thus, Rap1 is required for migrating border cell clusters to have an optimal number of cells.

We next asked if the observed reduction in cell numbers within the border cell cluster was due to Rap1 function in border cell specification or in the recruitment of cells due to cell survival. We examined anterior follicle cells at stage 8 for a reporter of JAK/STAT activity, 10XSTAT::GFP (Bach et al., 2007). These cells are fated to become the migratory border cells (Beccari et al., 2002; Silver and Montell, 2001). When both polar cells were present, we did not

detect changes in either the pattern of 10XSTAT:GFP or the levels of nuclear STAT, and hence activity, in the three follicle cells immediately adjacent to the polar cells at stages 7-8 in DN-Rap1^{N17} compared to control (Fig. 2.12 Sup. 5 A-C). These results suggest that border cell fate specification at stage 8 of oogenesis is normal under conditions when both polar cells are present and does not rely on Rap1 activity. However, we cannot rule out a subtle decrease in the JAK/STAT activity gradient when only one polar cell survives to stage 8 in DN-Rap1^{N17} egg chambers.

Finally, we determined if the smaller number of cells per border cell cluster was due to the increased apoptotic activity observed upon Rap1 inhibition. We co-expressed DN-Rap1^{N17} with either a UAS-LacZ control or the apoptosis inhibitor p35 (Fig. 2.7 D-F). We quantified the number of cells per cluster at stages 9 and 10, when border cell clusters have already formed and have either begun to migrate or finished their migration. Border cell clusters that co-expressed DN-Rap1^{N17} and LacZ had an average of 4.8 cells per cluster, resembling the phenotypes observed when expressing DN-Rap1^{N17} alone (Fig. 2.7 D, D', F compared to Fig. 2.7 C). In contrast, border cell clusters co-expressing DN-Rap1^{N17} and p35 had an average of 6.4 cells per cluster (Fig. 2.7 E-F), matching control border cell clusters (Fig. 2.7 A, A', C). Thus, the observed smaller border cell clusters caused by loss of Rap1 activity is likely due to apoptotic cell death of mature polar cells just prior to recruitment of border cells. Together, these data support a model in which Rap1 promotes mature polar cell survival by preventing apoptosis through upregulation of DIAP1, thus promoting an optimal number of cells being recruited to form the migrating border cell cluster.

2.4 Discussion

A key challenge is to understand how epithelia and constituent cells survive and maintain shape in response to changes in tissue shape and size during normal development. Here we focused on understanding how the small GTPase Rap1 maintains cell and tissue shapes during *Drosophila* egg chamber growth. Prior work has shown requirements for Rap1 in epithelial morphogenesis (Asha et al., 1999; Boettner and Van Aelst, 2007; Choi et al., 2013; Bonello et al., 2018), but whether and how Rap1 maintains epithelia during tissue growth and homeostasis was unclear. Here we used a model of developmental tissue growth in the *Drosophila* ovary to interrogate the function of Rap1. We found that Rap1 promotes epithelial follicle cell shape, polar cell shape, and local tissue shapes during a period of major egg chamber growth. We propose that this function of Rap1 in maintenance of epithelial integrity is through regulation of dynamic linkages between adherens junctions and the contractile actomyosin cytoskeleton. Our experiments revealed an unexpected and new role for Rap1 in regulating cell survival, especially of the mature polar cells, which leads to the assembly of a migratory border cell cluster with the optimal number of cells.

Rap1 maintains cell and tissue shapes by modulating adherens junction-cytoskeleton linkages during tissue growth

Here we report that Rap1 is required to maintain polar cell and follicle cell shapes and proper tissue shapes of the anterior follicular epithelium during egg chamber elongation. Our quantitative analyses of individual cell shapes and local tissue deformation demonstrated that Rap1 maintained tissue and epithelial morphology. Moreover, Rap1-deficient polar cell shapes were highly affected. Most of these phenotypes were at stages 7-8, a period of dramatic egg

chamber growth (Crest et al., 2017). Previous work using *Rap1* null flies that were rescued to viable adults by expression of heat shock-driven Rap1 revealed egg chambers that degenerated and had distorted follicle cell shapes (Asha et al., 1999). Notably, these phenotypes seemed to be more severe during mid-to-late stages of oogenesis, stages that overlap with egg chamber elongation, thus supporting a role for Rap1 in tissue maintenance. We obtained similar, albeit less severe egg chamber defects, by specifically expressing DN-Rap1^{N17} in follicle cells. These results indicate a requirement of Rap1 in tissue shape maintenance.

How does Rap1 contribute to cell and tissue shape maintenance within the follicular epithelium during tissue expansion? Rap1 regulates early Bazooka/Par3 localization and adherens junction positioning during *Drosophila* embryogenesis (Bonello et al., 2018). *Rap1* mutant embryos fail to localize spot adherens junctions properly during cellularization and complete embryogenesis with fragmented cuticles suggesting a loss of tissue integrity (Choi et al., 2013). Similarly, Rap family proteins are required for adherens junctions and tight junction formation in MDCK cells (Sasaki et al., 2020). Our results showed that Rap1 is required specifically for the enrichment of E-Cadherin at the apical side of polar cells, which we propose helps promote proper polar cell shapes. We also observed stretching of the anterior epithelial follicle cells, which may indicate altered adhesion in these cells. Although E-cadherin appeared to be localized to apical puncta between follicle cells consistent with the formation of adherens junctions, these junctions may not be completely normal thus contributing to the stretched epithelial shapes. We thus propose that Rap1 maintains (or helps assemble) the proper positioning of the apical adherens junction, at least in polar cells. Further work will be needed to determine if and how Rap1 mechanistically maintains adherens junctions in the follicle cells.

The functions of adherens junctions to maintain cell-to-cell contacts within an epithelium are also coupled to actomyosin contractility, which can drive cell shape changes. Rap1 and its effector Canoe (Cno) regulate actomyosin contractility in apically constricting mesodermal cells during *Drosophila* ventral furrow invagination (Sawyer et al., 2009; Spahn et al., 2012). Similarly, Rap1 is required for Shroom dependent apical constriction in *Xenopus* (Haigo et al., 2003). These studies led us to ask if, in addition to its role in positioning adherens junctions during egg chamber elongation, Rap1 was responsible for proper actomyosin contractility. We found that Myo-II was required for proper tissue shape during egg chamber elongation, but surprisingly Rap1 was dispensable for Myo-II localization in polar cells. Taken together with the stretched individual cell shapes and deformed egg chambers observed for α-Catenin RNAi, these data support our model that Rap1 maintains the strength of adherens junction-actin linkages as was reported for the known Rap1 effector Cno (Sawyer et al., 2009).

We found that Rap1 regulates egg chamber shape during a period of major tissue growth. The inherent on-off activity states of GTPases like Rap1 make them particularly useful for dynamic processes that require discrete bursts of activity in response to cellular or tissue level cues (Gloerich and Bos, 2011). In apical constriction, for example, myosin pulsatility is coupled to progressive tightening of the apical domain (Martin and Goldstein, 2014; Martin et al., 2009). The transient nature of pulsatile myosin may require a fast-acting molecular switch that can be activated and inactivated quickly to couple motor behaviors to changes at the cell cortex. While we did not observe Myo-II localization defects when Rap1 was inhibited, the requirement for α-Catenin indicates that linkage to the actomyosin cytoskeleton is critical for epithelial cell and tissue shapes. Atypical Protein Kinase C (aPKC) promotes an optimal level of actomyosin to maintain an intact and organized follicle cell epithelium (Osswald et al., 2022). Indeed, acute

loss of aPKC causes the follicle cell layer to apically constrict and rupture, due to growth of the egg chamber. While the effects caused by loss of Rap1 activity did not cause the epithelium to rupture, the tissue instead locally deformed. The basement membrane becomes thinner at the anterior and posterior ends during tissue elongation, allowing further growth along the anterior-posterior axis (Balaji et al., 2019; Crest et al., 2017). We suggest that loss of Rap1, in conjunction with a permissive region of the basement membrane, allows the tissue to widen in response to egg chamber growth. Thus, we propose that Rap1, through apical enrichment of adherens junction proteins, reinforces strong epithelial connections and resistance to growth of the germline.

The signal relay mechanisms that act upstream to regulate the various Rap1 activities in the follicle cell epithelium are unknown. Nor is it known which Rap1 effectors mediate the direct control of adherens junction-actomyosin linkages in this context. The GTPase activating protein Rapgap1 acts as one regulatory layer controlling Rap1 α-Catenin modulation in regulating dorsal fold morphogenesis and is expressed in the ovary (Wang et al., 2013; Sawant et al., 2018). *Drosophila* has several known guanine nucleotide exchange factors (GEFs), including PDZ-GEF (also known as Dizzy), C3G, and Epac. Whether one or more GEFs have differential functions during these stages of oogenesis, and in cell survival, remains to be tested. A well-known Rap1 effector, Cno, acts as a key signal relay mechanism downstream of Rap1. For example Cno mediates Rap1 functions in *Drosophila* morphogenesis including mesoderm invagination, head involution, and dorsal closure through modular biochemical functions (Perez-Vale et al., 2021; Sawyer et al., 2009). Whether these or other upstream and downstream regulators mediate Rap1 functions in epithelial tissue maintenance and cell survival remain to be determined.

Rap1 promotes follicle cell and polar cell survival during oogenesis

We found that Rap1 maintains epithelial cell viability during oogenesis. One possibility is that the role for Rap1 in adherens junction protein localization is coupled to cell survival. Cell-cell contacts are essential for cell viability in certain contexts (Guillot and Lecuit, 2013). We found that the adherens junction-cytoskeleton linker protein α-Catenin not only supported proper epithelial and tissue shapes, but also promoted cell survival during oogenesis. Thus, cell-cell adhesions may be coupled to cell viability during tissue growth during oogenesis. Indeed, this period of dramatic tissue growth places extra strain on the epithelial follicle cells (Osswald et al., 2022), which could result in fewer cells surviving. Another major role for Rap1 was in promoting survival of the mature polar cells. The consequence of fewer polar cells surviving was a smaller border cell cluster, which is critical for optimal migration speed and ability to reach their final position at the oocyte (Cai et al., 2016; Stonko et al., 2015). Thus, Rap1's role in promoting cell viability is critical for normal oogenesis.

We do not yet have a clear understanding of the mechanism by which Rap1 promotes cell survival and suppresses apoptosis. Our results suggest that Rap1 may have independent functions in cell survival other than (or in addition to) regulation of adherens junction proteins. Although knocking down α-Catenin resulted in apoptotic cells, the phenotype was overall much milder than that observed with Rap1 inhibition. Normally, DIAP1 must be maintained in the two mature polar cells to prevent their apoptosis (Borensztejn et al., 2013; Khammari et al., 2011). We observed a decrease in DIAP1 accumulation in the mature polar cells upon Rap1 inhibition, which is unlikely to be directly associated with defects in cell-cell adhesion. During stages 7 to 8, the overall levels of DIAP1 undergo a global reduction, which serves as a checkpoint mechanism to terminate unhealthy egg chambers rather than commit additional nutritional and energy

resources (Baum et al., 2007). Rap1 promotes levels of DIAP1 before and during these stages, thus protecting the mature polar cells and likely other follicle cells from undergoing abnormal cell death. It remains to be tested whether Rap1 generally maintains cell survival of follicle cells by more directly fine tuning DIAP1 levels at the molecular level, or if the regulation of DIAP1 by Rap1 is indirect, for example due to disruption of epithelial integrity when Rap1 is inhibited. It is also unclear how cellular mechanics function together with transcription of DIAP1 to promote cell survival during tissue growth of the ovary. Further work will also be needed to determine if the function for Rap1 in cell survival and maintenance of epithelial shapes in growing tissues is conserved in other developing tissues and organs.

2.5 Materials and Methods

Drosophila genetics

All fly stocks used in this study are listed in Table 2.1 and the complete genotypes for each experiment can be found in Table 2.2. Crosses were typically set up and maintained at 25˚C. In cases where transgene expression impacted organism viability, the crosses were set up and maintained at 18˚C. The tub-GAL80ts ('tsGAL80') transgene (McGuire et al., 2004) was present in the genetic background of many crosses in this study to repress GAL4 expression during other stages of development. Flies were shifted to 29˚C for 12-72 hours prior to dissection to ensure optimal GAL4 expression and repression of tsGAL80, unless otherwise noted.

Immunostaining

Antibodies, sources, and dilutions used are listed in Table 2.3. Fly ovaries from 2- to 8-day old females were dissected in Schneider's *Drosophila* Medium (Thermo Fisher Scientific, Waltham, MA, USA) supplemented with 10% fetal bovine serum (Seradigm FBS; VWR, Radnor, PA, USA). Ovaries were either kept whole or dissected further into ovarioles and fixed for 10 mins using 16% methanol-free formaldehyde (Polysciences, Inc., Warrington, PA, USA) diluted to a final concentration of 4% in 1X Phosphate Buffered Saline (PBS). Following fixation, tissues were washed ≥4x with 'NP40 block' (50 mM Tris-HCL, pH 7.4, 150mM NaCl, 0.5% NP40, 5mg/ml bovine serum albumin [BSA]) and rocked in the solution for ≥30 mins prior to antibody incubation. Primary and secondary antibody incubation as well as all other subsequent wash steps were also performed in NP40 block. Dissected and stained ovarioles and egg chambers were mounted on slides with Aqua-PolyMount (Polysciences, Inc.) media and allowed to harden prior to imaging.

Microscopy

Images of fixed egg chambers were acquired on a Zeiss LSM 880 confocal laser scanning microscope (KSU College of Veterinary Medicine Confocal Core) using either a 20 X 0.75 numerical aperture (NA) or a 40 X 1.3 NA oil-immersion objective controlled by Zeiss Zen 14 software.

Image Processing and Data Analysis

Measurements were performed using FIJI (Schindelin et al., 2012). Egg chamber local deformation measurements were determined by measuring the width between the apical follicle

cell surfaces at 20% of the anterior-posterior (A-P) length of the egg chamber (the very anterior tip is 0% of the A-P length). The polar cell aspect ratio was measured by analyzing Z-stacks taken of egg chambers stained with FasIII (to identify polar cells), E-Cadherin, and DAPI; the length and width was measured at the widest point of each polar cell. The aspect ratio was then calculated by dividing the width by length.

E-Cadherin accumulation in polar cells (identified by FasIII) was measured by analyzing Z-stacks acquired of egg chambers stained for E-Cadherin, FasIII, and DAPI. A 7μm line was drawn to quantify pixel intensity, starting within the germline (an adjacent nurse cell), extending through the apical polar cell-polar cell contact, then continuing along the lateral interface (see line in Fig. 2.3 A' and 2.3 B'). Only images in which both polar cells could be viewed in the same Z-slice were used for quantitation. The "Plot Profile" function in FIJI was used to obtain a list of pixel intensity values corresponding to points along this line. These values were normalized to the highest pixel intensity measured in the experiment and plotted. Staining and imaging conditions were kept consistent between samples.

Dying cells during oogenesis were quantified by scanning through dissected whole ovarioles stained and imaged for cDcp-1, DAPI, and FasIII. Nuclei positive for caspase activity (cDcp-1-expressing nuclei) from stages 2 through 8 were quantified. Death of mature polar was scored by analyzing cDcp-1 expressing nuclei specifically in stage 7-8 egg chambers. DIAP1 accumulation in polar cells was assessed by acquiring Z-stacks through the polar cells in stages 4-6 and stages 7-8 egg chambers and analyzing qualitative reduction in the DIAP1 signal compared to adjacent cells. Polar cells were identified using a GFP protein trap in FasIII.

Quantification of the number of cells per border cell cluster were measured by acquiring Z-stacks through border cell clusters visualized using the nuclear envelope marker Lamin (also

known as Lamin Dm_0) and DAPI. Whenever possible, E-Cadherin was used to determine the boundaries of fully delaminated border cell clusters. Z-stacks encompassing the entire cluster including both border cells and polar cells were acquired and nuclei were manually counted using the Lamin signal.

Apical Myo-II accumulation was quantified by acquiring Z-stacks of stage 7-8 egg chambers expressing a fluorescent Myo-II reporter, Sqh::GFP, and co-stained for E-Cadherin and DAPI. A 2μm line was drawn at the apical surface of polar cells (identified by enrichment of E-Cadherin) and the "Plot Profile" function in FIJI was used to obtain a list of intensity values for each line. The intensity values were normalized to the highest pixel intensity measured in the experiment and plotted. Samples of inferior staining quality were eliminated from analysis. Staining and imaging conditions were kept consistent between samples.

Supernumerary polar cell load during oogenesis was scored by scanning through whole ovarioles and counting the number of polar cells present at each pole using FasIII and Eya as markers for polar cell fate. Nuclear STAT intensity at stages 7-8 was quantified by measuring 10XSTAT::GFP reporter intensity by drawing lines across three nuclei on either side of polar cells The mean GFP intensity of each line was normalized to the mean DAPI signal for each nuclear measurement. All measurements were then normalized to the highest relative GFP intensity value measured in the experiment.

Figures, graphs, and statistics

Images were processed in FIJI and figures were assembled using Affinity Photo (Serif, Nottingham, United Kingdom). Illustrations were designed in Affinity Photo. Graphs and statistical tests were performed using GraphPad Prism 7 or Prism 9 (GraphPad Software, San

Diego, CA, USA). All statistical tests and significance levels are listed in the figure legends for the figures in which they appear and in Table 2.4.

Acknowledgements

We would like to thank Denise Montell, Michelle Starz-Gaiano, Nick Brown, and Hyung Don Ryoo, the Vienna *Drosophila* Resource Center (VDRC), the Bloomington *Drosophila* Stock Center (BDSC), and the Developmental Studies Hybridoma Bank (DSHB) at the University of Iowa for fly protocols, fly stocks, and antibodies. We also thank Gibson Hoefgen and Manuel Garcia for general project assistance and maintenance of *Drosophila* strains and Emily Burghardt, Rehan Khan, and Yujun Chen for helpful comments on the manuscript. We acknowledge the Confocal Core, funded by the Kansas State University (KSU) College of Veterinary Medicine, which provided use of the Zeiss LSM 880 confocal microscope. We thank the KSU Statistics Consulting Laboratory for statistics advice. This work was supported by the National Science Foundation (NSF 2027617) to J.A.M. and a KSU Johnson Cancer Research Center Graduate Student Summer Stipend Award to C.L.M. and J.A.M. The authors declare no competing financial interests.

Author Contributions

C. Luke Messer: Conceptualization, Formal analysis, Validation, Investigation, Visualization, Methodology, Writing - Original Draft, Writing - Review & Editing; Jocelyn A. McDonald: Conceptualization, Supervision, Funding acquisition, Methodology, Writing - Original Draft, Writing - Review & Editing.

2.6 Figures and Tables

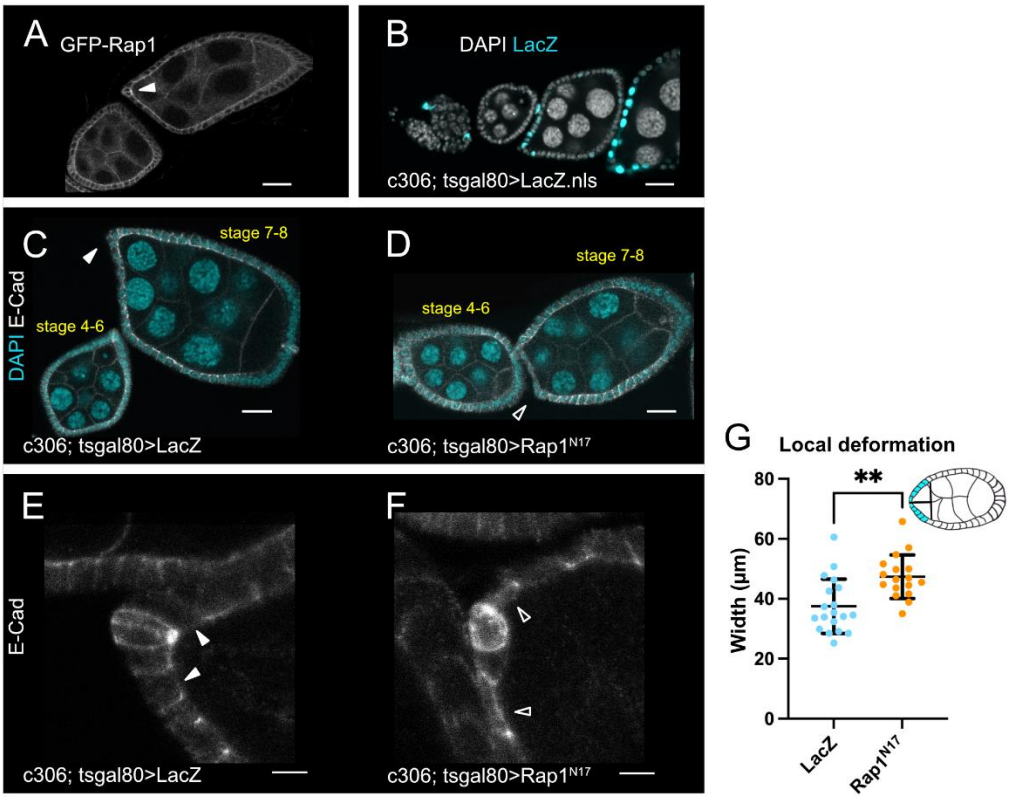

Figure 2.1 Rap1 is required in the anterior epithelium to maintain follicle cell and egg chamber shapes

(A) Ovariole with GFP tagged Rap1 illustrates Rap1 enrichment in follicle cells. Arrowhead indicates apical Rap1 accumulation in anterior epithelium. (B) Ovariole expressing UAS-LacZ driven by *c306*-GAL4 to demonstrate the *c306*-GAL4 expression pattern. (C-D) LacZ control (C) or DN-Rap1^{N17} (D) egg chambers. Anterior epithelia are distorted at stages 7-8 in DN-Rap1^{N17}. Arrowheads indicate anterior region of stage 7-8 egg chambers. Solid arrowhead points to normal anterior epithelium of control (C), while open arrowhead indicates distorted anterior region for DN-Rap1^{N17} (D). (E-F) Anterior regions of stage 7-8 egg chambers showing normal cuboidal epithelium in control (E) or stretched cell shapes in DN-Rap1^{N17} (F). Solid arrowheads indicate cuboidal shaped cells in E. Open arrowheads indicate stretched cells in F. (G)

Quantification of local deformation measures taken at 20% of egg chamber length (illustrated by egg chamber schematic in G). ** $p \leq 0.01$ two-tailed unpaired t-test. $N \geq 17$ egg chambers measured per genotype. (A-D) Scale bars 20μm. (E-F) Scale bars 5μm. Anterior is to the left in this and the following figures.

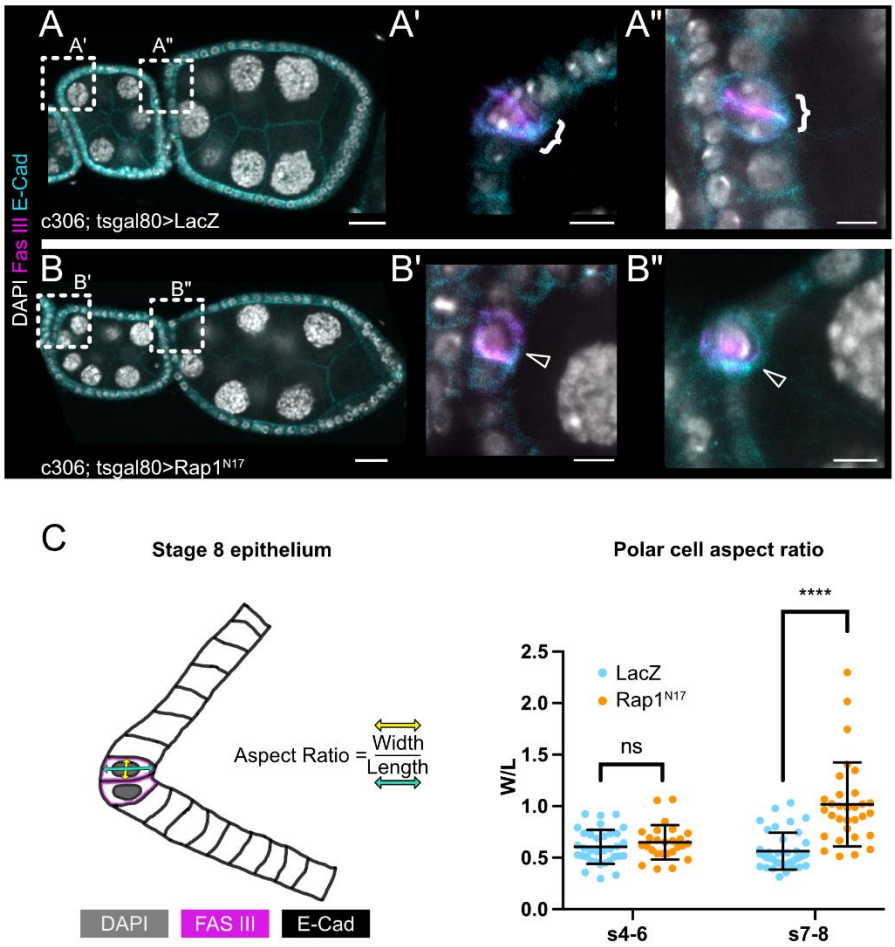

Figure 2.2 Rap1 is required for proper polar cell shape

(A-B) LacZ (A) and DN-Rap1^{N17} (B) ovarioles imaged for polar cell shape. Dashed boxes indicate the regions expanded in A', A", B', and B". (A'-A", B'-B") Close-up views of anterior egg chamber regions. Control stage 4-6 (A') and stage 7-8 (A") egg chamber polar cells. Brackets indicate intact polar cell pairs. (B'-B") DN-Rap1^{N17} stage 4-6 (B') and stage 7-8 (B") egg chamber polar cells. (B') Only one polar cell is present at stage 4-6. (B") One spherical polar cell is present at stage 7-8. Open arrowheads indicate only one polar cell is present. (C) Aspect ratio schematic and quantification. Aspect ratio (AR) was defined as the dorsoventral (DV, yellow arrow) width divided by the anterior-posterior (AP, cyan arrow) length. AR measurements plotted for stage 4-6 and stage 7-8 egg chamber polar cells. DN-Rap1^{N17} polar

cells are more spherical at stage 7-8 indicated by average AR=1.02 vs average AR=0.56 for control. **** $p \leq 0.0001$ two-tailed unpaired t test. $N \geq 26$ polar cells measured per genotype per egg chamber stage. (A-B) Scale bars 20μm. (A'-B") Scale bars 5μm.

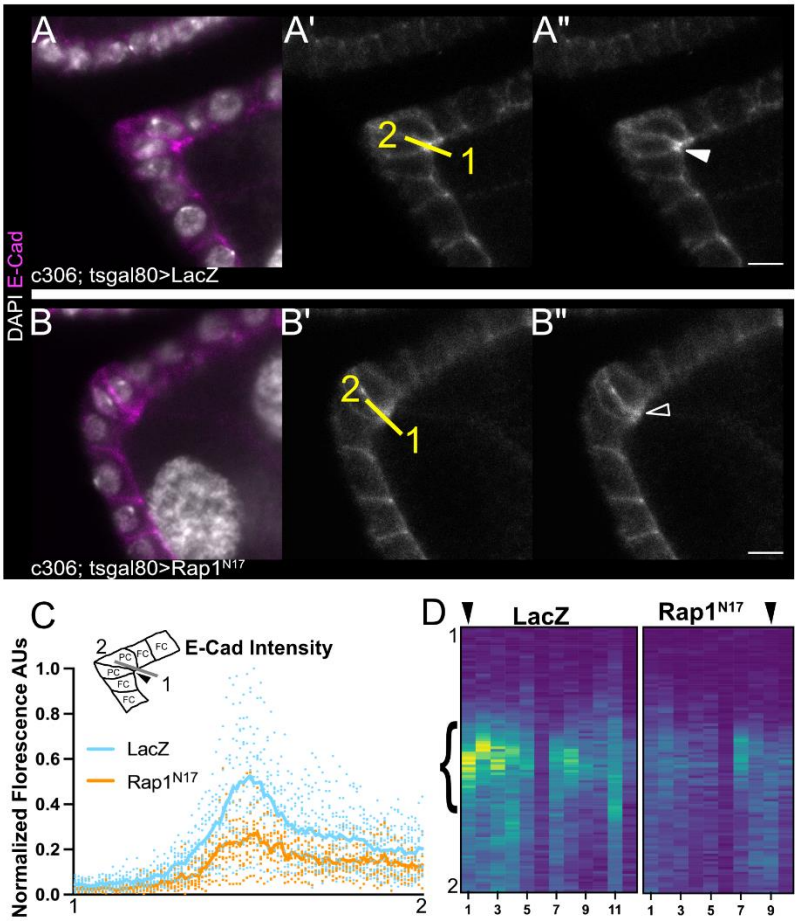

Figure 2.3 Rap1 is required for apical E-Cadherin enrichment in polar cells

(A-B) Anterior regions of stage 7-8 egg chambers for LacZ control (A) and DN-Rap1^{N17} egg chambers (B). (A'-B") Single channel panels of A and B showing E-Cadherin (gray) enrichment. (A', B') Yellow line indicates region of measurement beginning over nurse cells (1) and ending along lateral polar cell-polar cell interface (2). Solid arrowhead indicates apical accumulation of E-Cadherin. Open arrowhead indicates reduced E-Cadherin enrichment. (A", B") Same as A' and B' without line overlays for clarity. Image brightness adjusted for presentation purposes. (C) Measurement schematic and quantification of fluorescence intensities measured along lines drawn as in A' and B' and normalized to highest signal. Lines represent mean intensity. (D) Heat map representation of C. Bracket indicates area of heat map corresponding to apical enrichment

of E-Cadherin in polar cells. Arrowheads at the top of heat map indicate the lanes corresponding to A” and B”. Scale bars 5µm.

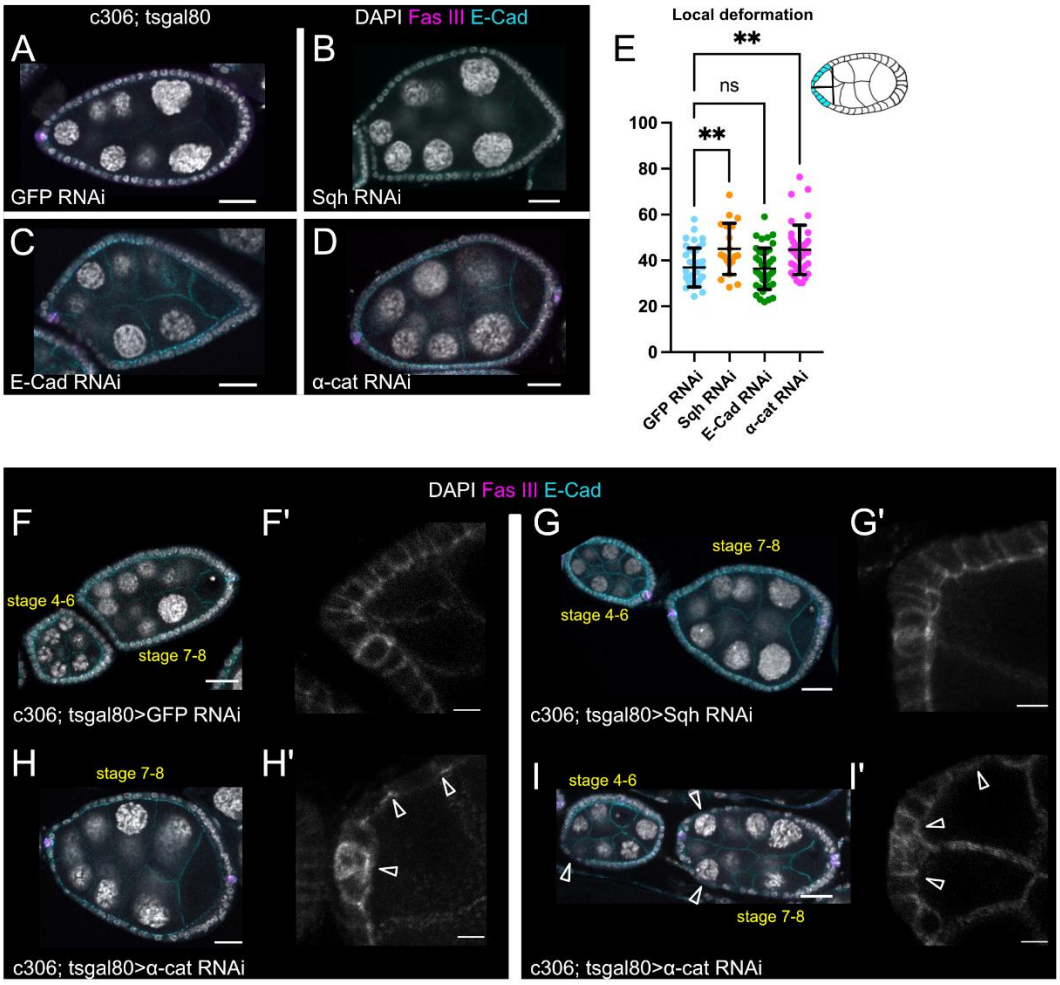

Figure 2.4 Sqh and α-Catenin maintain local tissue shape and α-Catenin is required for epithelial integrity

(A-D) Stage 7-8 GFP RNAi (A), Sqh RNAi, (B) E-Cadherin RNAi (C), and α-cat RNAi (D) egg chambers imaged for egg chamber shape. (E) Schematic and quantification of local deformation measurement. ** $p \leq 0.01$ One-way ANOVA followed by Dunnett's multiple comparisons test. $N \geq 19$ egg chambers per genotype. (F-I) GFP RNAi (F), Sqh RNAi (G), and α-cat RNAi (H-I) ovarioles imaged to show egg chamber shape and anterior epithelium. (F'-I') Maximum intensity projections of anterior regions of stage 7-8 egg chambers pictured in the main panels. Open

arrowheads in H', I, and I' indicate "stretched" or clustered cells observed in α-cat RNAi egg chambers. (A-D, F-I) Scale bars 20μm. (F'-I') Scale bars 5μm.

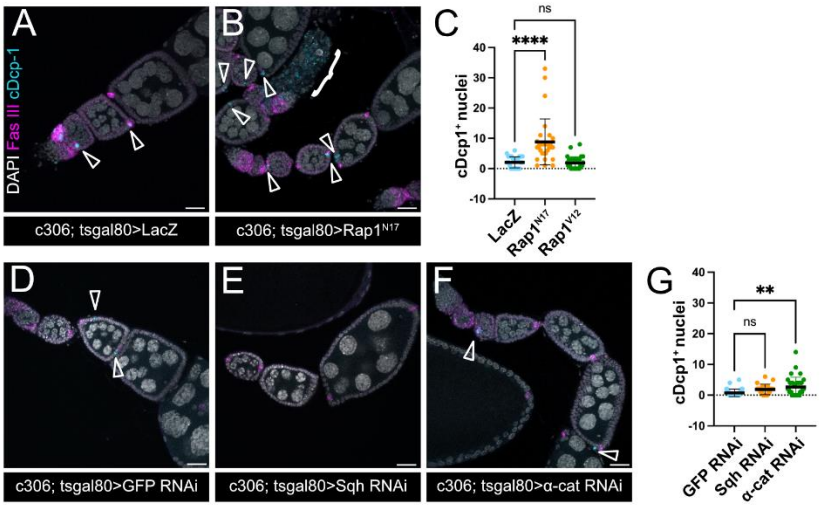

Figure 2.5 Rap1 and α-Catenin are required for cell viability during oogenesis

(A-B) Maximum intensity projections of ovarioles showing caspase positive nuclei for LacZ (A) and DN-Rap1^{N17} (B). Open arrowheads in A and B indicate cDcp1 positive nuclei and the bracket in B indicates a degenerating egg chamber. (C) Quantification of cDcp1 positive nuclei per ovariole (egg chamber stages 2-8 only). DN-Rap1^{N17} ovarioles have greater number of cDcp1 positive nuclei. **** $p \leq 0.0001$ One-way ANOVA followed by Dunnett's multiple comparisons test. $N \geq 29$ ovarioles per genotype. (D-F) Maximum intensity projections of ovarioles for GFP RNAi (D), Sqh RNAi (E), and α-cat RNAi (F). Open arrowheads indicate cDcp1 positive nuclei. (G) Quantification of cDcp1 positive nuclei. ** $p \leq 0.01$ One-way ANOVA followed by Dunnett's multiple comparisons test. $N \geq 20$ ovarioles per genotype. Scale bars 20μm.

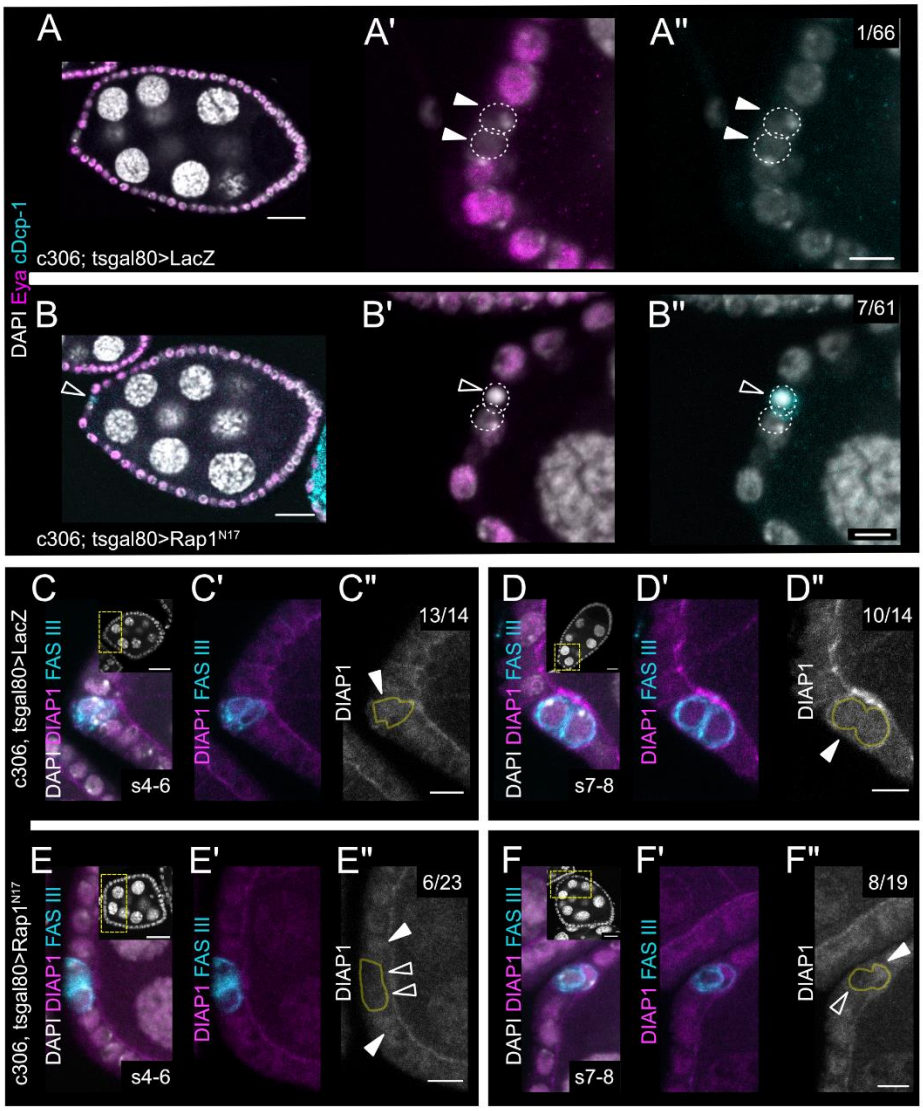

Figure 2.6 Rap1 is required for polar cell viability and proper DIAP1 accumulation

(A-B) Stage 7-8 LacZ (A) and DN-Rap1^{N17} (B) egg chambers scored for cDcp1 positive polar cells . (A', B') Close-up views of anterior regions of the egg chambers depicted in A and B, showing only DAPI and Eya staining. (A", B") Same images as A' and B' showing only DAPI and cDcp1. Filled arrowheads in A' and A" indicate viable mature polar cells. Open arrowheads in B' and B" indicate a cDcp1 positive dying polar cell. Numbers in A" and B" indicate number of observations of cDcp1 positive polar cells per stage 7-8 egg chambers scored. (C-C", E-E") Stage 4-6 LacZ (C-C") and DN-Rap1^{N17} (E-E") egg chambers. (C', E') Same images as C and E

showing only DIAP1 and FasIII. (C", E") DIAP1 only. (D-D", F-F") Stage 7-8 LacZ (D-D") and DN-Rap1^{N17} (F-F") egg chambers. (C-F) Insets show DAPI-stained whole egg chambers corresponding to zoomed regions with yellow boxes outlining the approximate region depicted in main panels. (C"-F") Polar cells are outlined in yellow. Solid arrowheads indicate normal DIAP1 accumulation. Open arrowheads indicate reduced DIAP1. The number of egg chambers with normal DIAP1 accumulation out of total egg chambers scored is reported in the upper right of C", D", E", and F". (A-F) Scale bars 20μm. (C"-F") Scale bars 5μm.

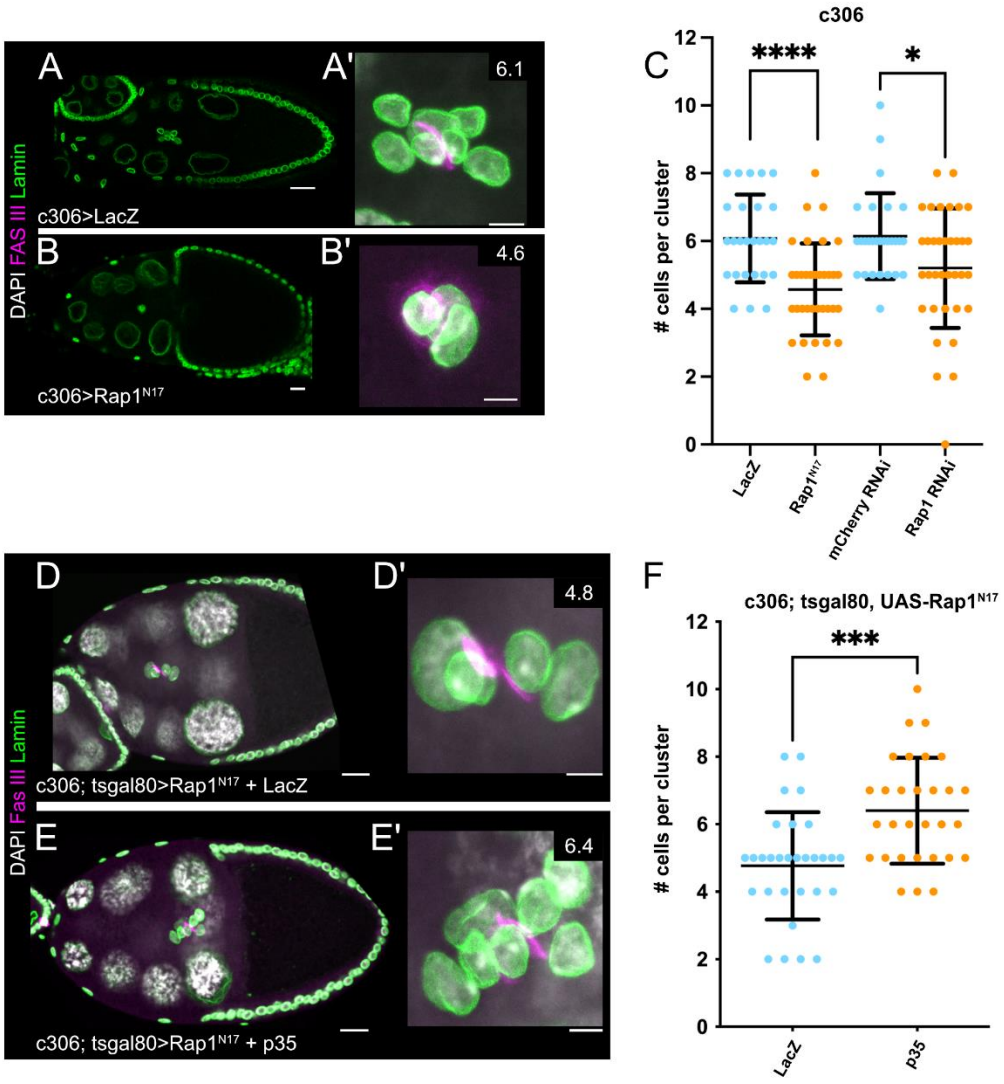

Figure 2.7 Rap1 dependent cell viability is required for proper border cell cluster assembly

(A-B) Stage 9-10 egg chambers for LacZ (A) and DN-Rap1^{N17} (B). (A'-B') Maximum intensity projections of border cell clusters from egg chambers pictured in A and B. Numbers at top right are average number of cells observed for each genotype. (C) Quantification of cell number per cluster for each genotype. * $p \leq 0.05$ **** $p \leq 0.0001$ two-tailed unpaired t test. $N \geq 26$ border cell clusters per genotype. (D-E) Stage 9-10 egg chambers for DN-Rap1^{N17} + LacZ expression control (D) or DN-Rap1^{N17} + p35 (E). (D'- E') Maximum intensity projections of border cell clusters from egg chambers pictured in D and E. Numbers at top right are average number of

cells observed for each genotype. (F) Quantification of cell number per cluster for each genotype. *** $p \leq 0.001$ two-tailed unpaired t test. N=30 border cell clusters per genotype. (A-B, D-E) Scale bars 20μm. (A'-B', D'-E') Scale bars 5μm.

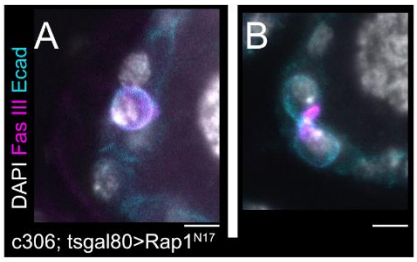

Figure 2.8 Sup. 1 Rap1 inhibition causes polar cell loss and distorted polar cell shapes

(A-B) Anterior regions of two different DN-Rap1^{N17} stage 7-8 egg chambers. (A) Only one mature polar cell is present. (B) A pair of polar cells stretched along the dorsoventral axis. Scale bars 5µm.

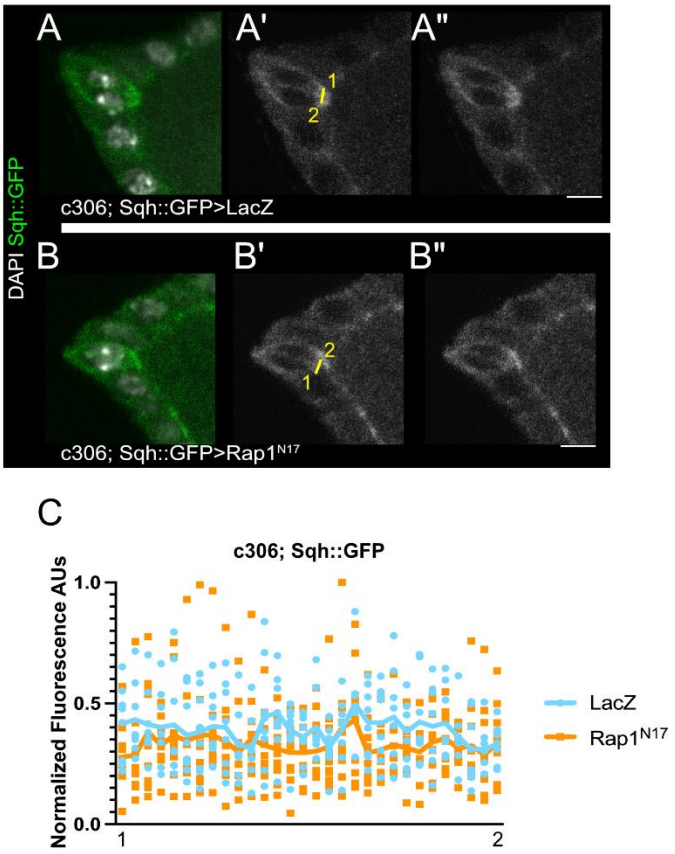

Figure 2.9 Sup. 2 Rap1 is dispensable for Sqh apical localization in polar cells

(A-B) Anterior regions of stage 7-8 egg chambers for LacZ (A) or DN-Rap1^{N17} (B). (A'-B') Single channel images of A and B showing GFP (gray) with yellow lines indicating region of measurement for Sqh::GFP intensity. The numbers correspond to the plot intensity profiles in C. (A"-B") Single channel images as in A' and B' with line removed for clarity. The image brightness was adjusted for presentation purposes but not used for quantification. (C) Profile of the intensity values along the measurement lines, plotted and normalized to highest signal. The numbers on the x-axis correspond to the lines drawn on A' and B'. Solid plot lines represent the mean intensity. N ≥ 8 egg chambers per genotype. Scale bars 5µm.

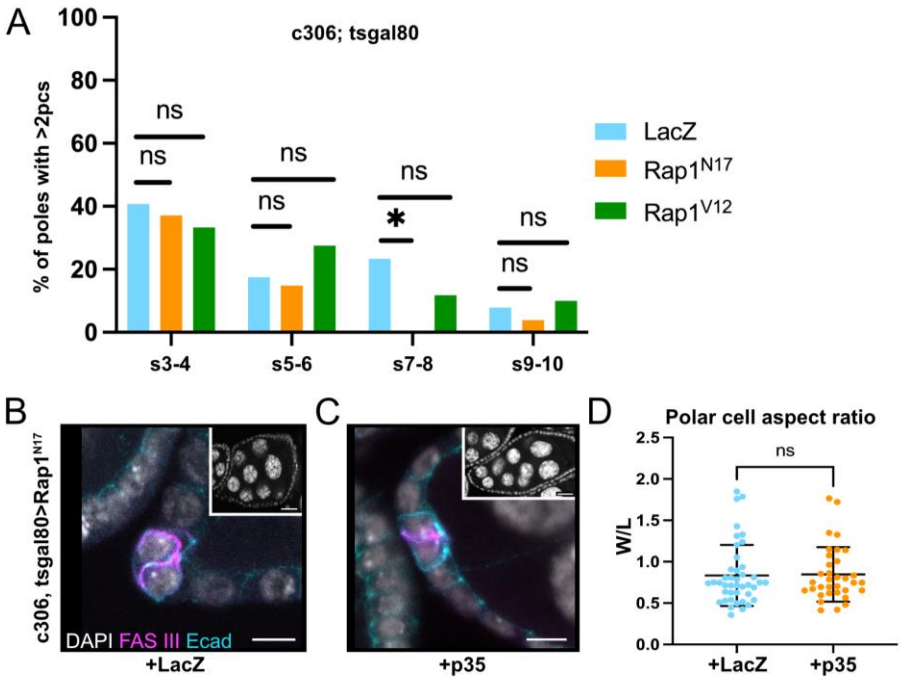

Figure 2.10 Sup. 3 Rap1 does not regulate early elimination of supernumerary polar cells and maintains mature polar cell shape independent of apoptosis

(A) Quantification showing frequency of egg chamber poles with supernumerary polar cells during specific stages of oogenesis. * p≤0.05 two-sided Fisher's exact test. N≥30 egg chamber poles per stage per genotype. Supernumerary polar cells are present early for all genotypes. (B-C) Anterior region of stage 7-8 egg chambers, DN-Rap1^{N17} with LacZ expression control (A) or DN-Rap1^{N17} with apoptosis inhibitor p35 (B). Whole egg chambers stained for DAPI are shown in the insets. (D) Polar cell aspect ratio quantification. Mean AR of DN-Rap1^{N17} + LacZ control = 0.84. Mean AR of DN-Rap1^{N17} + p35 = 0.85. NS two-tailed unpaired t test. N≥34 polar cells per genotype. Main panel scale bars 5μm. Inset scale bars 20μm.

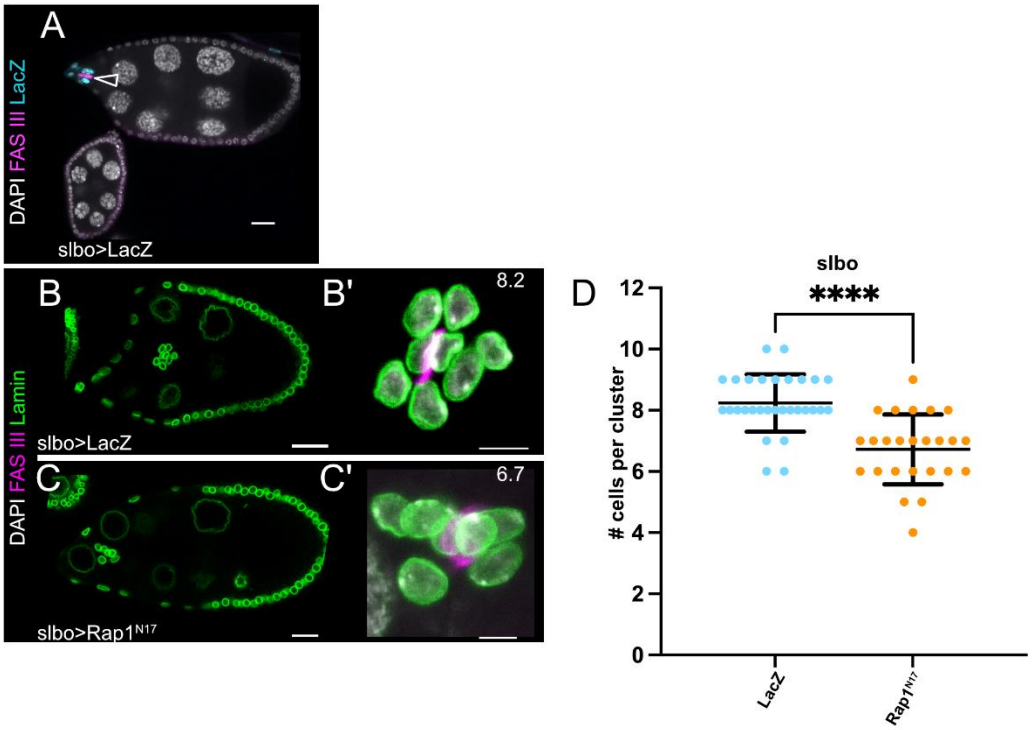

Figure 2.11 Sup. 4 Effects of late Rap1 inhibition on border cell numbers

(A) Ovariole region expressing UAS-LacZ indicates the expression pattern of *slbo*-GAL4. (B-C) Stage 9-10 LacZ (B) and DN-Rap1^{N17} (C) egg chambers showing mid-migration border cells. (B'-C') Maximum intensity projections of border cell clusters from B and C. Numbers in the upper right indicate the average number of cells per cluster. (D) Quantification of cell number per cluster for Rap1 inhibition using *slbo*-GAL4. **** $p \leq 0.0001$ two-tailed unpaired t test. $N \geq 25$ border cell clusters per genotype. (A-C) Scale bars 20µm. (B'-C') Scale bars 5µm.

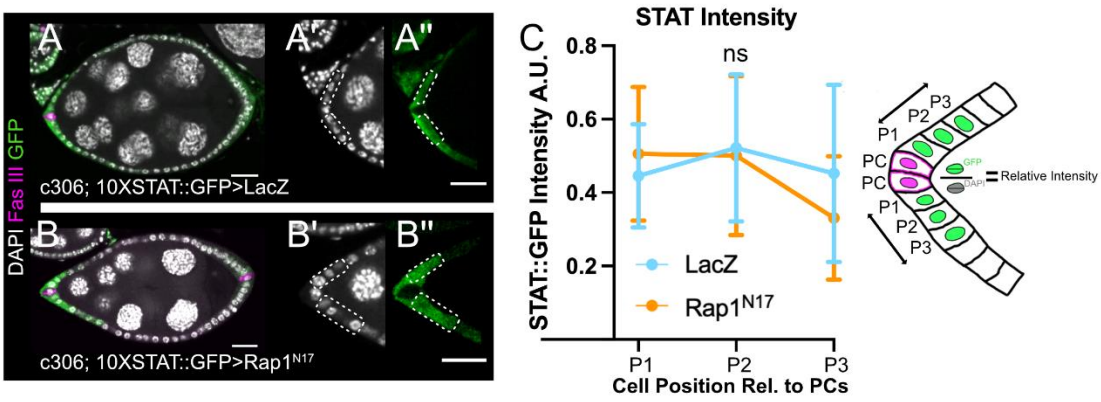

Figure 2.12 Sup. 5 Rap1 is dispensable for STAT levels in follicle cells fated to become border cells

(A, B) Stage 8 LacZ (A) and DN-Rap1^{N17} (B) egg chambers with 10XSTAT::GFP reporter expression enriched adjacent to anterior polar cells. (A'-A", B'-B") Insets of the anterior end of the egg chambers in A and B, which was used to measure the intensity of nuclear 10XSTAT::GFP. (A'-B') DAPI. (A"-B") 10XSTAT::GFP. Dashed rectangles indicate the cell positions next to polar cells used for analyzing STAT levels. (C) Schematic and plot of STAT intensity values relative to the DAPI signal and normalized to the highest intensity STAT measurement. NS, unpaired two-tailed t-test. N≥12 follicle cells at each position pooled from N≥6 stage 8 egg chambers for each genotype. (A-B) Scale bars 20μm. (A"-B") Scale bars 5μm.

Table 2.1 Fly strains used in this study.

Fly Stock	Source	Appears in Figures
c306-GAL4		7
c306-GAL4; 10XSTAT92E-GFP	M. Starz-Gaiano	S5
c306-GAL4; UAS-Rap1N17, tsgal80	This study	7, S3
c306-GAL4; Sqh::GFP	P. Majumder	S2
c306-GAL4; tsgal80	P. Majumder	1, 2, 3, 4, 5, 6, S1, S3
c306-GAL4, tsgal80; PT Fas III (GFP)	This study	6
slbo-GAL4	BDSC 58435	S4
GFP-Rap1	N. Brown	1
UAS-α-Catenin RNAi	VDRC v107298	4, 5
UAS-E-Cadherin RNAi	VDRC v103962	4
UAS-GFP RNAi	VDRC v60102	4, 5
UAS-LacZ.nls	D. Montell	1, 2, 3, 5, 6, 7, S2, S3, S4, S5
UAS-mCherry RNAi	BDSC 35785	7
UAS-p35.H	BDSC 5072	7, S3
UAS-Rap1N17	B. Boettner	1, 2, 3, 5, 6, 7, S1, S2, S3, S4, S5
UAS-Rap1 RNAi	VDRC v33437	7
UAS-Rap1V12	B. Boettner	5, S3
UAS-Sqh RNAi	VDRC v7916	4, 5

Table 2.2 Genotypes in this study.

Figure	Genotypes
1A	w; P[w+ GFP-Rap1]
1B	c306-GAL4/w; tsgal80/+; UAS-LacZ.nls/+
1C	c306-GAL4/w; tsgal80/+; UAS-LacZ.nls/+
1D	c306-GAL4/w; tsgal80/UAS-Rap1N17; TM2/+
1E	c306-GAL4/w; tsgal80/+; UAS-LacZ.nls/+
1F	c306-GAL4/w; tsgal80/UAS-Rap1N17; TM2/+
1G	c306-GAL4/w; tsgal80/+; UAS-LacZ.nls/+ c306-GAL4/w; tsgal80/UAS-Rap1N17; TM2/+
2A-A"	c306-GAL4/w; tsgal80/+; UAS-LacZ.nls/+
2B-B"	c306-GAL4/w; tsgal80/UAS-Rap1N17; TM2/+
2C	c306-GAL4/w; tsgal80/+; UAS-LacZ.nls/+ c306-GAL4/w; tsgal80/UAS-Rap1N17; TM2/+
3A-A"	c306-GAL4/w; tsgal80/+; UAS-LacZ.nls/+
3B-B"	c306-GAL4/w; tsgal80/UAS-Rap1N17; TM2/+
3C-D	c306-GAL4/w; tsgal80/+; UAS-LacZ.nls/+ c306-GAL4/w; tsgal80/UAS-Rap1N17; TM2/+
4A	c306-GAL4/w; tsgal80/UAS-GFP-RNAi
4B	c306-GAL4/w; tsgal80/UAS-Sqh-RNAi
4C	c306-GAL4/w; tsgal80/UAS-E-Cadherin-RNAi
4D	c306-GAL4/w; tsgal80/UAS-α-Catenin-RNAi
4E	c306-GAL4/w; tsgal80/UAS-GFP-RNAi c306-GAL4/w; tsgal80/UAS-Sqh-RNAi c306-GAL4/w; tsgal80/UAS-E-Cadherin-RNAi c306-GAL4/w; tsgal80/UAS-α-Catenin-RNAi
4F-F'	c306-GAL4/w; tsgal80/UAS-GFP-RNAi
4G-G'	c306-GAL4/w; tsgal80/UAS-Sqh-RNAi
4H-H'	c306-GAL4/w; tsgal80/UAS-α-Catenin-RNAi
4I-I'	c306-GAL4/w; tsgal80/UAS-α-Catenin-RNAi
5A	c306-GAL4/w; tsgal80/+; UAS-LacZ.nls/+
5B	c306-GAL4/w; tsgal80/UAS-Rap1N17; TM2/+
5C	c306-GAL4/w; tsgal80/+; UAS-LacZ.nls/+ c306-GAL4/w; tsgal80/UAS-Rap1N17; TM2/+ c306-GAL4/w; tsgal80/BL; UAS-Rap1V12/+
5D	c306-GAL4/w; tsgal80/UAS-GFP-RNAi
5E	c306-GAL4/w; tsgal80/UAS-Sqh-RNAi
5F	c306-GAL4/w; tsgal80/UAS-α-Catenin-RNAi
5G	c306-GAL4/w; tsgal80/UAS-GFP-RNAi c306-GAL4/w; tsgal80/UAS-Sqh-RNAi c306-GAL4/w; tsgal80/UAS-α-Catenin-RNAi
6A-A"	c306-GAL4/w; tsgal80/+; UAS-LacZ.nls/+
6B-B"	c306-GAL4/w; tsgal80/UAS-Rap1N17; TM2/+
6C-C"	c306-GAL4, tsgal80/w; PT Fas III (GFP)/+; UAS-LacZ.nls/+
6D-D"	c306-GAL4, tsgal80/w; PT Fas III (GFP)/+; UAS-LacZ.nls/+
6E-E"	c306-GAL4, tsgal80/w; PT Fas III (GFP)/UAS-Rap1N17; TM2/+
6F-F"	c306-GAL4, tsgal80/w; PT Fas III (GFP)/UAS-Rap1N17; TM2/+

7A-A'	c306-GAL4/w; G13, L[2]/+; UAS-LacZ.nls/+
7B-B'	c306-GAL4/w; G13, L[2]/UAS-Rap1N17; TM2/+
7C	c306-GAL4/w; G13, L[2]/+; UAS-LacZ.nls/+ c306-GAL4/w; G13, L[2]/UAS-Rap1N17; TM2/+ c306-GAL4/w; G13, L[2]/+; UAS-mCherry-RNAi/+ c306-GAL4/w; G13, L[2]/+; UAS-Rap1-RNAi/+
7D-D'	c306-GAL4/w; tsgal80, UAS-Rap1N17/+; UAS-LacZ.nls/+
7E-E'	c306-GAL4/w; tsgal80, UAS-Rap1N17/UAS-p35.H
7F	c306-GAL4/w; tsgal80, UAS-Rap1N17/+; UAS-LacZ.nls/+ c306-GAL4/w; tsgal80, UAS-Rap1N17/UAS-p35.H
S1A-B	c306-GAL4/w; tsgal80/UAS-Rap1N17; TM2/+
S2A-A"	c306-GAL4/w; Sgh::GFP/+; UAS-LacZ.nls/+
S2B-B"	c306-GAL4/w; Sqh::GFP/UAS-Rap1N17; TM2/+
S2C	c306-GAL4/w; Sqh::GFP/+; UAS-LacZ.nls/+ c306-GAL4/w; Sqh::GFP/UAS-Rap1N17; TM2/+
S3A	c306-GAL4/w; tsgal80/+; UAS-LacZ.nls/+ c306-GAL4/w; tsgal80/UAS-Rap1N17; TM2/+ c306-GAL4/w; tsgal80/BL; UAS-Rap1V12/+
S3B	c306-GAL4/w; tsgal80, UAS-Rap1N17/+; UAS-LacZ.nls/+
S3C	c306-GAL4/w; tsgal80, UAS-Rap1N17/UAS-p35.H
S3D	c306-GAL4/w; tsgal80, UAS-Rap1N17/+; UAS-LacZ.nls/+ c306-GAL4/w; tsgal80, UAS-Rap1N17/UAS-p35.H
S4A	w; slbo-GAL4/UAS-LacZ.nls
S4B-B'	w; slbo-GAL4/UAS-LacZ.nls
S4C-C'	w; UAS-Rap1N17/+; slbo-GAL4/TM2
S4D	w; slbo-GAL4/UAS-LacZ.nls w; UAS-Rap1N17/+; slbo-GAL4/TM2
S5A-A"	c306-GAL4/w; 10XSTAT92E-GFP/+; UAS-LacZ.nls/+
S5B-B"	c306-GAL4/w; 10XSTAT92E-GFP/UAS-Rap1N17; TM2/+
S5C	c306-GAL4/w; 10XSTAT92E-GFP/+; UAS-LacZ.nls/+ c306-GAL4/w; 10XSTAT92E-GFP/UAS-Rap1N17; TM2/+

Table 2.3 Antibodies used in this study.

Antibody	Concentration	Source	Appears in Figures
Dcp-1 (Asp215)	(1:50-1:100)	Cell Signaling Technology	5, 6
DE-cadherin (DCAD2)	(1:10)	DSHB	1, 2, 3, 4, S1, S3
DIAP1	(1:100)	H. D. Ryoo	6
Eya (10H6)	(1:50-1:100)	DSHB	6
Fas3 (7G10)	(1:5-1:10)	DSHB	2, 4, 5, 7, S1, S3, S4, S5
GFP (12E6)	(1:10)	DSHB	1, S2
GFP (ab13970)	(1:100)	abcam	6, S5
LacZ (40-1a)	(1:10)	DSHB	1, S4
Lamin (ADL67.10)	(1:10)	DSHB	7, S4

Secondary antibodies used at a concentration of 1:400
Alexa Fluor Chicken 488 IgG H+L
Alexa Fluor Mouse 488 IgG H+L
Alexa Fluor Mouse 488 IgG1
Alexa Fluor Mouse 568 IgG H+L
Alexa Fluor Mouse 568 IgG2a
Alexa Fluor Rabbit 647 IgG H+L
Alexa Fluor Rat 488 IgG H+L
Alexa Fluor Rat 647 IgG H+L
DAPI (Millipore Sigma) was used at 0.05 µg/ml

Table 2.4 Statistics in this study.

Figure	Experimental Unit	Measurement	Experiments per Genotype (n)	Statistical Test	Significance
1G	Egg chamber	Anterior width	≥17	Unpaired two-tailed t test	**
2C	Polar cell	Aspect ratio	≥26	Unpaired two-tailed t test	ns, ****
3C	Egg chamber	Apical E-Cad Intensity	≥10	N/A	N/A
4E	Egg chamber	Anterior width	≥19	One-way ANOVA with Dunnett's Multiple Comparisons test	ns, **
5C	Ovariole	cDcp+ nuclei	≥29	One-way ANOVA with Dunnett's Multiple Comparisons test	ns, ****
5G	Ovariole	cDcp+ nuclei	≥20	One-way ANOVA with Dunnett's Multiple Comparisons test	ns, **
7C	Border cell clusters	Cells per cluster	≥26	Unpaired two-tailed t test	*, ****
7F	Border cell clusters	Cells per cluster	30	Unpaired two-tailed t test	***
S2C	Egg chamber	Apical Sqh Intensity	≥8	N/A	N/A
S3A	Egg chamber pole	Supernumerary polar cells	≥30	Fisher's exact test	ns, *
S3D	Polar cell	Aspect ratio	≥34	Unpaired two-tailed t test	ns
S4D	Border cell clusters	Cells per cluster	≥25	Unpaired two-tailed t test	****
S5C	Nucleus	Stat reporter intensity	≥12	Unpaired two-tailed t test	ns

Significance values: * $P \leq 0.05$, ** $P \leq 0.01$, *** $P \leq 0.001$, **** $P < 0.0001$.

2.7 References

Abramson, J. and Anderson, G. (2017). Thymic Epithelial Cells. *Annu. Rev. Immunol.* **35**, 85–118.

Asha, H., de Ruiter, N., Wang, M. and Hariharan, I. (1999). The Rap1 GTPase functions as a regulator of morphogenesis invivo. *The EMBO Journal* **18**, 605–615.

Bach, E. A., Ekas, L. A., Ayala-Camargo, A., Flaherty, M. S., Lee, H., Perrimon, N. and Baeg, G.-H. (2007). GFP reporters detect the activation of the Drosophila JAK/STAT pathway in vivo. *Gene Expression Patterns* **7**, 323–331.

Bai, J. and Montell, D. (2002). Eyes Absent, a key repressor of polar cell fate during *Drosophila* oogenesis. *Development* **129**, 5377–5388.

Balaji, R., Weichselberger, V. and Classen, A.-K. (2019). Response of epithelial cell and tissue shape to external forces *in vivo*. *Development* dev.171256.

Baum, J. S., Arama, E., Steller, H. and McCall, K. (2007). The Drosophila caspases Strica and Dronc function redundantly in programmed cell death during oogenesis. *Cell Death Differ* **14**, 1508–1517.

Beccari, S., Teixeira, L. and Rørth, P. (2002). The JAK/STAT pathway is required for border cell migration during Drosophila oogenesis. *Mechanisms of Development* **111**, 115–123.

Besse, F. and Pret, A.-M. (2003). Apoptosis-mediated cell death within the ovarian polar cell lineage of *Drosophila melanogaster*. *Development* **130**, 1017–1027.

Blanpain, C. and Fuchs, E. (2009). Epidermal homeostasis: a balancing act of stem cells in the skin. *Nat Rev Mol Cell Biol* **10**, 207–217.

Boettner, B. and Van Aelst, L. (2007). The Rap GTPase Activator *Drosophila* PDZ-GEF Regulates Cell Shape in Epithelial Migration and Morphogenesis. *Mol Cell Biol* **27**, 7966–7980.

Boettner, B., Harjes, P., Ishimaru, S., Heke, M., Fan, H. Q., Qin, Y., Van Aelst, L. and Gaul, U. (2003). The AF-6 Homolog Canoe Acts as a Rap1 Effector During Dorsal Closure of the Drosophila Embryo. *Genetics* **165**, 159–169.

Bonello, T. T., Perez-Vale, K. Z., Sumigray, K. D. and Peifer, M. (2018). Rap1 acts via multiple mechanisms to position Canoe/Afadin and adherens junctions and mediate apical-basal polarity establishment. *Development* dev.157941.

Borensztejn, A., Boissoneau, E., Fernandez, G., Agnès, F. and Pret, A.-M. (2013). JAK/STAT autocontrol of ligand-producing cell number through apoptosis. *Development* **140**, 195–204.

Borensztejn, A., Mascaro, A. and Wharton, K. A. (2018). JAK/STAT signaling prevents excessive apoptosis to ensure maintenance of the interfollicular stalk critical for Drosophila oogenesis. *Developmental Biology* **438**, 1–9.

Bröer, S. (2008). Amino Acid Transport Across Mammalian Intestinal and Renal Epithelia. *Physiological Reviews* **88**, 249–286.

Cai, D., Dai, W., Prasad, M., Luo, J., Gov, N. S. and Montell, D. J. (2016). Modeling and analysis of collective cell migration in an in vivo three-dimensional environment. *Proc Natl Acad Sci U S A* **113**, E2134-2141.

Choi, W., Harris, N. J., Sumigray, K. D. and Peifer, M. (2013). Rap1 and Canoe/afadin are essential for establishment of apical–basal polarity in the *Drosophila* embryo. *MBoC* **24**, 945–963.

Clem, R. J., Fechheimer, M. and Miller, L. K. (1991). Prevention of Apoptosis by a Baculovirus Gene During Infection of Insect Cells. *Science* **254**, 1388–1390.

Crest, J., Diz-Muñoz, A., Chen, D.-Y., Fletcher, D. A. and Bilder, D. (2017). Organ sculpting by patterned extracellular matrix stiffness. *eLife* **6**, e24958.

Duhart, J. C., Parsons, T. T. and Raftery, L. A. (2017). The repertoire of epithelial morphogenesis on display: Progressive elaboration of Drosophila egg structure. *Mechanisms of Development* **148**, 18–39.

Duszyc, K., Gomez, G. A., Schroder, K., Sweet, M. J. and Yap, A. S. (2017). In life there is death: How epithelial tissue barriers are preserved despite the challenge of apoptosis. *Tissue Barriers* **5**, e1345353.

Gloerich, M. and Bos, J. L. (2011). Regulating Rap small G-proteins in time and space. *Trends in Cell Biology* **21**, 615–623.

Guillot, C. and Lecuit, T. (2013). Mechanics of Epithelial Tissue Homeostasis and Morphogenesis. *Science* **340**, 1185–1189.

Haigo, S. L. and Bilder, D. (2011). Global Tissue Revolutions in a Morphogenetic Movement Controlling Elongation. *Science* **331**, 1071–1074.

Haigo, S. L., Hildebrand, J. D., Harland, R. M. and Wallingford, J. B. (2003). Shroom Induces Apical Constriction and Is Required for Hingepoint Formation during Neural Tube Closure. *Current Biology* **13**, 2125–2137.

Harris, T. J. C. and Tepass, U. (2010). Adherens junctions: from molecules to morphogenesis. *Nat Rev Mol Cell Biol* **11**, 502–514.

Hay, B. A., Wolff, T. and Rubin, G. M. (1994). Expression of baculovirus P35 prevents cell death in Drosophila. *Development* **120**, 2121–2129.

Hay, B. A., Wassarman, D. A. and Rubin, G. M. (1995). Drosophila homologs of baculovirus inhibitor of apoptosis proteins function to block cell death. *Cell* **83**, 1253–1262.

Irvine, K. D. and Wieschaus, E. (1994). Cell intercalation during Drosophila germband extension and its regulation by pair-rule segmentation genes. *Development* **120**, 827–841.

Keller, R. E. (1981). An experimental analysis of the role of bottle cells and the deep marginal zone in gastrulation ofXenopus laevis. *J. Exp. Zool.* **216**, 81–101.

Khammari, A., Agnès, F., Gandille, P. and Pret, A.-M. (2011). Physiological apoptosis of polar cells during Drosophila oogenesis is mediated by Hid-dependent regulation of Diap1. *Cell Death Differ* **18**, 793–805.

Kim, Y. S., Fan, R., Lith, S. C., Dicke, A.-K., Drexler, H. C. A., Kremer, L., Kuempel-Rink, N., Hekking, L., Stehling, M. and Bedzhov, I. (2022). Rap1 controls epiblast morphogenesis in sync with the pluripotency states transition. *Developmental Cell* **57**, 1937-1956.e8.

Knox, A. L. and Brown, N. H. (2002). Rap1 GTPase Regulation of Adherens Junction Positioning and Cell Adhesion. *Science* **295**, 1285–1288.

Lebo, D. P. V. and McCall, K. (2021). Murder on the Ovarian Express: A Tale of Non-Autonomous Cell Death in the Drosophila Ovary. *Cells* **10**, 1454.

Li, M., Sun, S., Priest, J., Bi, X. and Fan, Y. (2019). Characterization of TNF-induced cell death in Drosophila reveals caspase- and JNK-dependent necrosis and its role in tumor suppression. *Cell Death Dis* **10**, 613.

Loyer, N., Kolotuev, I., Pinot, M. and Le Borgne, R. (2015). *Drosophila* E-cadherin is required for the maintenance of ring canals anchoring to mechanically withstand tissue growth. *Proc. Natl. Acad. Sci. U.S.A.* **112**, 12717–12722.

Martin, A. C. and Goldstein, B. (2014). Apical constriction: themes and variations on a cellular mechanism driving morphogenesis. *Development* **141**, 1987–1998.

Martin, A. C., Kaschube, M. and Wieschaus, E. F. (2009). Pulsed contractions of an actin–myosin network drive apical constriction. *Nature* **457**, 495–499.

McGuire, S. E., Mao, Z. and Davis, R. L. (2004). Spatiotemporal gene expression targeting with the TARGET and gene-switch systems in Drosophila. *Sci STKE* **2004**, pl6.

Munjal, A. and Lecuit, T. (2014). Actomyosin networks and tissue morphogenesis. *Development* **141**, 1789–1793.

Niewiadomska, P., Godt, D. and Tepass, U. (1999). DE-Cadherin Is Required for Intercellular Motility during Drosophila Oogenesis. *Journal of Cell Biology* **144**, 533–547.

Osswald, M., Barros-Carvalho, A., Carmo, A. M., Loyer, N., Gracio, P. C., Sunkel, C. E., Homem, C. C. F., Januschke, J. and Morais-de-Sá, E. (2022). aPKC regulates apical constriction to prevent tissue rupture in the Drosophila follicular epithelium. *Current Biology* S0960982222013859.

Peifer, M., Orsulic, S., Sweeton, D. and Wieschaus, E. (1993). A role for the Drosophila segment polarity gene armadillo in cell adhesion and cytoskeletal integrity during oogenesis. *Development* **118**, 1191–1207.

Perez-Vale, K. Z., Yow, K. D., Johnson, R. I., Byrnes, A. E., Finegan, T. M., Slep, K. C. and Peifer, M. (2021). Multivalent interactions make adherens junction–cytoskeletal linkage robust during morphogenesis. *Journal of Cell Biology* **220**, e202104087.

Perez-Vale, K. Z., Yow, K. D., Gurley, N. J., Greene, M. and Peifer, M. (2022). Rap1 regulates apical contractility to allow embryonic morphogenesis without tissue disruption and acts in part via Canoe-independent mechanisms. *MBoC* mbc.E22-05-0176.

Potla, U., Ni, J., Vadaparampil, J., Yang, G., Leventhal, J. S., Campbell, K. N., Chuang, P. Y., Morozov, A., He, J. C., D'Agati, V. D., et al. (2014). Podocyte-specific RAP1GAP expression contributes to focal segmental glomerulosclerosis–associated glomerular injury. *J. Clin. Invest.* **124**, 1757–1769.

Royou, A., Field, C., Sisson, J. C., Sullivan, W. and Karess, R. (2004). Reassessing the Role and Dynamics of Nonmuscle Myosin II during Furrow Formation in Early *Drosophila* Embryos. *MBoC* **15**, 838–850.

Ruohola, H., Bremer, K. A., Baker, D., Swedlow, J. R., Jan, L. Y. and Jan, Y. N. (1991). Role of neurogenic genes in establishment of follicle cell fate and oocyte polarity during oogenesis in Drosophila. *Cell* **66**, 433–449.

Sarpal, R., Pellikka, M., Patel, R. R., Hui, F. Y. W., Godt, D. and Tepass, U. (2012). Mutational analysis supports a core role for *Drosophila* α-Catenin in adherens junction function. *Journal of Cell Science* **125**, 233–245.

Sasaki, K., Kojitani, N., Hirose, H., Yoshihama, Y., Suzuki, H., Shimada, M., Takayanagi, A., Yamashita, A., Nakaya, M., Hirano, H., et al. (2020). Shank2 Binds to aPKC and Controls Tight Junction Formation with Rap1 Signaling during Establishment of Epithelial Cell Polarity. *Cell Reports* **31**, 107407.

Sawant, K., Chen, Y., Kotian, N., Preuss, K. M. and McDonald, J. A. (2018). Rap1 GTPase promotes coordinated collective cell migration in vivo. *MBoC* **29**, 2656–2673.

Sawyer, J. K., Harris, N. J., Slep, K. C., Gaul, U. and Peifer, M. (2009). The Drosophila afadin homologue Canoe regulates linkage of the actin cytoskeleton to adherens junctions during apical constriction. *Journal of Cell Biology* **186**, 57–73.

Schindelin, J., Arganda-Carreras, I., Frise, E., Kaynig, V., Longair, M., Pietzsch, T., Preibisch, S., Rueden, C., Saalfeld, S., Schmid, B., et al. (2012). Fiji: an open-source platform for biological-image analysis. *Nat Methods* **9**, 676–682.

Silver, D. L. and Montell, D. J. (2001). Paracrine Signaling through the JAK/STAT Pathway Activates Invasive Behavior of Ovarian Epithelial Cells in Drosophila. *Cell* **107**, 831–841.

Spahn, P., Ott, A. and Reuter, R. (2012). The PDZ-GEF Dizzy regulates the establishment of adherens junctions required for ventral furrow formation in *Drosophila*. *Journal of Cell Science* jcs.101196.

Spradling A. C. (1993). Developmental genetics of oogenesis. In *The Development of Drosophila Melanogaster*, pp. 1-70. CSHL Press.

Starz-Gaiano, M., Melani, M., Wang, X., Meinhardt, H. and Montell, D. J. (2008). Feedback Inhibition of JAK/STAT Signaling by Apontic Is Required to Limit an Invasive Cell Population. *Developmental Cell* **14**, 726–738.

Stonko, D. P., Manning, L., Starz-Gaiano, M. and Peercy, B. E. (2015). A mathematical model of collective cell migration in a three-dimensional, heterogeneous environment. *PLoS One* **10**, e0122799.

Tai, K., Cockburn, K. and Greco, V. (2019). Flexibility sustains epithelial tissue homeostasis. *Current Opinion in Cell Biology* **60**, 84–91.

Wang, Y.-C., Khan, Z. and Wieschaus, E. F. (2013). Distinct Rap1 Activity States Control the Extent of Epithelial Invagination via α-Catenin. *Developmental Cell* **25**, 299–309.

Wang, A., Dunn, A. R. and Weis, W. I. (2022). Mechanism of the cadherin–catenin F-actin catch bond interaction. *eLife* **11**, e80130.

Williams-Masson, E. M., Malik, A. N. and Hardin, J. (1997). An actin-mediated two-step mechanism is required for ventral enclosure of the C. elegans hypodermis. *Development* **124**, 2889–2901.

Yan, N., Wu, J.-W., Chai, J., Li, W. and Shi, Y. (2004). Molecular mechanisms of DrICE inhibition by DIAP1 and removal of inhibition by Reaper, Hid and Grim. *Nat Struct Mol Biol* **11**, 420–428.

Yonemura, S., Wada, Y., Watanabe, T., Nagafuchi, A. and Shibata, M. (2010). α-Catenin as a tension transducer that induces adherens junction development. *Nat Cell Biol* **12**, 533–542.

Chapter 3 - An X chromosome deficiency screen for Rap1 GTPase dominant interacting genes in *Drosophila* border cell migration

C. Luke Messer and Jocelyn A. McDonald

Division of Biology, Kansas State University, Manhattan, KS 66506

In preparation for submission

3.1 Abstract

Collective cell migration is critical to embryonic development, wound healing, the immune response, and acts as a driver of tumor dissemination. Understanding how collectives coordinate migration in-vivo is a challenge with therapeutic benefits ranging from addressing developmental defects to designing cancer treatments. Small GTPases have distinct activity states acting as molecular switches that link extracellular signals to organized cell behaviors. The small GTPase Rap1 contributes to both embryogenesis and cancer cell migration. How active Rap1 coordinates downstream signaling functions required for coordinated collective migration is poorly understood. *Drosophila* border cells undergo a stereotyped and genetically tractable in-vivo migration within the developing egg chamber of the ovary. This group of 6-8 cells migrates through a densely packed tissue microenvironment and serves as an excellent model for collective cell migration during development or disease. Proper regulation of Rap1 activity states is essential for successful border cell migration. Using the known requirement for Rap1 in border cell migration we conducted a dominant suppressor screen for genes whose heterozygous loss modifies the migration defects observed upon constitutively active $Rap1^{V12}$ expression. Here we identified seven genomic regions on the *X* chromosome that interact with $Rap1^{V12}$. Further, we mapped three of these interacting regions down to single genes. This screening approach provides high confidence hits as well as additional regions that can be refined to single gene resolution.

3.2 Introduction

Cell migration is critical to metazoan development, homeostasis and contributes to pathological processes ranging from arthritis to cancer (Ridley et al., 2003). Directed cell migration is a

cyclical process. Coordinated movement first requires cell polarization in response to a stimulus or guidance cue. Generation of membrane protrusions at the newly established leading edge then works alongside cell-substrate attachment to generate forces required for locomotion. Finally, release of adhesive attachments at the rear allows efficient migration (Lauffenburger and Horwitz, 1996).

Complex regulatory mechanisms govern the seemingly simple processes required for cell migration. Linking external guidance cues to intracellular reorganization required for cell migration relies on several additional players. Cell-substrate adhesion and actin-rich protrusions are two of the most obvious examples. Endocytic transport is one regulatory node facilitating guidance cue processing and cell adhesion molecule turnover (Ulrich and Heisenberg, 2009). Similarly, small GTPases like Rho and Rac often lie between receptor activation at the plasma membrane and actin nucleation required to generate protrusions (Insall and Machesky, 2009). Therefore, a carefully managed program linking guidance cues to cellular response is required for efficient migration.

Cells migrating as collectives similarly require careful regulation of actin-rich protrusions and adhesion molecules but face the challenge of coordinating these behaviors across the entire group. Collectively migrating cells must establish leader-follower dynamics that requires the careful restriction of protrusions to the leading edge. Collectives also maintain cell-cell linkages required to keep cells together and transmit information from one side of the cluster to the other (Friedl and Gilmour, 2009; Roberto and Emery, 2022; Scarpa and Mayor, 2016). Despite the advances made in the field of cell migration, how collectives respond to external factors and coordinate behavior across the group to migrate efficiently towards their destination remains poorly understood.

Small GTPases act as molecular switches with discrete “on” and “off” states. GTPases are active when bound to GTP and inactive when bound to GDP. GTPase activating proteins (GAPs) speed up GTP hydrolysis and result in inactive, GDP bound GTPases. Guanine nucleotide exchange factors (GEFs) conversely promote dissociation of GDP allowing GTP to bind. Once active, GTPases signal through numerous downstream effectors to coordinate cellular functions including collective migration (Cherfils and Zeghouf, 2013; Zegers and Friedl, 2014). The well-conserved Ras-related small GTPase Rap1 has roles ranging from axon guidance in the *Drosophila* nervous system to breast cancer cell migration, but context-specific Rap1 effector molecules remain poorly understood (McSherry et al., 2011; Yang et al., 2016).

Rap1 is required for *Drosophila* border cell migration, a genetically tractable in-vivo model of collective cell migration. A group of 4-8 epithelial cells are specified and recruited as a migratory cohort during stages 8-9 of oogenesis, and then migrate between germline derived nurse cells to reach the oocyte boundary by stage 10. This process requires integration of guidance cues and Rac1 GTPase activation leading to productive protrusions at the cluster leading edge (Montell et al., 2012; Roberto and Emery, 2022; Saadin and Starz-Gaiano, 2016; Scarpa and Mayor, 2016). Rap1 regulates actomyosin polarity, helps restrict protrusions to the leading edge, and contributes to proper E-Cadherin enrichment within the cluster (Chang et al., 2018; Sawant et al., 2018). We know very little however, about the downstream effectors involved in these Rap1 dependent processes.

Here we performed a genetic interaction screen to identify downstream targets of Rap1 and other interacting genes. We took advantage of the strong border cell migration defects caused by expression of constitutively active Rap1 ($Rap1^{V12}$) to conduct an unbiased modifier screen (Chang et al., 2018; Sawant et al., 2018). Using the first chromosome deficiency kit,

which removes ~98% of the *X* chromosome, we identified seven deficiency regions that dominantly suppressed the $Rap1^{V12}$ migration defects. We mapped three of the deficiency interacting regions to individual genes. Specifically, we identified *frizzled 4 (fz4), Ubiquitin specific protease 16/45 (Usp16-45),* and *strawberry notch (sno)* as genes whose heterozygous loss strongly modified the $Rap1^{V12}$ induced border cell migration defect. Furthermore, we found that loss of *Usp16-45* and *sno* on their own also impaired border cell migration. These results thus identify three genes and four additional genetic interacting regions that represent previously uncharacterized Rap1 interacting genes.

3.3 Results and Discussion

An unbiased dominant interaction screen of the *X* chromosome identifies seven Rap1-interacting genomic regions

Proper regulation of Rap1 activity is critical to Rap1 function in border cell migration. Expression of constitutively active Rap1 ($Rap1^{V12}$) strongly impedes border cell migration and results in ectopic protrusions and altered E-Cadherin enrichment. These results demonstrate a requirement for Rap1 in generating productive protrusions and managing cell-cell adhesions in migration but Rap1 effector molecules in this context remain unclear (Chang et al., 2018; Sawant et al., 2018).

For the primary screen we used the Bloomington Drosophila Stock Center (BDSC) *X* chromosome deficiency kit (DK1), which consists of 93 lines and covers ~98% of the euchromatic *X* (Cook et al., 2012). Of the 93 lines within the kit 21 were untested due to complicated genetics or health issues resulting in an estimated 87% coverage of the *X*. We crossed the remaining female lines bearing *X* chromosome deficiencies to a male stock

expressing *CA-Rap1*^{V12} driven by a border cell specific driver *slbo-GAL4* (Figure 3.1 A). As a control, a stock expressing *slbo>Rap1*^{V12} was outcrossed to the *w*^{1118} strain, which is mutant for *white* and causes white eyes but is presumably otherwise wild type (Figure 3.1 A, D). Progeny expressing *CA-Rap1*^{V12} under control of *slbo-GAL4* in a *w*^{1118} background ("*slbo>Rap1*^{V12} + *w1118*") exhibited very strong border cell migration defects, with border cell clusters that pass the midpoint of migration only 22% of the time (Figure 3.1 A, B, D; Table 3.1). By contrast, *slbo-GAL4* driven expression of *mCD8GFP* in a *w*^{1118} background ("*slbo>mCD8GFP* + *w1118*") resulted in minimal defects with 96% of clusters passing the midpoint of migration (Figure 3.1 B, C). We used the strong migration defects observed for *slbo>Rap1*^{V12} border cells to screen for deficiencies on the *X* chromosome that partially restored migration. We considered a hit as a deficiency that restored migration past the halfway point to the oocyte in at least 50% of border cell clusters examined (Figure 3.1 A, E).

Using these methods, we identified seven deficiency regions that restored migration to the *slbo>Rap1*^{V12} background (Figure 3.1 B, D-E; Table 3.1). Each of these deficiencies results in complete or partial deletion of tens of genes. Using smaller deficiencies and available alleles we were able to map three of these regions to single gene interactions. We targeted each candidate with RNAi to independently assess its requirement in border cell migration as compared to a GFP RNAi control. A migration defect in this case is assessed as a border cell cluster that fails to reach ≥75% of migration by stage 10.

Mapping the Df(1)Sxl-bt region reveals an interaction between Rap1 and *fz4*

The strongest hit in this screen, *Df(1)Sxl-bt* (BDSC 3196) caused *slbo>Rap1*^{V12} border cell clusters to migrate past the midpoint 77% of the time (Figure 3.1 B, D, E; Table 3.1). This

deficiency removes an estimated 191-321kb (X:6,987,188-X:7,307,939) along the X chromosome resulting in the predicted deletion of 28 genes (Flybase; Figure 3.2 A). We next used a smaller deficiency *Df(1)BSC867* (BDSC 29990; X:6,981,859-X:7,041,515) to further refine the gene region (Flybase; Figure 3.2 A). Border cell clusters expressing *slbo>Rap1*^{V12} and heterozygous for *Df(1)BSC867* migrated past the midpoint only 14% of the time (Figure 3.2 C). We therefore considered it unlikely that Rap1 interacting genes reside on this segment of *Df(1)Sxl-bt*. We next focused on the region extending from the end of *Df(1)BSC867* to the end of *Df(1)Sxl-bt* (X:7,041,515-X:7,307,939). We screened this 266kb region for genes that are likely to contribute to border cell migration and have available alleles. We then tested *Sex lethal* (*Sxl)*, *Sxl*^{f2}, and *frizzled 4 (fz4), fz4*$^{3-1}$. Border cells migrated past the midpoint in only 1% of egg chambers scored for *slbo>Rap1*^{V12} *+ Sxl*^{f2} (Figure 3.2 C). Border cells for *slbo>Rap1*^{V12} *+ fz4*$^{3-1}$ egg chambers migrated much better, however, with 46% of clusters examined migrating past the midpoint compared to 18% in matched controls (Figure 3.2 B-C; Table 3.2; $p<0.0001$, Chi-squared test).

Single cell RNA sequencing data from the Fly Cell Atlas project revealed expression of *fz4* in both somatic and germline cells of the ovary indicating that *fz4* is expressed in the relevant tissue (Li et al., 2022). To determine whether *fz4* is required for border cell migration we assessed migration defect in the homozygous viable *fz4*$^{3-1}$ allele looking for border cell clusters that failed to reach 75% of egg chamber length by stage 10. We observed migration defects for only 3% of *fz4*$^{3-1}$ mutant border cell clusters scored compared to 2% in homozygous *w*^{1118} controls (Figure 3.2 C). We then targeted *fz4* with RNAi using two independent, non-overlapping RNAi lines (BDSC 64990, VDRC 102339) expressed under the control of a strong follicle cell driver, *c306-GAL4*. BDSC 64990 had no border cell clusters that failed to reach 75% of egg

chamber length (Figure 3.2 C). Similarly, VDRC 102339 resulted in a mild 5% migration defect that resembled the 3% defect observed in GFP RNAi controls (Figure 3.2 C; Table 3.3). We conclude that *fz4* on its own is dispensable for the ability of border cells to complete their migration to the oocyte.

Fz4 is a member of the Frizzled family of proteins that act as receptors for secreted Wnt proteins (Huang and Klein, 2004). Wnt inhibitor of Dorsal (WntD/Wnt8) and Wnt4 both bind Fz4 (Gordon et al., 2005; McElwain et al., 2011; Wu and Nusse, 2002). WntD functions in the Toll-Dorsal pathway to pattern the gastrulating embryo but has limited expression in ovarian follicle cells (Ganguly et al., 2005; Li et al., 2022; Rahimi et al., 2016). Wnt4, however, contributes to cell movement in the pupal ovary and is required for border cell migration (Cohen et al., 2002; Kotian et al., 2021). The role for Wnt4 in border cell migration however may be independent of Fz4 as Fz4 is not required for migration. Alternatively, Wnt4 may bind multiple Frizzled proteins to coordinate its function in border cell migration. Indeed, Wnt4 can bind both Fz and Fz2 in addition to Fz4 (Wu and Nusse, 2002).

It is unclear in this case how *fz4* heterozygosity restored migration to border cell clusters expressing $Rap1^{V12}$. Notably $Rap1^{V12}$ border cell clusters accumulate excessive E-Cadherin at the cluster periphery (Sawant et al., 2018). It is possible that Wnt4 through Fz4 regulates adhesion in migratory border cells (Cohen et al., 2002; Kotian et al., 2021). Loss of *fz4*, therefore, may be sufficient to modify the adhesion defects caused by $Rap1^{V12}$, but insufficient to cause border cell migration defects on its own.

Mapping the Df(1)BSC533 region reveals an interaction between Rap1 and *Usp16-45*

Df(1)BSC533 (BDSC 25061) covers ~146kb (X:5,282,581-X:5,428,543) along the *X* chromosome and results in the predicted deletion of 21 genes (Flybase; Figure 3.3 A). Border cell clusters expressing *slbo>Rap1*^{V12} and heterozygous for *Df(1)BSC533* migrated past the midpoint 59% of the time (Figure 3.1 B; Table 3.1). We found that overlapping deficiencies *Df(1)BSC823* (BDSC 27584; X:5,282,581-X:5,332,808) and *Df(1)Exel6290* (BDSC 7753; X:5,364,532-5,428,543) also interact with *slbo>Rap1*^{V12} (Flybase; Figure 3.3 A, D). *Df(1)Exel6290* was stronger, however, and led us to focus on this segment of *Df(1)BSC533* (Figure 3.3 D). Screening this region for genes with available alleles led us to uncover *Ubiquitin specific protease 16/45 (Usp16-45).* A point mutation allele for this gene, *Usp16-45*$^{[B]}$, was able to partially replicate the interaction observed for this deficiency with *Rap1*^{V12}. Border cells migrated past the midpoint in 52% of *slbo>Rap1*^{V12} + *Usp16-45*^{B} egg chambers compared to 19% in matched controls (Figure 3.3 B, D; Table 3.2; $p<0.0001$, Chi-squared test).

Usp16-45 is a member of the Ubiquitin Specific Proteases (USP) sub-family of deubiquitinases (Clague et al., 2019). While Usp16-45 has no known roles in cell migration, the family member USP22 (non-stop) is required for border cell migration (Badmos et al., 2021). Single cell RNA sequencing data from the Fly Cell Atlas project revealed expression of *Usp16-45* in both somatic and germline cells of the ovary, indicating that *Usp16-45* is expressed in the relevant tissue (Li et al., 2022). To determine whether Usp16-45 is required for border cell migration we expressed RNAi under control of *c306-GAL4*. Two independent, non-overlapping RNAi constructs (VDRC 41976 and VDRC 110286) provided mixed results. VDRC 41976 RNAi expression resulted in moderately strong migration defects, with 24% of border cell clusters failing to reach 75% egg chamber length by stage 10 (Figure 3.3 C, D; Table 3.3). This value is significantly different than the 3% defect observed in controls (Figure 3.3 D; Table 3.3;

p<0.0001, Chi-squared test). VDRC 110286 RNAi, however, resulted in minimal (2%) migration defects (Figure 3.3 D; Table 3.3). Although VDRC 110286 failed to impact migration, it is possible that VDRC 41976 results in more efficient knockdown of *Usp16-45*. Furthermore, no off-targets are predicted for VDRC 41976 suggesting that the phenotypes observed are produced by specific *Usp16-45* knockdown. Given the dominant genetic interaction of a *Usp16-45* mutant allele with $Rap1^{V12}$ and the phenotypes caused by VDRC 41976 RNAi, we conclude that *Usp16-45* is required for border cell migration.

Usp16-45 has predicted cysteine-type deubiquitinase activity (FlyBase; Komander et al., 2009). Small GTPases like Rap1 are often regulated by post-translational modifications (Konstantinopoulos et al., 2007). Post-translational modification at the CAAX domain, for example, can facilitate membrane targeting of GTPases (Konstantinopoulos et al., 2007). Ubiquitination is a mode of post-translational modification that can regulate small GTPase stability, activity, and localization (Lei et al., 2021). Ubiquitination of endocytic GTPase Rab7, for example, results in enrichment at the membrane. The ubiquitin specific protease USP32 is required to release membrane localization and allow Rab7 function (Sapmaz et al., 2019). It is unclear whether Usp16-45 directly targets Rap1. PDZ-GEF1, an activating guanine nucleotide exchange factor for Rap1 whose ortholog PDZ-GEF (also known as Dizzy) is required for border cell migration, is known to be targeted for ubiquitination (Kim et al., 2015; Sawant et al., 2018). These data suggest that the addition or removal of ubiquitin could be critical in regulating Rap1 signaling in border cells. Further work will be required to determine if Usp16-45 targets Rap1 directly, a signaling partner such as PDZ-GEF, or another protein functioning with Rap1.

Mapping the Df(1)ED7170 region reveals an interaction between Rap1 and *sno*

Df(1)ED7170 (BDSC 8898) removes ~525kb (X:12,752,602-13,277,326) along the X (Flybase; Figure 3.4 A) and interacts strongly with *slbo>Rap1*^{V12}. Border cell clusters expressing *slbo>Rap1*^{V12} and heterozygous for *Df(1)ED7170* migrated past the midpoint in 69% of egg chambers (Figure 3.1 B; Table 3.1). *Df(1)ED7170* is predicted to delete or disrupt 60 genes. Using deficiencies *Df(1)ED7165* (BDSC 9058; X:12,752,602-X:13,138,948) and *Df(1)BSC713* (BDSC 26565; X:13,159,870-X:13,373,704) led us to focus on the region extending from X:13,159,870-X:13,277,326 covering from the beginning of *Df(1)BSC713* to the end of *Df(1)ED7170* (Flybase; Figure 3.4 A, G). Using available alleles of genes along this region led us to investigate the gene *strawberry notch (sno)*. Sno is a nuclear protein that functions in Notch signaling (Majumdar et al., 1997). Single cell RNA sequencing data from the Fly Cell Atlas project indicates *sno* expression in both germline and somatic cells of the ovary (Li et al., 2022). Using a GFP protein trap in *sno*, *sno*^{CC01032}, we found that Sno is found in the nuclei of all cells including the nurse cells, follicle cells, and border cells (Figure 3.4 B, B').

We were able to partially replicate the interaction observed for *Df(1)ED7170* with a loss of function allele for *sno, sno*^{EF531}. Border cells migrated past the midpoint in 37% of egg chambers scored for *slbo>Rap1*^{V12} + *sno*^{EF531} compared to 17% in matched controls (Figure 3.4 C, G; Table 3.2; $p<0.0001$, Chi-squared test). Genetic interaction experiments in wing and eye place Sno in the Notch pathway (Coyle-Thompson and Banerjee 1993). Rough eye and wing notching phenotypes of *sno* mutants are rescued by an extra copy of *Notch* (Coyle-Thompson and Banerjee 1993). Similarly, combining the hypomorphic *nd*^{1} allele of *Notch* with the temperature sensitive *sno*^{71e3} allele synergistically enhances mild wing phenotypes present in *nd*^{1} alone (Coyle-Thompson and Banerjee, 1993). Sno also binds to Supressor of Hairless Su(H) downstream of Epidermal Growth Factor Receptor (EGFR) signaling in *Drosophila* eye

development (Tsuda et al., 2002). Su(H), as visualized with a lacZ reporter construct, is highly expressed in migrating border cells (Schober et al., 2005, Wang et al., 2007). Therefore, to determine if the interaction between *sno* and $Rap1^{V12}$ is related to Sno-dependent regulation of Su(H), we next tested a *Su(H)* loss of function allele, $Su(H)^{[2]}$. Border cells migrated past the midpoint in 42% of $slbo>Rap1^{V12} + Su(H)^{[2]}$ egg chambers compared to 17% in controls (Figure 3.4 D, G; Table 3.2). These results were highly significant (Table 3.2) and suggest that *sno* and *Su(H)* are in the same pathway or contribute similar functions in border cell migration.

We next asked whether *sno* was essential for border cell migration on its own. Prior work indicates a role for Sno in successful oogenesis. Females homozygous for the *sno* allele sno^{71e1} had severe defects in oogenesis including a reduced number of ovarioles, dying cystoblasts, and disrupted cystoblast polarity (Coyle-Thompson and Banerjee 1993). To determine whether *sno* is required specifically in border cell migration, we targeted *sno* with RNAi lines expressed under the control of the follicle cell driver *c306-GAL4*. Using two independent, non-overlapping constructs (VDRC 23841 and VDRC 101404) we found that *sno* is essential for migration. VDRC 28341 RNAi resulted in a significant migration defect of 16% (Figure 3.4 E, G; Table 3.3). Similarly, we observed 36% migration defect for VDRC 101404 RNAi (Figure 3.4 F, G; Table 3.3). The difference in migration defects with the two RNAi lines is likely due to differences in knockdown efficiency.

How *sno* contributes to border cell migration via the Rap1 pathway is unclear. However, *Notch* and its ligand Delta are required for normal border cell migration (Schober et al., 2005, Wang et al., 2007). Both active Notch and *Su(H)* are expressed during migration (Wang et al., 2007). One downstream target of Notch-Su(H) is Anterior open (Aop; also known as Yan) (Schober et al., 2005). Aop regulates the turnover of E-Cadherin required for efficient border cell

migration (Schober et al., 2005). One possibility is that Sno could regulate Aop, which in turn impacts migration efficiency via E-Cadherin turnover. The interaction between *sno* and *Rap1*^{V12} could thus be explained by a common target, E-Cadherin. Further work will be required to determine if this hypothesis is true, or if another mechanism is at play.

Conclusions

The goal of this screen was to identify factors downstream of Rap1 GTPase that are relevant for collective cell migration. Here we report seven deficiency regions that partially restored migration in the severe *slbo>Rap1*^{V12} border cell migration defect background. Of these seven regions, three were mapped to single genes. *Fz4, Usp16-45,* and *sno* may function either as effectors of Rap1 GTPase or act as parallel factors that similarly regulate border cell migration. *Sno* and *Usp16-45* were each required for border cell migration on their own while *fz4* was not. It is important to note that heterozygous loss of these genes did not completely recapitulate the interaction of the relevant deficiency with Rap1^{V12}. This could be due to the presence of additional genes in these genomic regions that interact with Rap1 or because of the nature of the mutant alleles used. Further work will be needed to determine which of these two possibilities is true. Future identification of the relevant genes from the four other interacting deficiencies may also reveal new Rap1 effectors in border cells. This report thus identified new factors that genetically interact with Rap1 during border cell migration. Further work will be needed to fully characterize the extent that each of these genes cooperates with Rap1 to facilitate border cell migration and how these data are applicable to other types of collective cell migration.

3.4 Materials and Methods

Drosophila deficiency screen and genetics

The *X* chromosome deficiency kit (DK1) was obtained from the Bloomington *Drosophila* Stock Center (BDSC). The *X* chromosome was chosen on the basis that chromosomes II and III had been screened previously (Chang et al., 2018). Females from the balanced *X* deficiency lines were crossed to *slbo-GAL4*/CyO; *UAS-Rap1*^{V12}/TM6b, *tubGal80* males (Figure 3.1 A). F1 progeny lacking the balancer chromosomes were selected. In the case of w^{1118} controls, females of the *slbo>Rap1*^{V12} stock were crossed to w^{1118} males. Progeny were fattened overnight (~12-24 hours) on supplemental yeast at 27°C prior to dissection. These conditions allowed sufficient GAL4-UAS expression to observe border cell migration defects. Each deficiency was tested at least once; potential interacting deficiency 'hits' were further evaluated. We set a cutoff of 50% border cell clusters migrating >50% of egg chamber length for the primary screen. This value is greater than two standard deviations above the mean of control egg chambers scored in the primary screen and allowed us to capture high confidence hits. All reported hit lines were tested a minimum of three times. For RNAi knockdown of candidate genes, each RNAi line was crossed to the early follicle cell driver *c306-GAL4*, which is a strong driver of RNAi in border cells (Aranjuez et al., 2016, Miao et al., 2022, Plutoni et al., 2019) . Resultant progeny were temperature shifted to 29°C for two days before being fattened overnight (~12-24 hours) on supplemental yeast at 29°C to ensure enough time for RNAi knockdown.

Immunostaining and imaging

Ovaries were dissected in Schneider's *Drosophila* Medium (Thermo Fisher Scientific, Waltham, MA, USA) supplemented with 10% fetal bovine serum (Seradigm FBS; VWR, Radnor, PA, USA). Ovaries were then fixed for 10 mins using 16% methanol-free formaldehyde (Polysciences, Inc., Warrington, PA, USA) diluted to a final concentration of 4% in 1X Phosphate Buffered Saline (PBS). Following fixation, tissues were washed ≥4x with 'NP40 block' (50 mM Tris-HCL, pH 7.4, 150mM NaCl, 0.5% NP40, 5mg/ml bovine serum albumin [BSA]) and rocked in the solution for ≥30 mins prior to antibody incubation. Primary antibodies, obtained from the Developmental Studies Hybridoma Bank (DSHB, University of Iowa, Iowa City, IA, USA), were used at the following dilutions: rat anti-E-Cadherin 1:10 (DCAD2) and mouse anti-Singed 1:10-1:25 (Sn7C). For GFP detection, rabbit anti-GFP (A11122, Thermo Fisher Scientific) was used at 1:1000 dilution. Anti-rat, anti-mouse, or anti-rabbit secondary antibodies conjugated to Alexa Flour-488 or -568 (Thermo Fisher Scientific) were used at 1:400 dilution. 4', 6'-Diamidino-2-phenylindole (DAPI, Millipore Sigma) was used at 2.5 µg/ml to label nuclei. Primary and secondary antibody incubation as well as all other subsequent wash steps were also performed in NP40 block. Dissected and stained ovarioles and egg chambers were mounted on slides with Aqua-PolyMount (Polysciences, Inc.). Images of fixed egg chambers were acquired on a Zeiss LSM 880 confocal laser scanning microscope (KSU College of Veterinary Medicine Confocal Core) using either a 20 X 0.75 numerical aperture (NA) or 40 X 1.3 NA oil-immersion objective controlled by Zeiss Zen 14 software. Images were processed in FIJI (Schindelin et al., 2012) and figures were assembled using Affinity Photo (Serif, Nottingham, United Kingdom). Illustrations were designed in Affinity Photo.

Tables and statistics

Tables were assembled using Excel (Microsoft, Redmond, WA, USA) or Affinity Photo (Serif). Deficiency regions that were considered "hits" were analyzed for migration a minimum of three times, with a minimum of 20 egg chambers scored per trial. The average of all trails for each "hit" exceeds 50% of the migration pathway. This value was determined as >2σ above the mean "migration" for w^{1118} controls. To determine the genes required for border cell migration, we defined a migration defect as the fraction of border cell clusters that failed to reach ≥75% of the migration path. Chi-squared tests were performed to assess significance level for each experiment using GraphPad Prism 9 (GraphPad Software, San Diego, CA, USA). See Tables 3.2 and 3.3 for statistics.

3.5 Figures and Tables

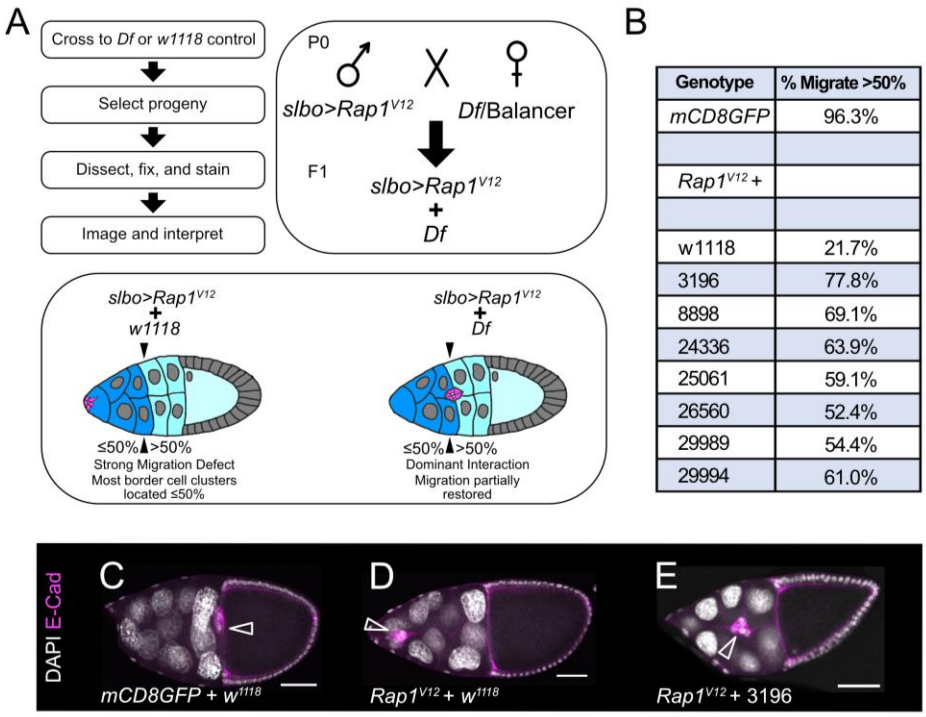

Genotype	% Migrate >50%
mCD8GFP	96.3%
Rap1^{V12} +	
w1118	21.7%
3196	77.8%
8898	69.1%
24336	63.9%
25061	59.1%
26560	52.4%
29989	54.4%
29994	61.0%

Figure 3.1 Screen to identify *Rap1^{V12}* interacting regions

(A) Screen design to assess deficiency regions that restore migration to *slbo>Rap1^{V12}* expressing border cell clusters. (B) Seven hit regions identified by their BDSC stock number (Genotype) followed by the percent of border cell clusters that migrated more than halfway along the length of the egg chamber to the oocyte. All positive hits increased the fraction of clusters that were able to migrate greater than halfway to the oocyte by ≥50%. (C-E) Stage 10 egg chambers stained for E-cadherin (magenta) to label cell membranes and the border cells (arrowheads) and DAPI to label cell nuclei (white). (C) A representative *slbo>mCD8GFP + w^{1118}* control egg chamber showing border cells (arrowhead) that completed their migration to the oocyte. (D) A *slbo>Rap1^{V12} + w^{1118}* control egg chamber that failed to migrate and stopped ~10% along the migration pathway. (E) An example of a *slbo>Rap1^{V12} + Df(1)Sxl-bt* (3196) border cell cluster that migrated to the egg chamber midpoint. Scale bars, 50μm.

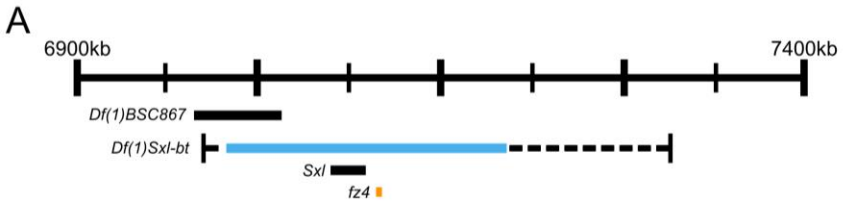

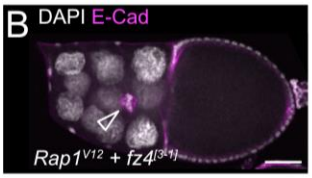

C

Genotype	% Migrate >50%	Interaction
Rap1^{V12} + w1118	17.6%	Control
Rap1^{V12} + Df(1)BSC867	14.3%	No
Rap1^{V12} + Sxl^{f2}	1.1%	No
Rap1^{V12} + fz4$^{[3-1]}$	45.6%	Yes
Genotype	**% Migrate <75%**	**Defect**
w^{1118}	2.3%	Control
fz4$^{[3-1]}$	3.1%	No
60102 GFP RNAi	3%	Control
64990 fz4 RNAi	0%	No
102339 fz4 RNAi	4.5%	No

Figure 3.2 *Fz4* lies within *Df(1)Sxl-bt* and interacts with *Rap1^{V12}*

(A) Schematic illustrating the location of *fz4* within *Df(1)Sxl-bt* along with companion deficiencies and genes tested. The numbers refer to the genomic location of the deficiency. (B) A stage 10 *Rap1^{V12} + fz4$^{[3-1]}$* egg chamber showing restored migration, with the border cells (arrowhead) moving past 50% of the egg chamber length. E-cadherin (magenta) labels all cell membranes including the border cells and DAPI labels cell nuclei (white). Scale bar 50μm. (C) Table of migration data indicating the percentage of border cell clusters that migrate (>50% of egg chamber length) or the percentage of border cell clusters with migration defect (those that migrate <75% of egg chamber length).

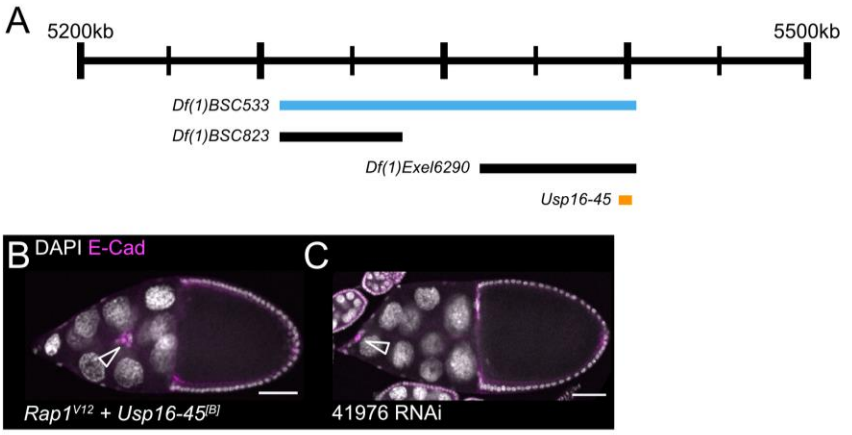

D

Genotype	% Migrate >50%	Interaction
Rap1^{V12} + w1118	18.8%	Control
Rap1^{V12} + Df(1)BSC823	37.5%	Yes
Rap1^{V12} + Df(1)Exel6290	46.9%	Yes
Rap1^{V12} + Usp16-45$^{[B]}$	52.3%	Yes
Genotype	**% Migrate <75%**	**Defect**
60102 GFP RNAi	3.1%	Control
41976 Usp16-45 RNAi	24%	Yes
110286 Usp16-45 RNAi	2.2%	No

Figure 3.3 *Usp16-45* lies within *Df(1)BSC533,* interacts with *Rap1^{V12}*, and is required for border cell migration

(A) Schematic illustrating where *Usp16-45* lies within *Df(1)BSC533* along with companion deficiencies tested. (B-C) Stage 10 egg chambers stained for E-cadherin (magenta), which labels all cell membranes including the border cells and DAPI to label cell nuclei (white). Arrowheads indicate border cell clusters. Scale bars 50µm. (B) A *Rap1^{V12} + Usp16-45$^{[B]}$* egg chamber showing restored migration, with the border cells (arrowhead) moving past 50% of the egg chamber length. (C) A VDRC 41976 RNAi egg chamber with a strong border cell migration defect. (D) Table of migration data indicating the percentage of border cell clusters that migrate

(>50% of egg chamber length) or the percentage of border cell clusters with migration defect (those that migrate <75% of egg chamber length).

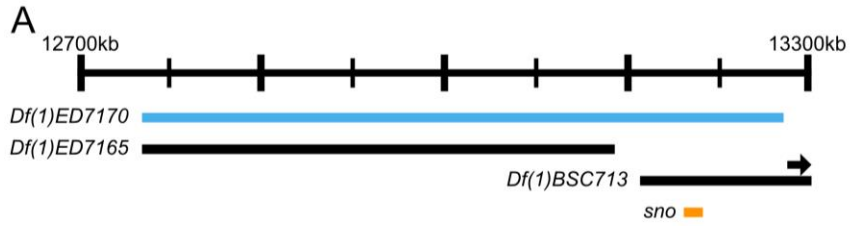

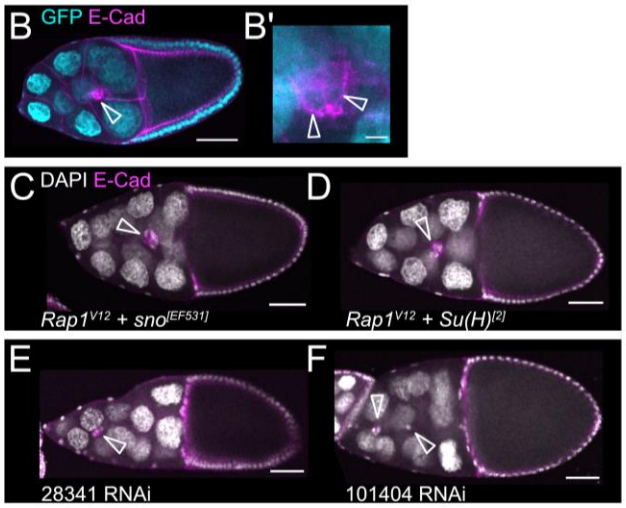

G

Genotype	% Migrate >50%	Interaction
Rap1^{V12} + w1118	17%	Control
Rap1^{V12} + Df(1)ED7165	12.5%	No
Rap1^{V12} + Df(1)BSC713	57.1%	Yes
Rap1^{V12} + sno$^{[EF531]}$	36.5%	Yes
Rap1^{V12} + Su(H)$^{[2]}$	42%	Yes
Genotype	**% Migrate <75%**	**Defect**
60102 GFP RNAi	3%	Control
23841 sno RNAi	16.3%	Yes
101404 sno RNAi	36.2%	Yes

Figure 3.4 *Sno* lies within *Df(1)ED7170*, interacts with *Rap1^{V12}*, and is required for border cell migration

(A) Schematic illustrating where *sno* lies along *Df(1)ED7170* along with companion deficiencies tested. Arrow indicates *Df(1)BSC713* extends beyond the region depicted here. (B) Egg chamber with GFP protein trap in *sno*, *sno*^{CC01032}, shows Sno nuclear expression (cyan). E-cadherin

(magenta) labels cell membranes including the border cells (arrowhead). (B') Close-up view of the same border cell cluster in B. Arrowheads indicate Sno expression in border cells (C-F) Stage 10 egg chambers stained for E-cadherin (magenta), which labels all cell membranes including the border cells and DAPI to label cell nuclei (white). Arrowheads indicate border cell clusters. Scale bars 50μm. (C) A $Rap1^{V12}$ + $sno^{[EF531]}$ egg chamber showing restored migration, with border cells moving past 50% of the egg chamber length. (D) A $Rap1^{V12}$ + $Su(H)^{[2]}$ egg chamber showing restored migration past 50%. (E) A VDRC 28341 RNAi egg chamber showing a migration defect. (F) A VDRC 101404 RNAi egg chamber indicating a migration defect. (G) Table of migration data indicating the percentage of border cell clusters that migrate (>50% of egg chamber length) or the percentage of border cell clusters with migration defect (those that migrate <75% of egg chamber length).

Table 3.1 Primary screen data

Symbol	Stock #	Observed Bkpts R6 or Cyto Bands	Estimated Cyto Locs	Hit (Y/N)	Fraction Migrating ≤50%	Fraction Migrating >50%	# of expts	# egg chambers
Df(1)BSC843	27887	X:254968-255277;X:334685 (Df)	1A1;1A3 (Df)	N	70.49%	29.51%	1	122
Df(1)BSC530	25058	X:364350; X:623478-623577 (Df)	1A5;1B12 (Df)	N	73.21%	26.79%	1	56
Df(1)G1	34050	X:644873; X:654238 (Df)	1B13; 1B13 (Df)	N	66.95%	33.05%	2	214
Df(1)ED6443	9053	X:656023; X:1026707 (Df)	1B14; 1E1 (Df)	N	98.55%	1.45%	3	268
Df(1)BSC534	25062	X:841105; X:1453730 (Df)	1D1;2A3 (Df)	N	82.69%	17.31%	1	52
Df(1)BSC719	26571	X:1453730;X:1865709 (Df)	2A3;2B13 (Df)	N	90.01%	9.99%	2	122
Df(1)BSC717	26569	X:2251580;X:2545663 (Df)	2F2;3A4 (Df)	N	98.55%	1.45%	3	99
Df(1)ED411	8031	X:2469859;X:2642686 (Df)	3A3;3A8 (Df)	N	70.63%	29.38%	1	160

Df(1)ED6584	9348	X:2636213;X:2685435 (Df)	3A8;3B1 (Df)	N	97.26%	2.74%	3	199
Df(1)ED6630	8948	X:2685540;X:3036910 (Df)	3B1;3C5 (Df)	N	99.60%	0.40%	3	200
Df(1)BSC531	25059	X:2913683-2913782;X:3672682 (Df)	3C3;3E2 (Df)	N	52.83%	47.17%	1	53
Df(1)BSC834	27886	X:3288956;X:3845727 (Df)	3C11;3F3 (Df)	N	96.53%	3.47%	3	227
Df(1)ED6712	9169	X:3432535;X:3789615 (Df)	3D3;3F1 (Df)	N	94.74%	5.26%	2	96
Df(1)ED6716	24145	X:3799196;X:4204584 (Df)	3F2;4B3 (Df)	N	94.54%	5.46%	3	242
Df(1)BSC580	25414	X:4101232-4101613;X:4688080 (Df)	4A5;4C13 (Df)	N	69.83%	30.17%	2	102
Df(1)ED6727	8956	X:4325174;X:4911061 (Df)	4B6;4D5 (Df)	N	85.71%	14.29%	1	49
Df(1)JC70	944	X:4679537-4919558;X	4C12-4D6;4F4-	N	95.98%	4.02%	2	177

		:5309242-5412386 (Df)	4F9 (Df)					
Df(1)BSC533	25061	X:5282581-5282584;X:5428543 (Df)	4F4;4F10 (Df)	Y	40.92%	59.08%	4	333
Df(1)Exel6235	7709	X:5516611;X:5593966 (Df)	5A2;5A6 (Df)	N	58.10%	41.90%	2	185
Df(1)BSC571	25114	X:5545559;X:5662787 (Df)	5A4;5A10 (Df)	N	66.07%	33.93%	1	56
Df(1)ED6802	8949	X:5679980;X:5965880 (Df)	5A12;5D1 (Df)	N	56.07%	43.93%	2	172
Df(1)ED6829	8947	X:5901976;X:6353095 (Df)	5C7;5F3 (Df)	N	77.50%	22.50%	1	80
Df(1)Exel6239	7713	X:6344333;X:6516952-6538013 (Df)	5F2;6B1-6B2 (Df)	N	51.06%	48.94%	2	127
Df(1)Exel6240	7714	X:6543963;X:6669857-6669858 (Df)	6B2;6C4 (Df)	N	60.13%	39.87%	1	153
Df(1)BSC535	25063	X:6625450;X:6707019 (Df)	6C2;6C8 (Df)	N	69.12%	30.88%	1	136

Df(1)BSC351	24375	X:6748387-6748403;X:6860753 (Df)	6C11;6D7 (Df)	N	97.36%	2.64%	3	189
Df(1)BSC882	30587	X:6824174;X:7015408 (Df)	6D3;6E4 (Df)	N	77.67%	22.33%	1	103
Df(1)Sxl-bt	3196	X:6987188-7004151;X:7195487-7307939 (Df)	6E4;7A3-7B1 (Df)	Y	22.20%	77.80%	5	439
Df(1)ED6906	8955	X:7195084;X:7405806 (Df)	7A3;7B2 (Df)	N	73.82%	26.18%	2	96
Df(1)BSC536	25064	X:7338653;X:7891613 (Df)	7B2;7C1 (Df)	N	83.11%	16.89%	2	88
Df(1)C128	949	X:7901331-7956278;X:8061645-8115848 (Df)	7C2-7D1;7D5-7D6 (Df)	N	82.03%	17.97%	2	184
Df(1)BSC866	29989	X:8086993;X:8157322 (Df)	7D5;7D16 (Df)	Y	45.61%	54.39%	3	149

Df(1)BSC662	26514	X:8116248;X:8489613 (Df)	7D6;7F1 (Df)	N	50.63%	49.37%	3	270
Df(1)M38-C5	5706	X:8877627-8933650;X:9554623-9594143 (Df)	8B5-8C1;8E7-8E12 (Df)	N	69.70%	30.30%	1	33
Df(1)ED6957	8033	X:8891795;X:9135037 (Df)	8B6;8C13 (Df)	N	75.63%	24.37%	1	119
Df(1)BSC712	26564	X:9606595;X:10086569 (Df)	8F1;9B1 (Df)	N	76.02%	23.98%	3	186
Df(1)ED7005	9153	X:10071922;X:10585431 (Df)	9B1;9D3 (Df)	N	96.94%	3.06%	3	212
Df(1)BSC755	26853	X:10454979;X:10848473 (Df)	9C4;9F5 (Df)	N	70.80%	29.20%	1	113
Df(1)BSC540	25068	X:10772545;X:11065010 (Df)	9E8;10A3 (Df)	N	61.97%	38.03%	1	71
Df(1)v-L1	6219	X:10854869-10925631; X:11108482-11136887 (Df)	9F5-9F11; 10A4-10A6 (Df)	N	74.60%	25.40%	1	63

Df(1)BSC572	25391	X:10890940;X:11092253 (Df)	9F8;10A4 (Df)	N	78.03%	21.97%	1	132
Df(1)BSC287	23672	X:11182121;X:11426241 (Df)	10A10;10B11 (Df)	N	99.62%	0.38%	3	299
Df(1)ED7147	9171	X:11714383;X:12004800 (Df)	10D6;11A1 (Df)	N	91.24%	8.76%	3	252
Df(1)ED7161	9217	X:12007087;X:12750866 (Df)	11A1;11B14 (Df)	N	93.11%	6.89%	3	247
Df(1)ED7170	8898	X:12752602;X:13277326 (Df)	11B15;11E8 (Df)	Y	30.90%	69.10%	7	532
Df(1)ED7225	24146	X:13784406;X:14322206 (Df)	12C4;12E8 (Df)	N	100.00%	0.00%	1	61
Df(1)ED7229	9352	X:14222234;X:14653944 (Df)	12E5;12F2 (Df)	N	57.26%	42.74%	2	126
Df(1)ED7261	9218	X:14653809;X:14839412 (Df)	12F2;12F5 (Df)	N	87.67%	12.33%	5	424
Df(1)BSC310	24336	X:14842413;X:15089556 (Df)	12F5;13A10 (Df)	Y	36.07%	63.93%	4	175
Df(1)ED7289	29732	X:15024777;X:15125750 (Df)	13A5;13A12 (Df)	N	96.48%	3.52%	5	543

Df(1)ED7294	8035	X:15175415;X:15450298 (Df)	13B1; 13C3 (Df)	N	69.33%	30.67%	1	150
Df(1)ED7331	9219	X:15450255;X:15813523 (Df)	13C3; 13F1 (Df)	N	87.50%	12.50%	3	239
Df(1)BSC714	26566	X:15758351;X:16086028 (Df)	13E1 4;14A8 (Df)	N	81.08%	18.92%	1	37
Df(1)BSC758	26855	X:16005260;X:16367112 (Df)	14A6; 14C1 (Df)	N	53.67%	46.33%	2	191
Df(1)BSC772	26869	X:16302976;X:16423105 (Df)	14B9; 14C4 (Df)	N	75.21%	24.79%	1	117
Df(1)FDD-0024486	23295	X:16423105;X:16463156 (Df)	14C4; 14D1 (Df)	N	77.42%	22.58%	1	31
Df(1)BSC760	26857	X:16526332;X:16632102 (Df)	14E1; 14F2 (Df)	N	50.14%	49.86%	2	154
Df(1)BSC582	25416	X:16680721;X:17091833 (Df)	15A1; 15E2 (Df)	N	79.94%	20.06%	4	501
Df(1)ED7374	8954	X:16695187;X:17107632 (Df)	15A1; 15E3 (Df)	N	91.33%	8.67%	3	253
Df(1)BSC405	24429	X:17830759-17830846;	16D5; 16F6 (Df)	N	83.33%	16.67%	1	30

		X:18092832 (Df)						
Df(1)ED13478	29733	X:18085406;X:18102011 (Df)	16F6; 16F7 (Df)	N	88.55%	11.45%	2	218
Df(1)BSC352	24376	X:18117467;X:18374885 (Df)	16F7; 17A8 (Df)	N	94.62%	5.38%	3	274
Df(1)BSC716	26568	X:18243732;X:18800267 (Df)	17A3; 17D6 (Df)	N	84.64%	15.36%	2	148
Df(1)ED7424	9350	X:18657253;X:19298773 (Df)	17D1; 18C1 (Df)	N	86.87%	13.13%	2	147
Df(1)Exel7468	7768	X:19264512;X:19509637 (Df)	18B7; 18C8 (Df)	N	75.00%	25.00%	1	52
Df(1)BSC275	23171	X:19496689;X:19580079 (Df)	18C8; 18D3 (Df)	N	100.00%	0.00%	1	22
Df(1)BSC871	29994	X:19617601;X:19788713 (Df)	18D7; 18F2 (Df)	Y	38.96%	61.04%	4	193
Df(1)BSC586	25420	X:19788713;X:20429928 (Df)	18F2; 19D1 (Df)	N	90.91%	9.09%	1	44
Df(1)BSC644	25734	X:20243402;X:21061001 (Df)	19C1; 19E7 (Df)	N	80.49%	19.51%	1	41
Df(1)DCB1-35b	977	X:20939503-	19E5-19F5;	N	61.76%	38.24%	1	34

		21345088; X:2298072 2-23542271 (Df)	20F3-h32 (Df)					
Df(1)BSC708	26560	X:2102829 6;X:21623 866 (Df)	19E7; 20A4 (Df)	Y	47.56%	52.44%	5	351
Df(1)Exel 6255	7723	X:2151920 3;X:22517 665 (Df)	20A1; 20C1 (Df)	N	50.22%	49.78%	4	390

Table 3.2 Candidate allele data

Allele	Sample size	Migrating >50%	Statistical Test	Significance
fz4[3-1]	393	180	Chi-square test	****, P<0.0001
matched control	287	49		
Usp16-45[B]	292	159	Chi-square test	****, P<0.0001
matched control	354	64		
sno[EF531]	525	198	Chi-square test	****, P<0.0001
matched control	411	67		
Su(H)[2]	410	173	Chi-square test	****, P<0.0001
matched control	287	49		

N=number of egg chambers.

Table 3.3 Candidate RNAi data

RNAi	Sample size	Migrating <75%	Statistical Test	Significance
64990 *fz4* RNAi	238	0	Chi-square test	**, P<0.01
matched control	202	9		
102339 *fz4* RNAi	186	9	Chi-square test	ns
matched control	239	9		
41976 *Usp16-45* RNAi	152	35	Chi-square test	****, P<0.0001
matched control	239	9		
110286 *Usp16-45* RNAi	196	4	Chi-square test	ns
matched control	239	9		
23841 *sno* RNAi	185	28	Chi-square test	****, P<0.0001
matched control	239	9		
101404 *sno* RNAi	109	39	Chi-square test	****, P<0.0001
matched control	259	9		

N=number of egg chambers.

3.6 References

Aranjuez, G., Burtscher, A., Sawant, K., Majumder, P. and McDonald, J. A. (2016). Dynamic myosin activation promotes collective morphology and migration by locally balancing oppositional forces from surrounding tissue. *Mol Biol Cell* **27**, 1898–1910.

Badmos, H., Cobbe, N., Campbell, A., Jackson, R. and Bennett, D. (2021). Drosophila USP22/nonstop polarizes the actin cytoskeleton during collective border cell migration. *Journal of Cell Biology* **220**, e202007005.

Chang, Y. C., Wu, J. W., Hsieh, Y. C., Huang, T. H., Liao, Z. M., Huang, Y. S., Mondo, J. A., Montell, D. and Jang, A. C. C. (2018). Rap1 Negatively Regulates the Hippo Pathway to Polarize Directional Protrusions in Collective Cell Migration. *Cell Reports* **22**, 2160-2175.

Cherfils, J. and Zeghouf, M. (2013). Regulation of Small GTPases by GEFs, GAPs, and GDIs. *Physiological Reviews* **93**, 269–309.

Clague, M. J., Urbé, S. and Komander, D. (2019). Breaking the chains: deubiquitylating enzyme specificity begets function. *Nat Rev Mol Cell Biol* **20**, 338–352.

Cohen, E. D., Mariol, M.-C., Wallace, R. M. H., Weyers, J., Kamberov, Y. G., Pradel, J. and Wilder, E. L. (2002). DWnt4 Regulates Cell Movement and Focal Adhesion Kinase during Drosophila Ovarian Morphogenesis. *Developmental Cell* **2**, 437–448.

Cook, R. K., Christensen, S. J., Deal, J. A., Coburn, R. A., Deal, M. E., Gresens, J. M., Kaufman, T. C. and Cook, K. R. (2012). The generation of chromosomal deletions to provide extensive coverage and subdivision of the Drosophila melanogaster genome. *Genome Biol* **13**, R21.

Coyle-Thompson, C. A. and Banerjee, U. (1993). The strawberry notch gene functions with Notch in common developmental pathways. *Development* **119**, 377–395.

Friedl, P. and Gilmour, D. (2009). Collective cell migration in morphogenesis, regeneration and cancer. *Nature Reviews Molecular Cell Biology* **10**, 445–457.

Ganguly, A., Jiang, J. and Ip, Y. T. (2005). Drosophila WntD is a target and an inhibitor of the Dorsal/Twist/Snail network in the gastrulating embryo. *Development* **132**, 3419–3429.

Gordon, M. D., Dionne, M. S., Schneider, D. S. and Nusse, R. (2005). WntD is a feedback inhibitor of Dorsal/NF-kappaB in Drosophila development and immunity. *Nature* **437**, 746–749.

Huang, H.-C. and Klein, P. S. (2004). The Frizzled family: receptors for multiple signal transduction pathways. *Genome Biology* **5**, 234.

Insall, R. H. and Machesky, L. M. (2009). Actin Dynamics at the Leading Edge: From Simple Machinery to Complex Networks. *Developmental Cell* **17**, 310–322.

Kim, T. Y., Siesser, P. F., Rossman, K. L., Goldfarb, D., Mackinnon, K., Yan, F., Yi, X., MacCoss, M. J., Moon, R. T., Der, C. J., et al. (2015). Substrate Trapping Proteomics Reveals Targets of the βTrCP2/FBXW11 Ubiquitin Ligase. *Mol Cell Biol* **35**, 167–181.

Komander, D., Clague, M. J. and Urbé, S. (2009). Breaking the chains: structure and function of the deubiquitinases. *Nat Rev Mol Cell Biol* **10**, 550–563.

Konstantinopoulos, P. A., Karamouzis, M. V. and Papavassiliou, A. G. (2007). Post-translational modifications and regulation of the RAS superfamily of GTPases as anticancer targets. *Nat Rev Drug Discov* **6**, 541–555.

Kotian, N., Troike, K. M., Curran, K. N., Lathia, J. D. and McDonald, J. A. (2022). A Drosophila RNAi screen reveals conserved glioblastoma-related adhesion genes that regulate collective cell migration. *G3 Genes|Genomes|Genetics* **12**, jkab356.

Lauffenburger, D. A. and Horwitz, A. F. (1996). Cell Migration: A Physically Integrated Molecular Process. *Cell* **84**, 359–369.

Lei, Z., Wang, J., Zhang, L. and Liu, C. H. (2021). Ubiquitination-Dependent Regulation of Small GTPases in Membrane Trafficking: From Cell Biology to Human Diseases. *Front Cell Dev Biol* **9**, 688352.

Li, H., Janssens, J., De Waegeneer, M., Kolluru, S. S., Davie, K., Gardeux, V., Saelens, W., David, F. P. A., Brbić, M., Spanier, K., et al. (2022). Fly Cell Atlas: A single-nucleus transcriptomic atlas of the adult fruit fly. *Science* **375**, eabk2432.

Majumdar, A., Nagaraj, R. and Banerjee, U. (1997). strawberry notch encodes a conserved nuclear protein that functions downstream of Notch and regulates gene expression along the developing wing margin of Drosophila. *Genes Dev.* **11**, 1341–1353.

McElwain, M. A., Ko, D. C., Gordon, M. D., Fyrst, H., Saba, J. D. and Nusse, R. (2011). A Suppressor/Enhancer Screen in Drosophila Reveals a Role for Wnt-Mediated Lipid Metabolism in Primordial Germ Cell Migration. *PLOS ONE* **6**, e26993.

McSherry, E. A., Brennan, K., Hudson, L., Hill, A. D. and Hopkins, A. M. (2011). Breast cancer cell migration is regulated through junctional adhesion molecule-A-mediated activation of Rap1 GTPase. *Breast Cancer Res* **13**, R31.

Miao, G., Guo, L. and Montell, D. J. (2022). Border cell polarity and collective migration require the spliceosome component Cactin. *J Cell Biol* **221**, e202202146.

Montell, D. J., Yoon, W. H. and Starz-Gaiano, M. (2012). Group choreography: mechanisms orchestrating the collective movement of border cells. *Nature reviews. Molecular cell biology* **13**, 631–45.

Plutoni, C., Keil, S., Zeledon, C., Delsin, L. E. A., Decelle, B., Roux, P. P., Carréno, S. and Emery, G. (2019). Misshapen coordinates protrusion restriction and actomyosin contractility during collective cell migration. *Nat Commun* **10**, 3940.

Rahimi, N., Averbukh, I., Haskel-Ittah, M., Degani, N., Schejter, E. D., Barkai, N. and Shilo, B.-Z. (2016). A WntD-Dependent Integral Feedback Loop Attenuates Variability in Drosophila Toll Signaling. *Developmental Cell* **36**, 401–414.

Ridley, A. J., Schwartz, M. A., Burridge, K., Firtel, R. A., Ginsberg, M. H., Borisy, G., Parsons, J. T. and Horwitz, A. R. (2003). Cell migration: integrating signals from front to back. *Science* **302**, 1704–1709.

Roberto, G. M. and Emery, G. (2022). Directing with restraint: Mechanisms of protrusion restriction in collective cell migrations. *Seminars in Cell & Developmental Biology* **129**, 75–81.

Saadin, A. and Starz-Gaiano, M. (2016). Circuitous Genetic Regulation Governs a Straightforward Cell Migration. *Trends in Genetics* **32**, 660–673.

Sapmaz, A., Berlin, I., Bos, E., Wijdeven, R. H., Janssen, H., Konietzny, R., Akkermans, J. J., Erson-Bensan, A. E., Koning, R. I., Kessler, B. M., et al. (2019). USP32 regulates late endosomal transport and recycling through deubiquitylation of Rab7. *Nat Commun* **10**, 1454.

Sawant, K., Chen, Y., Kotian, N., Preuss, K. M. and McDonald, J. A. (2018). Rap1 GTPase promotes coordinated collective cell migration in vivo. *Molecular Biology of the Cell* **29**, 2656–2673.

Scarpa, E. and Mayor, R. (2016). Collective cell migration in development. *Journal of Cell Biology* **212**, 143–155.

Schindelin, J., Arganda-Carreras, I., Frise, E., Kaynig, V., Longair, M., Pietzsch, T., Preibisch, S., Rueden, C., Saalfeld, S., Schmid, B., et al. (2012). Fiji: an open-source platform for biological-image analysis. *Nat Methods* **9**, 676–682.

Schober, M., Rebay, I. and Perrimon, N. (2005). Function of the ETS transcription factor Yan in border cell migration. *Development* **132**, 3493–3504.

Tsuda, L., Nagaraj, R., Zipursky, S. L. and Banerjee, U. (2002). An EGFR/Ebi/Sno pathway promotes delta expression by inactivating Su(H)/SMRTER repression during inductive notch signaling. *Cell* **110**, 625–637.

Ulrich, F. and Heisenberg, C.-P. (2009). Trafficking and cell migration. *Traffic* **10**, 811–818.

Wang, X., Adam, J. C. and Montell, D. (2007). Spatially localized Kuzbanian required for specific activation of Notch during border cell migration. *Dev Biol* **301**, 532–540.

Wu, C. and Nusse, R. (2002). Ligand Receptor Interactions in the Wnt Signaling Pathway in Drosophila *. *Journal of Biological Chemistry* **277**, 41762–41769.

Yang, D.-S., Roh, S. and Jeong, S. (2016). The axon guidance function of Rap1 small GTPase is independent of PlexA RasGAP activity in Drosophila. *Dev Biol* **418**, 258–267.

Zegers, M. M. and Friedl, P. (2014). Rho GTPases in collective cell migration. *Small GTPases* **5**, e28997.

Chapter 4 - Discussion and Future Directions

This dissertation begins with an introductory chapter detailing well studied models of epithelial morphogenesis. In this closing chapter I will highlight key findings from my work that were presented in chapters 2 and 3, contextualize these findings by drawing from relevant literature in the field, and provide commentary on additional approaches that could be pursued to address key open questions.

4.1 Epithelial integrity and cell viability: keeping it together with Rap1

Chapter 2 describes my work investigating how Rap1 contributes to epithelial morphogenesis in a growing tissue, the developing *Drosophila* egg chamber. This model presents a unique opportunity to study how Rap1 contributes to epithelial integrity in a tissue that is undergoing dramatic changes in size and shape. The period of elongation that occurs after mitosis concludes at stage 6 may present a particularly acute challenge to tissue integrity. We found that Rap1 is required to promote proper shape of the anterior epithelium of growing egg chambers. This region lost its characteristic pointed shape upon Rap1 inhibition. Furthermore, individual cells within the anterior epithelium relied on Rap1 to retain cuboidal shapes and became obviously distorted in Rap1 deficient egg chambers. Focusing on the anterior polar cells revealed severe phenotypes with cells that appeared to be stretching along the dorsoventral axis. Using this easily identifiable cell type for further analysis, we found that polar cells in Rap1 deficient egg chambers failed to accumulate the homophilic cell-cell adhesion molecule E-Cadherin at their apical contact. In addition, we observed Rap1 deficient egg chambers with missing polar cells. Using markers for caspase activity we found that Rap1 is required for cell viability during egg chamber morphogenesis. Loss of Rap1 activity resulted in apoptotic follicle cells, missing polar cells, and ultimately failure to properly assemble the migratory border cell

cluster. Together these results suggest that Rap1 maintains epithelial integrity and cell viability within the developing egg chamber required for proper development and border cell cluster assembly.

4.1.1 Building or maintaining the adherens junction with Rap1

Adherens junctions are critical to epithelial integrity (Pinheiro and Bellaïche, 2018). A key question left unanswered by our study is how Rap1 recruits or maintains enrichment of E-Cadherin at adherens junctions in the anterior epithelium. A role for Rap1 in E-Cadherin recruitment may be related to cell polarity. First, consider how E-Cadherin is assembled into nascent adherens junctions. Work in the *Drosophila* embryo provides a good resource as adherens junction assembly can be studied as cells first form. Adherens junction formation and cell polarity are intimately linked, but epithelial polarity is ultimately upstream of adherens junction assembly. The cell polarity cue Bazooka/Par-3 localizes properly in E-Cadherin mutants, but E-Cadherin enrichment at adherens junctions requires Bazooka (Harris and Peifer, 2004).

Roles for Rap1 in cell polarity are well established (Bonello et al., 2018; Choi et al., 2013; Kim et al. 2022, Sasaki et al., 2020). In the embryo loss of Rap1 causes depolarization of Bazooka. Bazooka is normally observed in apically restricted puncta but disperses along the lateral membrane in Rap1 mutants (Bonello et al., 2018; Choi et al., 2013). One hypothesis is that Rap1 promotes E-Cadherin enrichment in the follicular epithelium by maintaining discrete distribution of polarity proteins.

First, it would be interesting to note if Rap1 regulates Bazooka localization in ovarian follicle cells. A Bazooka antibody with validated uses in the embryo is available (Bonello et al., 2018) in addition to a protein trap allele making it relatively straightforward to test Bazooka

localization in the egg chamber upon Rap1 inhibition. The next step would be to determine if E-Cadherin localization is dependent upon Bazooka activity. RNAi lines targeting Bazooka are available from the Vienna Drosophila Resource Center (VDRC). E-Cadherin localization could be probed upon Bazooka RNAi to determine if reducing Bazooka levels alters E-Cadherin recruitment at adherens junctions.

The *Drosophila* Rap1 effector Canoe/Afadin may also be involved in E-Cadherin recruitment in the ovary. Rap1 is required for Canoe recruitment at nascent spot adherens junctions in the embryo where Canoe and Rap1 are both essential for polarity establishment (Bonello et al., 2018; Choi et al., 2013). Therefore, it would be interesting to assess if Canoe is required for E-Cadherin enrichment at adherens junctions. RNAi lines for Canoe are available (VDRC) and both E-Cadherin enrichment and Bazooka localization could be probed upon Canoe depletion. These experiments would reveal whether Rap1 function in the ovary parallels the pathway observed for adherens junction assembly in the embryo.

Alternately, Rap1 may be required to maintain E-Cadherin levels at adherens junctions in the follicular epithelium. Adherens junctions are consistently challenged during morphogenesis and are thus robust, mechanosensitive linkages amenable to remodeling (Pinheiro and Bellaïche, 2018). Adherens junction maintenance and remodeling requires continuous turnover and recycling of E-Cadherin (Brüser and Bogdan, 2017). Therefore, it seems likely that Rap1 may regulate E-Cadherin enrichment at adherens junctions by contributing to E-Cadherin stablility. Indeed, Rap1 was shown to inhibit E-Cadherin endocytosis in both MDCK cells and a cell free assay (Hoshino et al., 2005). Moreover, fluorescence recovery after photobleaching (FRAP) experiments in *Drosophila* photoreceptors demonstrated that Rap1 inhibition increases the

mobile fraction of E-Cadherin suggesting that Rap1 stabilizes E-Cadherin at the zonula adherens (Walther et al., 2018).

To assess the role of Rap1 in E-Cadherin maintenance in the anterior epithelium FRAP experiments could be performed in egg chambers. This approach has been successfully implemented in the oocyte of egg chambers to track *gurken* (*grk*) dynamics (Jaramillo et al., 2008). Recovery of GFP tagged E-Cadherin could be assessed after photobleaching adherens junctions in the anterior epithelium of egg chambers that express Rap1 RNAi or a GFP RNAi control. If Rap1 is required for E-Cadherin stability, E-Cadherin recovery should be faster in Rap1 inhibited egg chambers as was reported for pupal photoreceptors (Walther et al., 2018). Since Rap1 functions in concert with Canoe/Afadin in preventing E-Cadherin endocytosis (Hoshino et al., 2005), it would also be beneficial to assess if Rap1 related E-Cadherin stability is Canoe dependent. Similar FRAP experiments could be performed using Canoe RNAi to address this possibility.

Finally, a minor companion experiment related to E-Cadherin maintenance should be pursued to fully evaluate the relationship between E-Cadherin enrichment and the cell and tissue shape deformations observed in Rap1 inhibited egg chambers. Weakened adherens junctions due to failed E-Cadherin accumulation is a plausible explanation for follicle cell deformations during the period of germline expansion. Targeting E-Cadherin with RNAi, however, failed to recapitulate the cell and tissue defects observed for Rap1 inhibition. This could be attributable to the compensatory function of N-Cadherin for E-Cadherin observed in *Drosophila* ring canals (Loyer et al., 2015) or insufficient knockdown of E-Cadherin. To further address this complication, null clones of E-Cadherin could be generating in follicle cells (Pacquelet and

Rørth, 2005) with or without the addition of N-Cadherin RNAi. These experiments would further determine the role of E-Cadherin in epithelial integrity.

4.1.2 Coupling contractility to the cell cortex

Our results indicate, that in addition to Rap1, both non-muscle myosin II (Myo-II) and α-Catenin are required for local tissue shape. We hypothesized that Rap1 functions to link actomyosin contractility to adherens junctions allowing the anterior epithelium to resist deformation imposed by germline growth. Indeed, Rap1 is required to couple actomyosin contractility to adherens junctions during ventral furrow formation (Sawyer et al., 2009). It, therefore, seems reasonable to suspect that Rap1 performs a similar function in the follicular epithelium.

Notably, our analysis of myosin regulatory light chain using Sqh-GFP failed to reveal any differences in Myo-II localization for Rap1 inhibited egg chambers compared to controls. A limitation to our approach was the use of fixed samples. Myosin contractility can be highly dynamic in epithelial cells. Consider apical constriction during ventral furrow formation, for example, where myosin pulses initiate contractions at the apical cell cortex (Martin et al., 2009). Similarly, dynamic myosin activity is required for border cell detatchment and migration (Aranjuez et al., 2016; Lamb et al., 2021; Majumder et al., 2012; Mishra et al., 2019). Given the highly dynamic nature of myosin contractility, a live imaging approach would be better suited to capture nuances in both myosin localization and activity.

Egg chambers could be live imaged using available E-Cadherin-GFP and Myosin-mCherry to visualize the relationship between myosin and adherens junctions (Martin et al., 2009). Rap1 inhibited egg chambers could be compared to those expressing an RNAi control. These experiments may reveal Rap1 dependent changes in myosin pulsatility. If Rap1 is required

to link actomyosin contractility to adherens junctions, Rap1 inhibited egg chambers may have obvious discontinuity between myosin activity and adherens junctions as was reported in the embryo (Sawyer et al., 2009).

4.1.3 Rap1 promotes follicle cell viability

Rap1 was required for follicle cell viability as noted by an increase of caspase positive cells in Rap1 inhibited egg chambers. Our study is not the first to report an increase in apoptotic epithelial cells upon Rap1 depletion. Rap1 is required for cell viability in mouse lens epithelium and in *Drosophila* neurons (Heo et al., 2017; Maddala et al., 2015). How Rap1 contributes to cell viability, however, remains unclear. Our results indicate a direct link between Rap1 and the apoptotic cascade. Rap1 was required to promote enrichment of the pro-survival factor DIAP1. Further work is required, however, to clarify the relationship between Rap1 function in epithelial integrity and a role in cell survival.

One method to distinguish a direct Rap1 dependent regulation of DIAP1 from secondary effects caused by loss of epithelial integrity is to disrupt epithelial integrity independently of Rap1 and examine DIAP1 accumulation. We observed regular epithelial disruptions and altered individual cell shapes in α-Catenin RNAi expressing egg chambers. The available *diap1-GFP* reporter (Zhang et al., 2008) could be used to determine whether disrupting epithelial integrity by α-Catenin RNAi reduces DIAP1 accumulation. We observed greater caspase accumulation, but less severe epithelial defects in Rap1 inhibited egg chambers as compared to α-Catenin RNAi expressing egg chambers. These results could suggest a pro-survival function of Rap1 that is independent of epithelial integrity. This experiment clarifies the dual contributions of Rap1 to epithelial integrity and cell viability.

In addition, a series of cell culture experiments could be performed to further define the relationship between Rap1 and the apoptotic cascade. GST tagged DIAP1 could be expressed in *Drosophila* S2 cells with Myc tagged Rap1 transgenes (Boettner et al., 2003; Geisbrecht and Montell, 2004). Experiments using pulldown of GST-DIAP1 followed by Myc antibody incubation could determine whether DIAP1 binds with either $Rap1^{V12}$ or $Rap1^{N17}$. Moreover, additional members of the apoptotic cascade could be interrogated using RT-PCR. Expression of upstream DIAP1 antagonists Reaper, Hid, and Grim could be probed in S2 cells expressing either $Rap1^{V12}$ or $Rap1^{N17}$ (Yalonetskaya et al., 2018). These experiments would be complementary to those reported in Chapter 2 and would help answer open questions about the role of Rap1 in cell viability.

4.1.4 Border cell cluster size impacts organ function

In addition to epithelial defects and cell viability issues, Rap1 inhibited egg chambers formed smaller border cell clusters. Border cell migration is essential to organ function as border cells help create a pore for sperm entry called the micropyle (Montell et al., 1992; Montell et al., 2012). Cluster size is a critical component of migration efficiency (Cai et al., 2016; Starz-Gaiano et al., 2008; Stonko et al., 2015). We lack a clear understanding of how cluster size impacts organ function for Rap1 inhibited egg chambers.

Given the severity of the defects observed in Rap1 inhibited egg chambers, it is surprising that border cell clusters form at all. To assess how well smaller border cell clusters migrate, live imaging could be performed (Prasad and Montell, 2007). Since border cell clusters in Rap1 inhibited egg chambers are smaller than the optimal size, it is reasonable to expect that they might migrate more slowly or fail to reach the oocyte boundary. Border cells change positions within the cluster along the migratory path and can occupy leading, trailing, and lateral

positions with respect to the cluster center (Prasad and Montell, 2007). Smaller clusters composed of less cells have fewer potential leaders so it would be interesting to evaluate the frequency with which cells change positions over the course of migration.

Finally, since border cell migration culminates at the oocyte boundary where they make a pore for sperm entry, it would be useful to determine if smaller border cell clusters cause fertility defects. To evaluate this possibility the number of progeny produced by Rap1 inhibited females could be compared to a wildtype control (Tootle and Spradling, 2008). These experiments would further define how border cell cluster size relates to organ function.

4.2 Identifying novel Rap1 interacting genes

Chapter 3 describes the results of the screen I performed for Rap1 effectors in *Drosophila* border cell migration. This system has several key advantages. It is a genetically accessible *in vivo* model of collective cell migration. In addition, a requirement for properly regulated Rap1 in border cell migration has already been reported. Using the strong migration defects present in constitutively active $Rap1^{V12}$ expressing border cells, I screened the *X* chromosome for deficiency regions that dominantly interacted with Rap1 and partially restored migration. Further analysis of interacting regions identified *fz4*, *Usp16-45*, and *sno* as candidate interacting genes contributing to border cell migration.

4.2.1 A dominant interaction screen identifies seven candidate gene regions

Roles for Rap1 in cell polarity, cell-cell adhesions, and cell migration have been identified in flies, mice, and zebrafish, but downstream effectors for each of these processes remain poorly understood (Bonello et al., 2018; Chang et al., 2018; Choi et al., 2013; Kim et al., 2022; Molina-Ortiz et al., 2018; Perez-Vale et al., 2022; Sawant et al., 2018). Our screen for

dominant Rap1 interacting genes revealed seven deficiencies as high confidence hits. Each hit results in the deletion of anywhere from a few to 60+ genes. We utilized available mutant alleles to refine three interacting genomic regions to single gene resolution. For the remaining four regions, a major limitation is the lack of available alleles for many of the genes contained in each deficiency region. Given the time and expense associated with making a new allele, it may not be feasible to follow up on every gene. To address this limitation, a targeted approach would be beneficial. The McDonald lab has an RNA sequencing dataset (Burghardt et al., unpublished) for genes that change expression during border cell migration. Each of these genes is positioned within a cluster of genes depending on how its expression changes during migration. These data could be used in conjunction with the list of genes from the screen that are currently untested to identify a short list of genes that may be important for border cell migration based upon their expression patterns. A gene ontology analysis could be performed on this list to further refine the candidates with likely roles in border cell migration. Of these remaining genes the top ten candidates could be assessed in border cell migration using RNAi lines where available. Based upon these data, the top two candidates could be used to generate alleles by CRISPR/Cas9 mutagenesis and tested for an interaction with Rap1. These experiments would provide further information on potential Rap1 effectors required in collective cell migration.

4.2.2 Strawberry notch (Sno) is a Rap1 interacting gene required for border cell migration

Of the three hit genes identified in Chapter 3, *Strawberry notch (Sno)* is the most promising candidate. We found that *sno* genetically interacts with Rap1, is required for border cell migration, and is expressed in border cells. Further work will be required to determine the relationship between *sno* and Rap1. Moreover, this is the first report of a role for *sno* in border cell migration.

Sno is required for proper eye and wing development in *Drosophila* and generates similar phenotypes as *Notch* mutants. Moreover, *Sno* mutant phenotypes in these tissues can be rescued by an extra copy of *Notch* (Coyle-Thompson and Banerjee, 1993). *Sno* mutants caused general oogenesis defects that resembled *Notch* mutants, suggesting that these two genes may function in the same pathway in the ovary as well (Coyle-Thompson and Banerjee, 1993; Xu et al., 1992). Antibody staining revealed nuclear localization of Sno in malpighian tubules, embryos, wing discs, and follicle cells of egg chambers (Majumdar et al., 1997). Our analysis of a GFP protein trap in Sno supports nuclear localization in follicle cells, but also in germline nurse cells and the migratory border cells.

The function of *sno* in border cell migration is unclear. Roles for *Notch* in border cell migration have been identified but are poorly defined. Notch is expressed in border cells and is required for border cell migration (Wang et al., 2007; Xu et al., 1992). Expression of a dominant negative form of Kuzbanian (KUZ), a metalloproteinase that activates Notch, resulted in reduced levels of both Notch and the downstream target Suppressor of Hairlesss [Su(H)] and caused significant border cell migration defects (Wang et al., 2007). Linking Notch signaling to a downstream cellular target required for border cell migration has been challenging. Notch is required to activate *slow border cells (slbo)*, the *Drosophila* C/EBP homolog, in both centripetal follicle cells and border cells (Levine et al., 2007; Schober et al., 2005). Moreover, *slbo* is required for border cell migration (Montell et al., 1992). Therefore, it is tempting to propose that Notch dependent *slbo* expression is required for proper border cell migration.

Notably, Notch signaling is required for detachment of the border cell cluster from the follicular epithelium, potentially through a cell-cell adhesion regulatory function (Prasad and Montell, 2007; Schober et al., 2005). Interestingly, a role for Notch in cell-cell adhesion has been

identified in border cell migration through the transcription factor Aop/Yan (Schober et al., 2005). Notch signaling promotes Yan expression and Yan may regulate the turnover of E-Cadherin adhesive complexes (Schober et al., 2005). Moreover, Slbo, another Notch target, also regulates E-Cadherin suggesting that Notch may function at multiple levels of E-Cadherin regulation in border cell migration (Levine et al., 2007; Niewiadomska et al., 1999; Schober et al., 2005). Properly regulated cell-cell adhesions are critical for border cell migration (Prasad and Montell, 2007; Sawant et al., 2018; Schober et al., 2005).

Given the known requirement of Notch signaling in border cell migration and the reported relationship between Notch and Sno in various tissues it would be beneficial to first assess if Sno has similar functions in border cell migration as Notch. Since Notch signaling promotes *slbo* expression in border cells it would be informative to determine whether *sno* performs a similar function. A lacZ enhancer trap allele in *slbo*, known as $slbo^{1}$ or $slbo^{1310}$, is a hypomorphic allele that allows the detection of slbo activity (Montell et al., 1992). This allele could be used in combination with sno RNAi or a temperature sensitive allele of *sno*, sno^{71e3}. If *sno* is required for *slbo* expression, then quantitative imaging of lacZ expression in border cells should reveal decreased signal upon *sno* inhibition. If the robust nature of lacZ precludes successful analysis, RNA-fluorescence in situ hybridization (FISH) could be perfromed to assess the levels of *slbo* mRNA. In addition genetic interaction experiments using alleles of *sno* and *slbo* could be performed to determine how different combinations influence border cell migration. A reasonable hypothesis is that mild migration defects may appear in transheterozygotes featuring an amorphic allele for each gene that are absent when each allele is alone.

Perhaps an even more exciting avenue of investigation is the relationship between Sno and E-Cadherin. Given that Rap1 regulates cell-cell adhesions in the border cell cluster, E-Cadherin could easily be a common target of both Sno and Rap1. The most direct approach to evaluate this possibility could utilize a temperature sensitive allele of *sno.* Quantitative imaging of E-Cadherin in border cell clusters could be perfomed on the same genotype with the only change being half the specimens are shifted to the restrictive temperature at a time point before dissection. Specimens kept at the permissive temperature would have functional Sno while those shifted to the restrictive temperature would not. If Sno promotes E-Cadherin turnover, it seems likely that egg chambers shifted to the restrictive temperature would either have increased accumulation or improper localization of E-Cadherin. This experiment would clearly identify whether E-Cadherin is a target of Sno.

Finally, targets of Sno are poorly defined. While the preceeding experiments present direct methods for testing two proposed targets, a broader approach may be needed to identify additional targets of Sno and reveal novel functions of Sno. *Sno* enocodes a nuclear protein that lacks DNA binding domains, but may function in concert with other proteins to regulate transcription (Majumdar et al., 1997). Su(H) is an intriguiging candidate based upon genetic interaction experiments (Majumdar et al., 1997). To assess how Sno contributes to gene expression, RNA-sequencing of *sno* mutants could be performed. Analyzing these data would help establish a set of target genes to perform an RNAi screen for genes critical to border cell migration. Existing Su(H) chromatin immunoprecipiation sequencing (ChiP-Seq) data could be used to identify common targets of Sno and Su(H) and further refine the candidate approach (Ozdemir et al., 2014). These methods would help identify a broader group of potential targets and define their requirement in border cell migration.

4.3 Summary

Here we report two studies of Rap1 function in the ovary. We propose that in this tissue, like the embryo, Rap1 maintains adherens junctions and adherens junction-actomyosin linkages required for proper tissue development. Moreover, we report a previously underappreciated function of Rap1 in cell viability with links to the apoptotic cascade through DIAP1. Although Rap1 has numerous functions, information about effector molecules used in each of these processes remains scant. We thus performed a dominant genetic interaction screen to identify genes contributing to Rap1 function in border cell migration. Here we report three candidate effectors of Rap1 and propose future experiments to clarify the relationship between Rap1 and our highest confidence hit, Sno. Together these results identify new roles for Rap1 in the *Drosophila* ovary and new candidate effectors. Epithelial morphogenesis and collective cell migration are highly conserved features of animal development, making these findings relevant to other organisms.

4.4 References

Aranjuez, G., Burtscher, A., Sawant, K., Majumder, P. and McDonald, J. A. (2016). Dynamic myosin activation promotes collective morphology and migration by locally balancing oppositional forces from surrounding tissue. *Mol Biol Cell* **27**, 1898–1910.

Boettner, B., Harjes, P., Ishimaru, S., Heke, M., Fan, H. Q., Qin, Y., Van Aelst, L. and Gaul, U. (2003). The AF-6 homolog canoe acts as a Rap1 effector during dorsal closure of the Drosophila embryo. *Genetics* **165**, 159–69.

Bonello, T. T., Perez-Vale, K. Z., Sumigray, K. D. and Peifer, M. (2018). Rap1 acts via multiple mechanisms to position Canoe and adherens junctions and mediate apical-basal polarity establishment. *Development* **145**, dev157941.

Brüser, L. and Bogdan, S. (2017). Adherens Junctions on the Move—Membrane Trafficking of E-Cadherin. *Cold Spring Harb Perspect Biol* **9**, a029140.

Cai, D., Dai, W., Prasad, M., Luo, J., Gov, N. S. and Montell, D. J. (2016). Modeling and analysis of collective cell migration in an in vivo three-dimensional environment. *Proceedings of the National Academy of Sciences of the United States of America* **113**, E2134–E2141.

Chang, Y.-C., Wu, J.-W., Hsieh, Y.-C., Huang, T.-H., Liao, Z.-M., Huang, Y.-S., Mondo, J. A., Montell, D. and Jang, A. C.-C. (2018). Rap1 Negatively Regulates the Hippo Pathway to Polarize Directional Protrusions in Collective Cell Migration. *Cell Reports* **22**, 2160–2175.

Choi, W., Harris, N. J., Sumigray, K. D. and Peifer, M. (2013). Rap1 and Canoe/afadin are essential for establishment of apical-basal polarity in the Drosophila embryo. *Molecular biology of the cell* **24**, 945–63.

Coyle-Thompson, C. A. and Banerjee, U. (1993). The strawberry notch gene functions with Notch in common developmental pathways. *Development* **119**, 377–395.

Geisbrecht, E. R. and Montell, D. J. (2004). A Role for Drosophila IAP1-Mediated Caspase Inhibition in Rac-Dependent Cell Migration. *Cell* **118**, 111–125.

Harris, T. J. C. and Peifer, M. (2004). Adherens junction-dependent and -independent steps in the establishment of epithelial cell polarity in Drosophila. *J Cell Biol* **167**, 135–147.

Heo, K., Nahm, M., Lee, M.-J., Kim, Y.-E., Ki, C.-S., Kim, S. H. and Lee, S. (2017). The Rap activator Gef26 regulates synaptic growth and neuronal survival via inhibition of BMP signaling. *Mol Brain* **10**, 62.

Hoshino, T., Sakisaka, T., Baba, T., Yamada, T., Kimura, T. and Takai, Y. (2005). Regulation of E-cadherin Endocytosis by Nectin through Afadin, Rap1, and p120ctn*. *Journal of Biological Chemistry* **280**, 24095–24103.

Jaramillo, A. M., Weil, T. T., Goodhouse, J., Gavis, E. R. and Schupbach, T. (2008). The Dynamics of Fluorescently Labeled Endogenous gurken mRNA in Drosophila. *J Cell Sci* **121**, 887–894.

Kim, Y. S., Fan, R., Lith, S. C., Dicke, A.-K., Drexler, H. C. A., Kremer, L., Kuempel-Rink, N., Hekking, L., Stehling, M. and Bedzhov, I. (2022). Rap1 controls epiblast morphogenesis in sync with the pluripotency states transition. *Dev Cell* **57**, 1937-1956.e8.

Lamb, M. C., Kaluarachchi, C. P., Lansakara, T. I., Mellentine, S. Q., Lan, Y., Tivanski, A. V. and Tootle, T. L. (2021). Fascin limits Myosin activity within Drosophila border cells to control substrate stiffness and promote migration. *eLife* **10**, e69836.

Levine, B., Jean-Francois, M., Bernardi, F., Gargiulo, G. and Dobens, L. (2007). Notch signaling links interactions between the C/EBP homolog slow border cells and the GILZ homolog bunched during cell migration. *Dev Biol* **305**, 217–231.

Loyer, N., Kolotuev, I., Pinot, M. and Le Borgne, R. (2015). Drosophila E-cadherin is required for the maintenance of ring canals anchoring to mechanically withstand tissue growth. *Proceedings of the National Academy of Sciences* **112**, 12717–12722.

Maddala, R., Nagendran, T., Lang, R. A., Morozov, A. and Rao, P. V. (2015). Rap1 GTPase is required for mouse lens epithelial maintenance and morphogenesis. *Dev Biol* **406**, 74–91.

Majumdar, A., Nagaraj, R. and Banerjee, U. (1997). strawberry notch encodes a conserved nuclear protein that functions downstream of Notch and regulates gene expression along the developing wing margin of Drosophila. *Genes Dev.* **11**, 1341–1353.

Majumder, P., Aranjuez, G., Amick, J. and McDonald, J. A. (2012). Par-1 Controls Myosin-II Activity Through Myosin Phosphatase to Regulate Border Cell Migration. *Curr Biol* **22**, 363–372.

Martin, A. C., Kaschube, M. and Wieschaus, E. F. (2009). Pulsed contractions of an actin-myosin network drive apical constriction. *Nature* **457**, 495–9.

Mishra, A. K., Mondo, J. A., Campanale, J. P. and Montell, D. J. (2019). Coordination of protrusion dynamics within and between collectively migrating border cells by myosin II. *MBoC* **30**, 2490–2502.

Molina-Ortiz, P., Orban, T., Martin, M., Habets, A., Dequiedt, F. and Schurmans, S. (2018). Rasa3 controls turnover of endothelial cell adhesion and vascular lumen integrity by a Rap1-dependent mechanism. *PLoS Genet* **14**, e1007195.

Montell, D. J., Rorth, P. and Spradling, A. C. (1992). slow border cells, a locus required for a developmentally regulated cell migration during oogenesis, encodes Drosophila CEBP. *Cell* **71**, 51–62.

Montell, D. J., Yoon, W. H. and Starz-Gaiano, M. (2012). Group choreography: mechanisms orchestrating the collective movement of border cells. *Nature reviews. Molecular cell biology* **13**, 631–45.

Niewiadomska, P., Godt, D. and Tepass, U. (1999). DE-Cadherin Is Required for Intercellular Motility during Drosophila Oogenesis. *Journal of Cell Biology* **144**, 533–547.

Ozdemir, A., Ma, L., White, K. P. and Stathopoulos, A. (2014). Su(H)-Mediated Repression Positions Gene Boundaries along the Dorsal-Ventral Axis of Drosophila Embryos. *Dev Cell* **31**, 100–113.

Pacquelet, A. and Rørth, P. (2005). Regulatory mechanisms required for DE-cadherin function in cell migration and other types of adhesion. *Journal of Cell Biology* **170**, 803–812.

Perez-Vale, K. Z., Yow, K. D., Gurley, N. J., Greene, M. and Peifer, M. (2022). Rap1 regulates apical contractility to allow embryonic morphogenesis without tissue disruption and acts in part via Canoe-independent mechanisms. *Mol Biol Cell* mbcE22050176.

Pinheiro, D. and Bellaïche, Y. (2018). Mechanical Force-Driven Adherens Junction Remodeling and Epithelial Dynamics. *Developmental Cell* **47**, 3–19.

Prasad, M. and Montell, D. J. (2007). Cellular and Molecular Mechanisms of Border Cell Migration Analyzed Using Time-Lapse Live-Cell Imaging. *Developmental Cell* **12**, 997–1005.

Sasaki, K., Kojitani, N., Hirose, H., Yoshihama, Y., Suzuki, H., Shimada, M., Takayanagi, A., Yamashita, A., Nakaya, M., Hirano, H., et al. (2020). Shank2 Binds to aPKC and Controls Tight Junction Formation with Rap1 Signaling during Establishment of Epithelial Cell Polarity. *Cell Reports* **31**, 107407.

Sawant, K., Chen, Y., Kotian, N., Preuss, K. M. and McDonald, J. A. (2018). Rap1 GTPase promotes coordinated collective cell migration in vivo. *Molecular Biology of the Cell* **29**, 2656–2673.

Sawyer, J. K., Harris, N. J., Slep, K. C., Gaul, U. and Peifer, M. (2009). The Drosophila afadin homologue Canoe regulates linkage of the actin cytoskeleton to adherens junctions during apical constriction. *Journal of Cell Biology* **186**, 57–73.

Schober, M., Rebay, I. and Perrimon, N. (2005). Function of the ETS transcription factor Yan in border cell migration. *Development* **132**, 3493–3504.

Starz-Gaiano, M., Melani, M., Wang, X., Meinhardt, H. and Montell, D. J. (2008). Feedback Inhibition of JAK/STAT Signaling by Apontic Is Required to Limit an Invasive Cell Population. *Developmental Cell* **14**, 726–738.

Stonko, D. P., Manning, L., Starz-Gaiano, M. and Peercy, B. E. (2015). A Mathematical Model of Collective Cell Migration in a Three-Dimensional, Heterogeneous Environment. *PLoS One* **10**, e0122799.

Tootle, T. L. and Spradling, A. C. (2008). Drosophila Pxt: a cyclooxygenase-like facilitator of follicle maturation. *Development* **135**, 839–847.

Walther, R. F., Burki, M., Pinal, N., Rogerson, C. and Pichaud, F. (2018). Rap1, Canoe and Mbt cooperate with Bazooka to promote zonula adherens assembly in the fly photoreceptor. *J Cell Sci* **131**, jcs207779.

Wang, X., Adam, J. C. and Montell, D. (2007). Spatially localized Kuzbanian required for specific activation of Notch during border cell migration. *Dev Biol* **301**, 532–540.

Xu, T., Caron, L. A., Fehon, R. G. and Artavanis-Tsakonas, S. (1992). The involvement of the Notch locus in Drosophila oogenesis. *Development* **115**, 913–922.

Yalonetskaya, A., Mondragon, A. A., Elguero, J. and McCall, K. (2018). I Spy in the Developing Fly a Multitude of Ways to Die. *J Dev Biol* **6**, 26.

Zhang, L., Ren, F., Zhang, Q., Chen, Y., Wang, B. and Jiang, J. (2008). The TEAD/TEF Family of Transcription Factor Scalloped Mediates Hippo Signaling in Organ Size Control. *Developmental Cell* **14**, 377–387.

Appendix A - Supplemental Figures

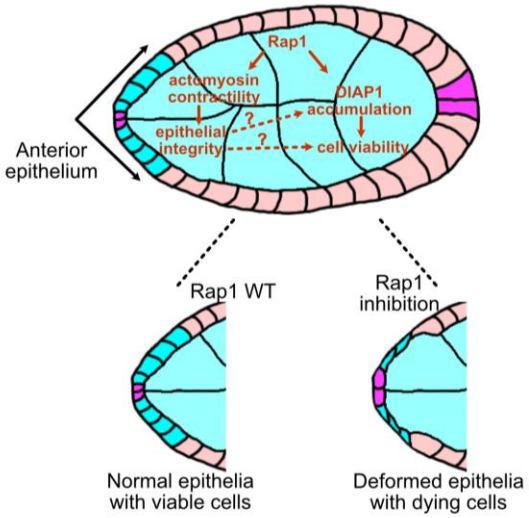

Appendix A.1 Chapter 2 Graphical Abstract

Rap1 promotes epithelial integrity and cell viability during oogenesis. Magenta indicates polar cells at the anterior and posterior of egg chamber schematic. Anterior follicle cells (cyan) lost proper shape in Rap1 inhibited egg chambers.

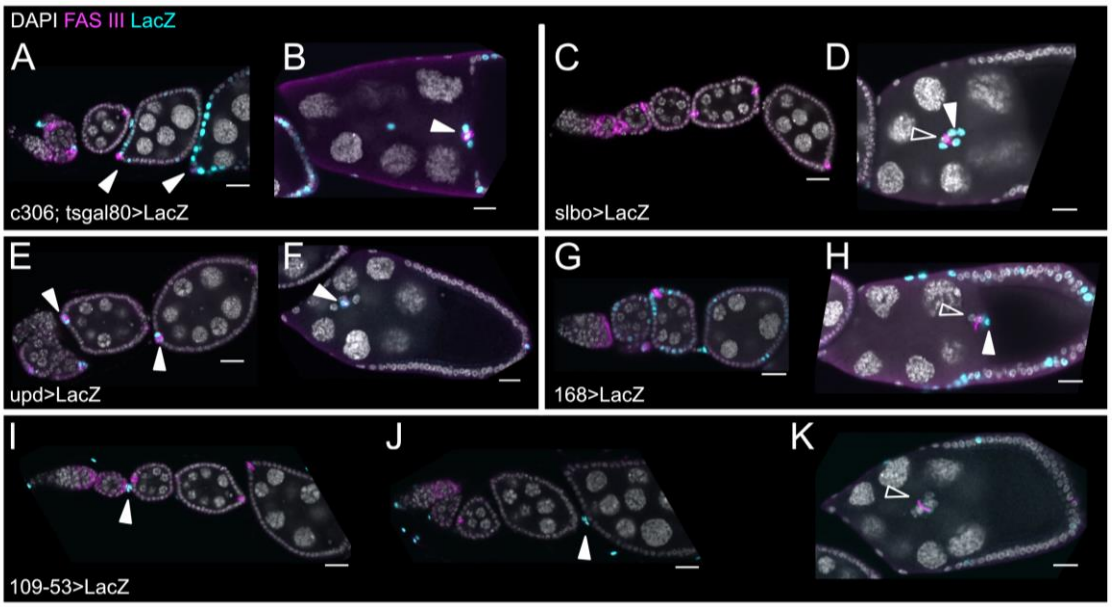

Appendix A.2 GAL4 Driver line expression patterns

(A-K) GAL4 driver line expression patterns visualized by LacZ antibody staining (cyan). All drivers used in Chapters 2 and 3 are presented along with drivers used for preliminary experiments. (A-B) *c306*-GAL4 is expressed in anterior follicle cells during oogenesis (A) and in border cell clusters including polar cells (B). Image in A also appears in Figure 2.1 B. (C-D) *slbo*-GAL4 is not expressed during early stages of oogenesis (C) but is expressed in border cells alone during migration (D). (E-F) *upd*-GAL4 is expressed in polar cells during early stages of oogenesis (E) and during migration (F). (G-H) *168*-GAL4 is expressed in some follicle cells during early oogenesis (G) and in border cells alone during migration (H). (I-K) *109-53*-GAL4 is expressed in interfollicular stalks (I-J) but not the migratory cluster (K). FAS III (magenta) marks polar cells. Solid arrowheads indicate LacZ expression. Open arrowheads indicate absence of LacZ. Scale bars 20µm.

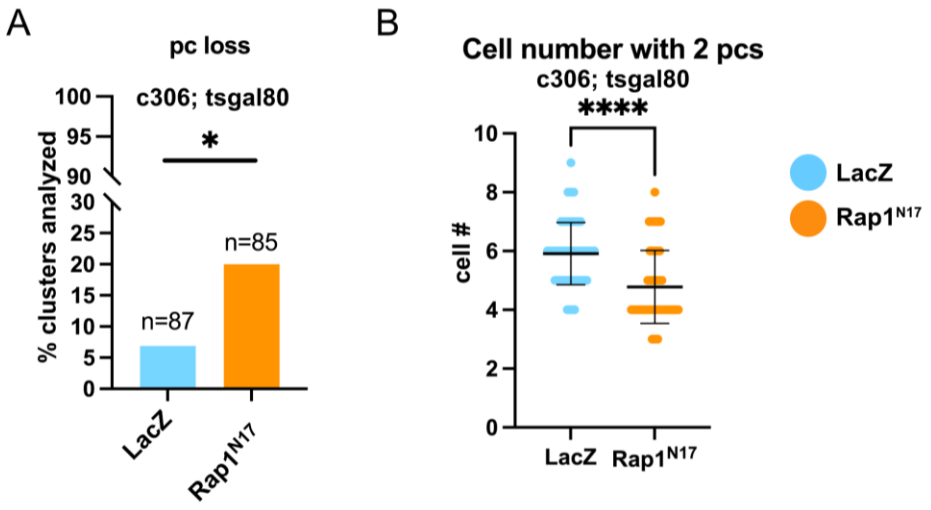

Appendix A.3 Rap1 is required for polar cell inclusion in migratory clusters

(A-B) Migratory border cell clusters were analyzed for presence of polar cells. (A) Loss of polar cells reported as percentage of migratory clusters scored that were missing one or both polar cells for LacZ control or DN-Rap1^{N17}. * $p<0.05$ Fisher's exact test. N≥85 border cell clusters analyzed per genotype. (B) Scatter plot analysis of total cells per cluster when both polar cells are present. Mean with standard deviation **** $p<0001$. Two-tailed unpaired t-test. N≥68 border cell clusters per genotype.